Public Interest Energy Research (PIER) Program

FINAL PROJECT REPORT

DEVELOPMENT OF FAULT CURRENT CONTROLLER TECHNOLOGY

Prototyping, Laboratory Testing, and Field Demonstration

Prepared for: California Energy Commission

Prepared by: University of California Irvine

JUNE 2011

CEC-XXX-XXXX-XXX

Prepared by:

Primary Author(s):
Keyue Smedley, Ph.D.
Alexander Abravomitz, Ph.D.
University of California, Irvine, CA 92697
949-824-6710
www.smedley@uci.edu

Contract Number: 500-02-004

Prepared for:

California Energy Commission

Jamie Patterson
Contract Manager

Pedro Gomez
Project Manager

Mike Gravely
Office Manager
Energy Systems Research

Laurie ten Hope
Deputy Director
Research & Development Division

Melissa Jones
Executive Director

ACKNOWLEDGEMENTS

University of California, Irvine acknowledges the financial support from the California Energy Commission and the California Institute for Energy & Environment, which made this project possible. We sincerely thank our collaborators at Southern California Edison Co., Zenergy Power plc, the Electric Power Research Institute (EPRI) and Silicon Power Corp. for their cooperation, teamwork, and support which made this project successful. Our appreciation also goes to our knowledgeable and supportive advisory group for their valuable advice, which has been of critical importance in each step of the project.

Contributing Authors:

Lloyd Cibulka, California Institute for Energy and Environment
Franco Moriconi, Francisco De La Rosa, Alonso Rodriguez, Albert Nielsen, Amandeep Singh, and Nick Koshnick, ZenergyPower Inc.
Christopher R. Clarke, Ed Kamia, Syed Ahmed, Southern California Edison Co.
Ram Adapa, Electric Power Research Institute (EPRI)
Mahesh Gandhi, Swapna Bhat, Simon Bird, Silicon Power Corporation.

Project Advisory Group:

Albert Nelson of Zenergy Power
Alfonso Orzoco, San Diego Gas & Electric Co.
Alonzo Rodrigues, Zenergy Power
Bob Yinger, Southern California Edison Co.
Christopher R. Clarke, Southern California Edison Co.
Ed Kamiab, Southern California Edison Co.
Russ Neal, Southern California Edison Co.
Ed Muljadi, National Renewable Energy Laboratory
Jim McHan, California Independent System Operator
Katie Speirs, San Diego Gas & Electric Co.
Ken Edwards, Bonneville Power Administration,
Lorraine Hwang, California Institute for Energy & Environment
Merwin Brown, California Institute for Energy & Environment
Jamie Patterson, California Energy Commission,
Raj Vora, So Cal Edison Co.,
Randy Hopkins, Pacific Gas & Electric Co.
Ron Meyer, Santa Margarita Water District
Tony Johnson, Southern California Edison Co.

UCI Participations:

Jun Wen
Franco Maddaleno
Liang Zhou
In Wha Jeong,
Marco Tedde
Sadigh Khoshkbar Arash,
Chaitanya Vartak,

Wensheng Song
Pengju Sun
ZhengSheng Wu,
Wenchao Xi,
Zhuo Zhao,
Fei Gu

PREFACE

The California Energy Commission Public Interest Energy Research (PIER) Program supports public interest energy research and development that will help improve the quality of life in California by bringing environmentally safe, affordable, and reliable energy services and products to the marketplace.

The PIER Program conducts public interest research, development, and demonstration (RD&D) projects to benefit California.

The PIER Program strives to conduct the most promising public interest energy research by partnering with RD&D entities, including individuals, businesses, utilities, and public or private research institutions.

PIER funding efforts are focused on the following RD&D program areas:

- Buildings End-Use Energy Efficiency
- Energy Innovations Small Grants
- Energy-Related Environmental Research
- Energy Systems Integration
- Environmentally Preferred Advanced Generation
- Industrial/Agricultural/Water End-Use Energy Efficiency
- Renewable Energy Technologies
- Transportation

- *Development of Fault Current Controller Technology* is the final report for the CEC/PIER project "Development of Fault Current Controller Technology" (contract number 500 - 02 - 004) conducted by University of California, Irvine. The information from this project contributes to PIER's Energy Systems Integration Program.

For more information about the PIER Program, please visit the Energy Commission's website at www.energy.ca.gov/research/ or contact the Energy Commission at 916-654-4878.

ABSTRACT

Fault current controller (FCC) technology, also frequently referred to as fault current limiter (FCL) technology, has been identified as a potentially viable solution for expanding the capacity of the transmission system and its service life to meet the growing demand for electricity, by addressing the impacts of the resulting higher fault currents. This document reports on the program supported by the California Institute for Energy and Environment under the California Energy Commission in the development of distribution class FCC technology. The project focused on test plan development, prototyping, laboratory test, and field demonstration, with a view toward potential further technical development and application of the technology in transmission-level systems. The University of California Irvine led the project with overall responsibility for project management, administration, coordination, and technical guidance, with the support of the California Institute for Energy & Environment (CIEE) at the University of California, Berkeley. Southern California Edison Co. (SCE) was the host utility for the field demonstration, providing on-site engineering personnel, expertise and support. Zenergy Power and the EPRI/Silicon Power team were engaged to prototype a passive type FCC and an active FCC, respectively, for laboratory testing and field demonstration.

A full-size three-phase distribution level high temperature superconductor (HTS) FCC prototype was designed, built, and field tested by Zenergy Power, plc. The prototype FCC went through several iterations of extensive testing at Powertech Labs Inc., Surrey, BC, Canada and at the High Voltage Laboratory of SCE's Westminster facility prior to field installation. It was then installed at SCE's Avanti "Circuit of the Future" for field demonstration from March 2009 through October 2010.

The EPRI/Silicon Power team has completed an initial design for a solid-state based FCC. Due to design changes that were necessary to improve the thermal management of the prototype but were beyond the scope of this project, this design did not advance to the laboratory and field test stages during the project period.

This report provides a technology survey of FCC technology, including both the saturable core and solid-state types represented by this project, followed by detailed design considerations, laboratory test procedures and results, field test installation and metering, and field demonstration outcomes. The report concludes with a summary of the lessons learned and recommendations for future research efforts.

Keywords: Fault Current, Fault Current Controller, FCC, Fault Current Limiter, FCL, Short Circuit Current, Power System Protection, Saturable Core Reactor FCL, Solid-State FCL, High Temperature Superconductivity, HTS.

Please use the following citation for this report:

Smedley, Keyue and Abramovitz, Alexander, (University of California Irvine). 2011. ***Development of Fault Current Controller Technology.*** California Energy Commission. Publication number: CEC-XXX-2010-XXX.

TABLE OF CONTENTS

EXECUTIVE SUMMARY

Introduction

Overall electric current loading on the transmission system has been rapidly climbing to meet the growth in demand for electricity. The resulting higher electrical energy levels have increased the potential fault current magnitudes at locations throughout the transmission system. Fault currents, in many instances, exceed the capability of existing protection systems (circuit breakers) to interrupt the faults safely and reliably. This also threatens other electric equipment along the line. Consequently, a utility must either upgrade breakers and equipment or reconfigure its system to reduce the potential fault current. Both solutions are costly, and frequently reduce system reliability and power transfer capability. Application of fault current controller (FCC) technology, also referred as fault current limiter (FCL) technology, has been identified as a potentially viable solution to reduce the fault currents to the rated short circuit capacity of the system in order to expand and extend the transmission system's capacity and service life. This approach allows utilities to meet the growing demand for electricity reliably and cost-effectively.

The California Institute for Energy and Environment (CIEE), with the financial support of the California Energy Commission (CEC), sponsored this project to develop and evaluate reliable, cost-effective, and environmentally acceptable technologies for the control of high fault currents. The proposed research aimed to establish the desired criteria for FCC performance and to test two different leading FCC technologies against those criteria, by means of controlled laboratory testing and field demonstration in a commercially operating Southern California Edison distribution system. The intended outcome of this project is to facilitate improved, safe and reliable operation of the power system by advancing the FCC technology as a cost-effective and environmentally-preferred option to breaker upgrades or system reconfiguration, and by evaluating the realistic potential of this technology to mitigate fault current levels at higher voltages in the electric system through real-world utility testing. The ultimate program goal is to enable the commercialization of FCC technology for the benefit of California and the United States.

Program Objectives

1. Establish an FCC test plan including test criteria, test protocol, test site selection, test scheduling, data collection plans, and interface requirements for both the laboratory testing and field demonstration.
2. Prototype two FCCs, one saturable-core type developed by ZenergyPower Inc., and one solid-state type developed by the Electric Power Research Institute (EPRI) and Silicon Power Corp. team.
3. Conduct laboratory testing of the two FCCs against the criteria, including pre-connection high-voltage insulation tests, normal operation tests, and fault current limiting tests.
4. Install the FCCs on the SCE distribution system and perform field demonstration for a minimum of six months.
5. Complete the evaluation of the technologies on the basis of performance, respective strengths and weaknesses, costs, reliability, installation, operation, and maintenance issues, potential for development to high-voltage design.

Program Outcomes

A research consortium was formed for this project, in which the University of California, Irvine as the Performing Institution was responsible for project management, administration, coordination, and technical guidance; Southern California Edison Co. (SCE) was the host utility for the field demonstration and support; while Zenergy Power and the EPRI/Silicon Power team were engaged to prototype and field test a passive type FCC and an active FCC, respectively. In addition, a Project Advisory Group was assembled with experts from utility companies, national laboratories, regulatory boards, and other relevant organizations to guide the process.

The project started in September 2007. This was not the first attempt in the United States to develop a distribution-level FCC and demonstrate it on an operating power system. However, none of the earlier efforts had led to a successful field demonstration in the US. The obstacles to be overcome were challenging. Firstly, there were no industry standards for such a device, complicating the development of testing protocols. Secondly, there were significant engineering challenges in developing the prototypes to withstand the currents and voltages in the field. Thirdly, the prototype FCCs had to meet SCE's specifications for field demonstration on their system. Fourthly, the FCCs had to withstand live circuit events and severe environmental conditions.

An important step taken at the early-stage was a focused effort to develop the test plan acceptable to SCE and workable for the teams. Zenergy Power worked closely with Georgia Tech's National Electric Energy Testing Research and Applications Center (NEETRAC) and several of its member utilities, including SCE to implement a detailed FCC test program based on selected IEEE and CIGRE standards and protocols for transformers and reactors. EPRI/Silicon Power team created their plan based on ANSI C39.09-1999 and ANSI C37.06-2000 covering the entire spectrum of possible tests that need to be carried out on their FCC, including component level factory tests, system level factory tests, acceptance tests and system field tests. Many technical issues related to laboratory test and field demonstration interfacing were resolved via a series of meetings with knowledgeable SCE engineers. Both teams completed their test plans, which provided valuable design and testing guidelines.

Zenergy Power HTS FCL

Zenergy Power, Inc. completed the design, construction, and testing of an FCC based on a saturable core concept. This type of FCC is basically a coil wound on an iron core and connected in series in the power line. In the normal state, the core is saturated by a dedicated DC electromagnet. Thus the inductance of the magnetically saturated coil and the corresponding voltage drop across the coil terminals are negligible. Therefore, the coil has no deleterious effect on the system. In the event of a fault, the magnetic core is driven out of saturation by the fault current. Consequently, the coil becomes highly inductive with a large impedance introduced into the power circuit to limit the fault current. The Zenergy Power FCC also incorporated a high temperature superconductor (HTS) winding for the DC bias circuit to reduce bias circuit power loss while increasing the intensity of the bias field, thus the Zenergy Power FCC is referred to as the HTS FCL[1] .

[1] As previously noted, while "fault current controller (FCC)" is the preferred terminology for the class of technologies that address the management of fault currents, "fault current limiter (FCL)" is also commonly used. Both Zenergy Power and EPRI/Silicon Power use "FCL" in reference to their devices, and their terminology has been preserved in this report in such references.

A full-scale three-phase 12 kV distribution level HTS FCL prototype was built for a rated load current of 1200 Amp (3 phase, 60 Hz), less than 1% normal voltage drop at maximum load (70V rms) and 20% fault current clipping capability.

The prototype HTS FCL went through a series of rigorous laboratory tests in BC Hydro's Powertech Laboratory in Surrey, BC, Canada. A total of 65 separate tests were performed, including 32 full-power fault tests with first peak fault current levels up to 59 kA at the rated voltage. Fault tests included individual fault events of 20-30 cycles duration, as well as multiple fault events in rapid sequence (to simulate automatic re-closer operation) and extended fault events of up to 82 cycles duration, simulating primary protection failure scenarios. The HTS FCL passed the test criteria in all cases. The unit was then transferred to the SCE Westminster High-Voltage Test Facility for acceptance test by SCE per IEEE Standard C57-12.01-2005.

Upon the successful acceptance test, the HTS FCL was installed on the SCE Avanti Circuit of the Future and operated from March 2009 through October 2010. The unit was integrated into SCE's SCADA system and operated in real-time to provide protection to the distribution circuit during its field demonstration.

Throughout the field demonstration, several deficiencies were revealed in the original design and construction, including a PLC RAM overflow programming issue, HVAC shutdown due to excessive ambient temperature, helium leaks in the cryogenic coolers, nitrogen pressure instabilities associated with the liquid nitrogen cooling system, and a terminal block short. It provided a valuable learning experience for the team to identify the design weakness and make necessary correction along the way, resulting in significant design and implementation enhancements. During the live grid demonstration, the FCL also experienced an in-service multiple-fault event, and it was able to limit the fault current throughout the individual faults.

The FCL survived and thrived during its nineteen-month field service demonstration (9 months on line, 10 months standby). The immediate research benefits obtained from the Zenergy Power FCL's operational experience included validation of the importance of a more compact, more reliable, and easier to maintain FCL design which is scalable to transmission voltages. The demonstration has also contributed to Zenergy Power's first commercial sale of a medium-voltage device. Furthermore, Zenergy Power has extended the research results to applications at the transmission voltage level.

EPRI/Silicon Power SSFCL

The Electric Power Research Institute (EPRI) and Silicon Power Corp. team completed an initial design for an FCC based on solid-state circuit technology employing their Super GTO (SGTO) thyristor switches. The FCC design consists of a set of standard building blocks (SBB), each containing an SGTO-based circuit, designed for 5kV blocking and 2000A continuous current ratings. The SBB are used in multiples to form standard power stack (SPS) assemblies rated for 2000A and 50kV blocking withstand voltage. One SPS per phase is required for the 15kV class system. Three SPS are then housed in an oil-filled tank to form a complete three-phase FCC, referred to as the Solid State FCL (SSFCL) unit. In the normal state, the SGTO switches are turned on, which allows continuous rated current to flow through the circuit; upon detection of a fault, the control circuits open the SGTO switches to insert a current limiting reactor (CLR) into the circuit to limit the fault current.

The 15kV 1200A SSFCL was designed for outdoor use according to the IEEE Standard for Standard General Requirements for Liquid-Immersed Distribution, Power, and Regulating Transformers. The overall package is similar to a typical substation transformer tank with an external radiator bank for the cooling system.

During initial simulation of the thermal performance of the FCL design, less than optimal thermal response was observed, which could have led to undesirable effects on the stability and reliability of the final, manufactured FCL. The designs of the thermal management system and the control boards were therefore modified during the course of the project, to provide a more efficient thermal management system and to improve the noise immunity of the controls. An unfortunate result of this necessary re-design was a much higher projected construction cost than allowed by the available project budget; therefore, this part of the project was terminated by mutual consent of the CEC, CIEE and EPRI at the conclusion of the design stage. EPRI was able to incorporate the lesson learned into a newer SSFCL design, which they intend to offer for demonstration in the future.

Conclusions:

Zenergy Power HTS FCL

The research in this period has led to the successful field demonstration of the Zenergy Power HTS FCL, marking a milestone event in the history of FCL development in the United States. The experience gained from the research contributed to a more reliable controller, a dramatic reduction of the FCL's size and weight, and the replacement of liquid nitrogen cryogenic refrigeration by a low maintenance dry cooling system.

The Zenergy Power HTS FCL was first laboratory tested successfully against FCL specifications and test criteria developed by US utilities, including the host utility Southern California Edison. The HTS FCL was then successfully demonstrated in actual field operation. The HTS FCL unit is rated at 15kV, 1200A, 110kV (BIL), steady state insertion impedance <1%, and a fault current reduction capability of 20% at 23kA maximum fault current.

The first-generation "spider-core" HTS FCL design had a dry-type transformer (air dielectric) structure, total overall dimensions of 19'x19'x7', and weighed approximately 50,000 lbs. The second-generation "compact" HTS FCL that followed from this demonstration employed innovative core architecture and oil dielectric transformer construction techniques that led to a much more compact size of approximately 8'x10'x11' (including electric bushings for AC circuit connection, which protrude from the side per customer-requirements) and a weight of approximately 67,000 lbs. The compact FCL had a power rating similar to the first device, but a much higher fault current limiting performance than the first generation "Spider core" FCL. The new Compact FCL design is an improved option for applications where real estate is limited.

Regarding the cost-effectiveness, as the first-generation device had a relatively low power rating, on the order of 25 MVA, the present manufacturing cost may not represent a high value proposition. This can be addressed, and is being addressed, in two directions - HTS FCL technology is being improved to reduce basic device manufacturing cost, and HTS FCL technology is being scaled up for higher voltages and current. The latter may be more important in terms of cost-effectiveness and value proposition, considering the fact that higher voltage substations can often be more crowded and have fewer options for expansion, and higher voltage components (switchgear, insulators, transformers, bus-work) are exponentially more expensive than their low-voltage counterparts. Further, large renewable power generators desire to connect to the electric grid, and high-voltage tie-lines have become increasingly more common as more power is wheeled from long distances and as grid interconnections occur to improve reliability and better control power flows. All of these factors are projected to continue to increase energy levels within the grid, leading to potentially unsafe fault current levels. In some cases, higher-rated components cannot be retrofitted in the available space, leading to lengthy and costly major upgrades of grid infrastructure. Economic studies and performance models show that at current performance levels and price points, FCC technologies can be very

cost-effective compared to major upgrade projects at high voltages. This becomes an especially important factor when the cost of the required construction outages of the existing facilities is taken into account, assuming the necessary outages will be allowed at all by independent system while connected to the circuit, several interventions were needed.

The HTS FCL demonstration project also brought out an issue with respect to reliability. While the HTS FCL device was maintained in good operating condition and performed satisfactorily as a demonstration unit, an improvement is needed for a commercial product. A desirable FCL needs to target "5-nines" reliability with only a single, scheduled, short-duration annual maintenance outage. Even better would be extending the maintenance interval to two years or longer, but an annual outage of a day or less would be acceptable if the FCL were reliable and required no other maintenance. If the FCC is to be relied upon for protection, then bypassing it from service temporarily for maintenance can be a risk for the circuit. Perhaps a scheduled bypass can be accomplished by splitting buses or otherwise configuring the system for short durations; but this might not be possible or acceptable for long-term operation. Thus an FCL should be designed, to the maximum extent possible, to allow essential routine maintenance, such as cryogenic maintenance, to be performed while the unit is energized. Zenergy Power is aggressively modifying their HTS FCL technologies for reduced maintenance requirements, higher mean time between failure (MTBF), and lower mean time to repair (MTTR).

A key area identified for improvement during the field test was that the nitrogen cooling system, which required periodic maintenance of the cryostat, including drying, establishing vacuum, and refilling the liquid nitrogen. This may not be practical considering the fact that the unit is typically installed in a high-voltage area. However, this issue was resolved in the second-generation FCL design by replacing the liquid nitrogen cooling system with a cryogen-free, "dry-type" conductive cryogenic cooling system, available as a commercial off-the-shelf unit, resulting in a more reliable and robust system requiring less maintenance.

Overall, the Zenergy Power HTS FCL project is considered as an important success and it has already led to a scaled-up design for a transmission level (138kV) application.

EPRI/Silicon Power SSFCL

The EPRI/Silicon Power SSFCL represents a potential cost-effective solution to the rapidly rising available fault currents seen in utility systems. One advantage of this type of FCL is the flexibility to be interruptive (i.e., act as a "solid-state breaker") or non-interruptive (limiting fault current but leaving fault interruption to existing protective devices). Furthermore, the solid state FCL may be used to limit the current of superconducting cable to enable the use of smaller cable sizes. The solid state FCL also has a unique capability to limit inrush current, even for capacitive loads.

EPRI/Silicon Power identified some thermal management issues in their initial design. An improved system design was completed, and the major technical design challenges, such as the thermal management system and control architecture, have been resolved. However, the resulting cost increase to actually construct the device was constrained by the project budget. Thus, this FCL did not advance to the laboratory test and field demonstration stages under this project.

According to the design prediction the system size and weight would be 6.5'x12'x12' and weight would be 62,000 lbs. with oil cooling. This size and weight specification would have been considered acceptable.

The SSFCL employs a modular and scalable design. The SSFCL designed for the 12kV line in this project period is composed of 10 SBBs in series. A consideration with this design is that

voltage sharing to maintain all the SBBs under the blocking voltage under dynamic conditions may be a technical challenge for transmission level applications where the voltage level is above 100kV.

Overall, the EPRI/Silicon Power team has made a creditable effort in the design and improvement of the SSFCL. During the project period, many engineering challenges were identified and a new design was completed.

Recommendations

Electricity is a vital force of our economy. It is an important goal of the California Institute for Energy and Environment and the California Energy Commission to support the technologies required satisfying a reliable, safe and environmentally responsible electrical energy supply. As such, FCC technology is a potentially cost-effective alternative to the capital-intensive upgrades of the power system that would ordinarily be required to meet growth in electrical demand. The demonstration projects in this phase have already resulted in two test plans, two full designs, and contributed to one commercial sale and one migration to a transmission-level application.

The consortium has accumulated extensive experience in the development of FCL technology, the operation, and support of field demonstration at Southern California Edison's Avanti Circuit. Further fast-paced and more advanced development of FCL technology is strongly recommended. As the demand for electrical energy rapidly increases, particularly in response to renewable power and "green technology" initiatives, tremendous investment investments on system upgrades will have to made on a fast-track in order to maintain the required levels of system availability and reliability. Significant amounts of these investment are potentially avoidable, if suitable FCL technologies are available to California utilities, and if California utilities are given reasonable incentives to deploy the new technologies. An accelerated program of FCL technology focused on reducing the cost, improving the reliability, and increasing the voltage and current ratings of FCC technology is needed in order for California utilities and ratepayers to reap the benefits. New and promising technologies are also important for the recovery of the economy and the creation of new jobs.

CHAPTER 1:

Introduction

The overall electric current loading on the transmission system has been increasing due to continuing growth in electricity demand. These higher power currents have increased the potential fault current magnitudes at locations throughout the transmission system. The fault currents, in many instances, exceed the capability of existing protection systems (circuit breakers) to interrupt the faults safely and reliably, as well as threaten the safety of electric equipment and utility personnel. Consequently, a utility must upgrade these breakers and equipment or reconfigure its system to reduce the available fault current. Both solutions are costly, and frequently reduce system reliability and power transfer capability. Fault current controller (FCC) technology has been identified in the research community as a potentially viable solution for limiting the fault current to the rated short circuit capacity, in order to meet the growing demand for electricity without the costly capital upgrades that would otherwise be required.

1.1 The Short Circuit Problem in Power Systems

Among the numerous faults occurring in power distribution systems, the short circuit fault is, probably, the most destructive one [1]. The short circuit fault can generate fault current more than 20 times the rated current. In less severe cases, the normal power flow is interrupted by the protection circuits, resulting in loss of service, under-voltage or over-voltage transients, and/or loss of synchronization. In the event of a serious fault, an extreme surge of power flowing through the short melts conductors and destroys insulation, which may lead to explosion and fire in equipment containing insulating oil. Moreover, intense magnetic forces imposed on the conductors and their support structures may damage the equipment causing outages and expensive repairs.

Distribution protection systems mainly rely on two customary and proven protection devices. A fuse is a simple, rugged, small and reliable protective device that can be used to interrupt fault currents as high as 200kA. It is a self-triggering device and requires neither sensors nor actuators. A fuse can open in less than half a cycle at current levels that are well under the peak fault current [2], [3]. The major disadvantage of a fuse is being a single-use device, which has to be manually replaced.

A Circuit Breaker (CB) is another proven and reliable piece of protection device [4]. A CB can be "tripped" and reset either automatically or remotely. However, CBs with high current interrupting capabilities are typically bulky and expensive. Furthermore, it is recognized that CBs require periodical maintenance and calibration and have a limited number of cycles of operation.

World economic growth poses a fast increasing demand for electrical power. Higher electrical loads, new consumers, and new distributed generation plants are constantly being added to the power grid. Higher fault current is a logical result of growing capacity of the power grid. The concern is that the expected fault current levels may exceed the interrupting capability of the existing CBs. Failure of protection equipment to interrupt the fault current may cause extensive damage and put at risk the integrity and stability of the power system. Replacement or upgrading of a great number of CBs is a possible, but costly solution to cope with the rising fault current levels. However, the problem extends beyond the cost of the CBs. An upgraded CB allows higher fault current to flow through the rest of the underrated distribution equipment,

which would be subjected to a much higher stress than originally designed for. The high stresses may incur damages even in the case that the CB trips. Furthermore, upgrading the CB to higher currents allows higher energy to the fault. Thus, in the event of the fault, the hazards to electrical installations may become increasingly higher. High fault current can also induce higher voltage in the grounding conductors and reduce the effectiveness of the grounding grid protective function. Thus, safety becomes an issue to consider. An additional concern is that, in certain cases, the mechanical support may need to be reinforced to withstand the higher stresses. Perhaps even the clearances between the conductors will need to be increased. Therefore, along with upgrading the CBs there may be a need to upgrade some other parts of the system as well. However, limited capital budgets may not allow such a massive upgrade of the existing installations.

There are several traditional approaches to suppress the fault current in the distribution systems [5]. System reconfiguration and bus splitting might be preferred for the fast growing areas. This approach comes at the cost of added grid complexity as well as the required switchgears. Another frequently used method is insertion of high impedance transformers or air-core reactors. This, however, breeds inefficiency and degrades the voltage regulation.

An alternative solution to the problem, which has gained much attention lately, is the application of a Fault Current Controller (FCC) [6]-[10], also known as a Fault Current Limiter (FCL). Funded by both government and private companies, research and development activities of various types of FCCs have been reported by many research institutions and private companies in many countries around the world [11], [12]. The recent trends of deregulation and restructuring of the power grid have invoked a renewed interest in innovative FCC technologies for implementation of reliable and economically feasible commercial devices for the grid.

1.2 The FCC Solution

1.2.1 FCC Features and Benefits

Application of FCCs is identified as one potentially viable approach for limiting the fault current to a safe level. An FCC is typically installed in series with the equipment to be protected. Under normal operating conditions, the FCC displays negligible impedance so that the power flow is unobstructed. In the event of a fault, however, the FCC's impedance rapidly increases, which limits the fault current.

An insight into FCC concepts and technologies can be found in several excellent references [13]-[15]. In general, FCCs may be classified by their principle of operation and key technological components used. As reported, FCCs can be implemented with passive non-linear elements, inductive devices, vacuum switches, semiconductor switches, superconductors, as well as their combos. FCCs may also be classified as an un-interrupting type or as an interrupting type. The task of an un-interrupting FCC is limiting the fault current magnitude to an acceptable level, which can be safely interrupted by the existing circuit breaker. An interrupting FCC type can also act as a circuit breaker and interrupt the fault current. Technical feasibility of various FCCs has been already demonstrated with full power prototypes or scaled models.

From literature review, discussions with utilities and FCC developers, it becomes apparent that for an FCC to be commercially successful, it shall have the following desired features.

In the normal state the FCC is expected to:

a) have a low insertion impedance;

b) be able to withstand distribution and transmission level voltage and current rating;
c) have a low voltage drop;
d) have a low power loss;
e) have a low distortion and provide high downstream power quality;
f) have low electromagnetic emissions.

In case of a fault, the FCC is required to:

a) be capable of limiting the first fault current peak;
b) display a large increase of impedance;
c) have a sufficient fault-condition impedance;
d) have an acceptable power loss;
e) tolerate the mechanical stresses;
f) endure the temperature rise;
g) withstand the fault condition for a sufficient time;
h) endure a sequence of recurring faults;
i) be capable of fast transition from normal to faulted state and vice versa.

On a system level the FCC is desired to:

a) be a fully autonomous system;
b) be remotely accessble;
c) operate with minimum down time;
d) have no special current sensors or actuators;
e) have no interference with existing protection schemes;
f) have a high reliability and fail-safe operation.

In order to become a commercially viable, the FCC needs to have:

a) an acceptable size, weight and cost;
b) simple installation;
c) low maintenance requirements;
d) long service life;
e) tolerance for harsh field conditions and weather extremes;
f) compliance with the basic isolation level or lightning tests according to the appropriate standards.

1.2.2 FCC in the Power Distribution System

An FCC can serve different purposes in the power system depending where it is installed. Figure 1 illustrates three possible configurations appropriate for FCC installation [16]. The FCC in position As, marked in Figure 1, can help reduce generator infeed fault currents, prevent transformer from damage, and help reduce the voltage sag on the upstream high-voltage bus during a fault on the medium-voltage bus. With FCC installed in position As, transformers with a low impedance can be used to maintain voltage regulation at a higher power level and to meet increased demand on a bus without CB and power equipment upgrades. An FCC can be installed in the bus tie position B as shown in Figure 1. In the event of a fault in one of buses, the FCC can help maintain the voltage level on the un-faulted one. High capacity is available to both buses resulting in a better transformer rating utilization. Smaller and less expensive FCCs can be installed in the feeder position, as shown in position C, to provide protection to overstressed equipment that is difficult to replace, such as underground cables or transformers in vaults.

Figure 1: Possible FCC positions in power grid.

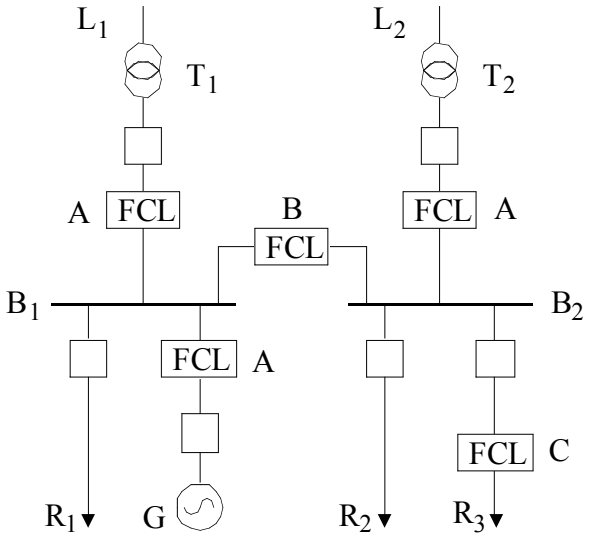

1.2.3 FCC Applications – Simulation Example

Many California and US substations are experiencing a steady increase in electrical loading due to economic growth, introduction of electric vehicles, and proliferation of renewable and distributed generation. In many cases, the substation fault current is approaching or exceeding the capabilities of the existing protective equipment, especially circuit breakers (CBs) with ratings of 63kA. Although 83kA CBs are also available, albeit large, expensive and sometimes difficult to obtain. Changing the power flow by splitting substation buses or reconfiguring circuits is possible, but can negatively impact system capacity and reliability. FCC technology offers a potentially cost-effective solution without degrading system capacity and reliability.

A PSCAD model of a hypothetical 230kV substation is shown in Figure 2. An FCC, modeled after the Zenergy Power HTS FCL, is installed in the feeder position and has a bypass switch. PSCAD simulation was performed with the following parameters: 230 kV Line, I_{peak} = 173 kA, I_{symm} = 63kA, K=173/63 = 2.75 and X/R = 55.06. The simulation results are given in Figure 3. According to the simulation study, the prospective fault current, with FCC bypassed, has 100kA

first peak and 63kA fault levels. Figure 3 shows the effect of an FCC that trims about 18% of the fault current. With such a device the fault current goes down to a safer 55kA level.

This simulation example gives an idea about the required specifications of a transmission level FCC. It is shown that a high voltage FCC, i.e., 66kV and up to 230kV, with 10-15% reduction of the fault current, is a feasible solution to the problem of high fault current. If an FCC proves to be commercially successful, the lifetime of a range of Californian substations with the 63KA existing CB limit can be extended. Keeping these substations operational for another decade or two has significant economic significance.

Figure 2: PSCAD model of hypothetical 230kV substation with FCC protection.

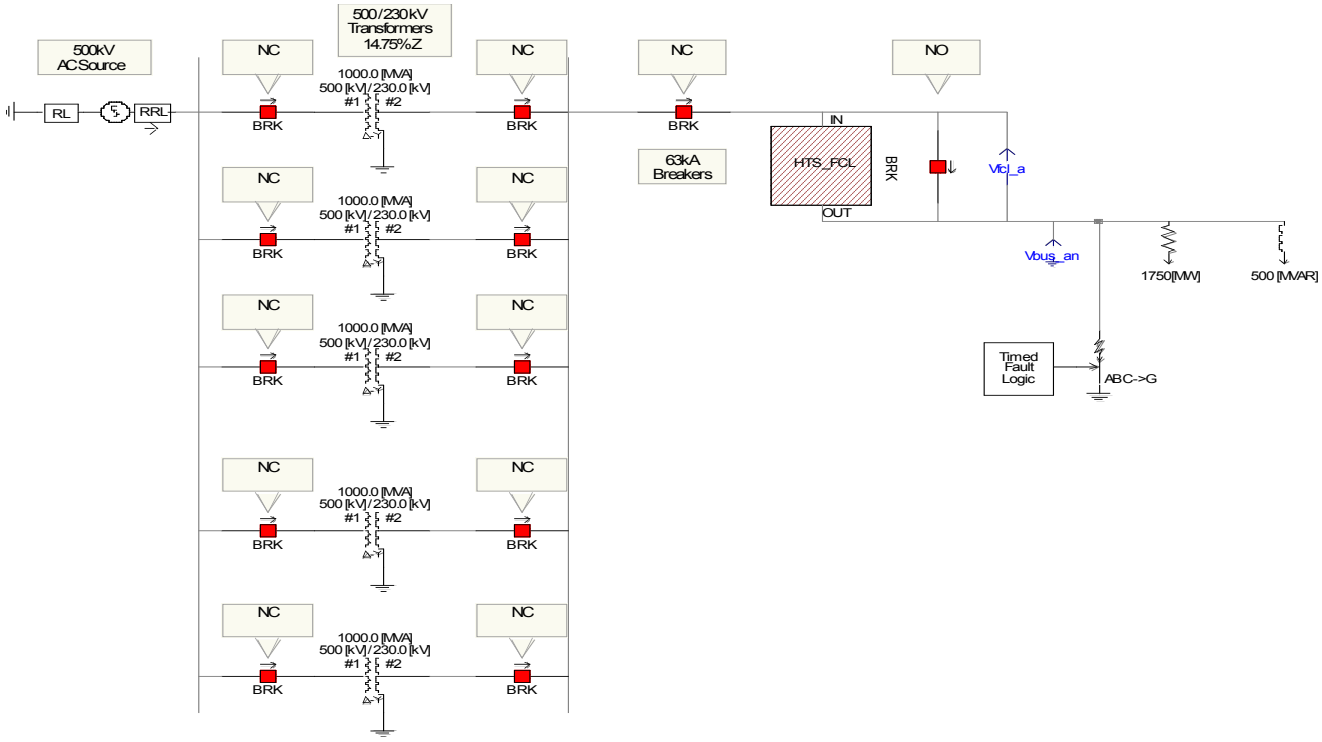

Figure 3: Comparison of PSCAD simulation waveforms of the fault current of a hypothetical 230kV substation with no protection device, with an air core inductor, and with an FCL. (a) top trace: instantaneous line currents; bottom trace: rms currents; (b) expanded view.

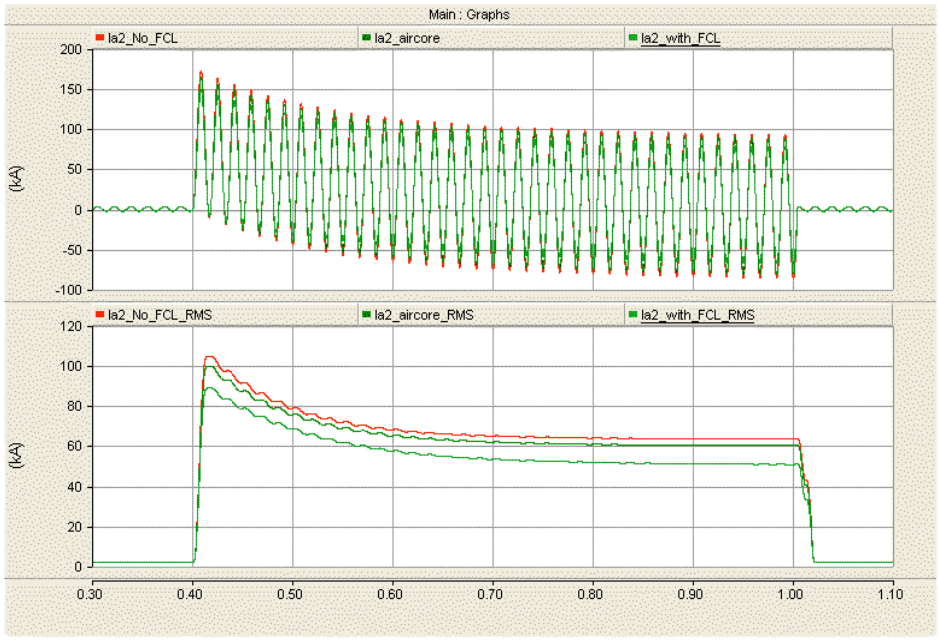

(a)

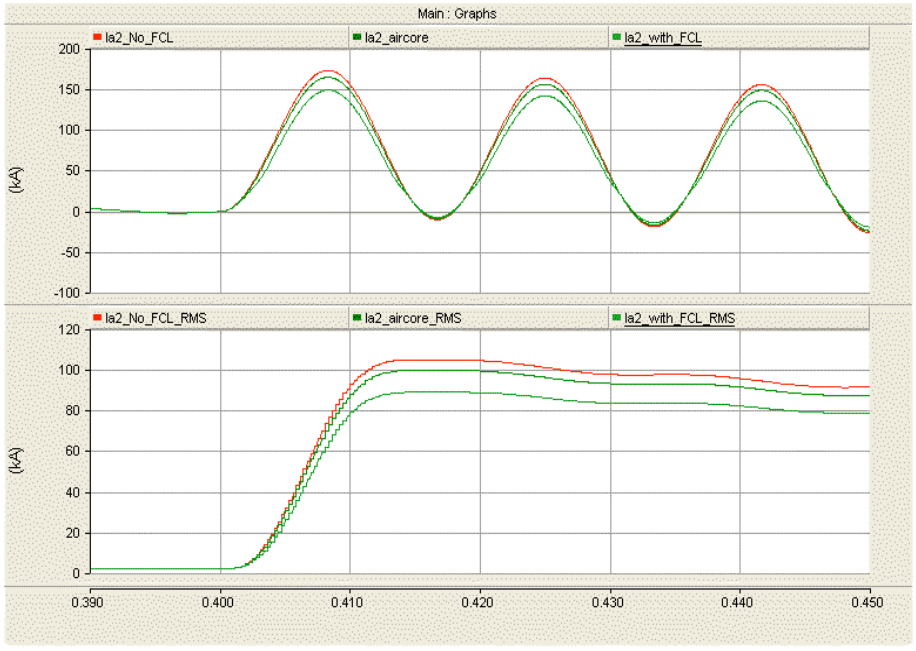

(b)

1.3 FCC Development Objectives

The California Institute for Energy and Environment (CIEE), with the financial sponsorship of the California Energy Commission(CEC), sponsored this project to develop a reliable, cost-effective, and environmentally acceptable technology to equip the transmission grid to handle higher fault currents. The proposed research under this work authorization aimed to establish the desired criteria for fault current controller performance and to test two different leading technologies against the criteria via controlled laboratory testing and field demonstration in an SCE distribution circuit. The objectives of the project are listed below:

1. Establish an FCC test plan including test criteria, test protocol, test site selection, test scheduling, data collection plans, and interface requirements for both the laboratory testing and field demonstration.
2. Prototype two FCCs, one saturable-core type developed by ZenergyPower Inc., and one solid-state type developed by the Electric Power Research Institute (EPRI) and Silicon Power Corp. team.
3. Conduct laboratory testing of the two FCCs against the criteria, including pre-connection high-voltage insulation tests, normal operation tests, and fault current limiting tests.
4. Install the FCCs on the SCE distribution system and perform field demonstration for a minimum of six months.
5. Complete the evaluation of the technologies on the basis of performance, respective strengths and weaknesses, costs, reliability, installation, operation, and maintenance issues, potential for development to high-voltage design.

A research consortium was formed for this project, in which the University of California, Irvine as the Performing Institution was responsible for project management, administration, coordination, and technical guidance; Southern California Edison Co. (SCE) was the host utility for the field demonstration and support; while Zenergy Power and the EPRI/Silicon Power team were engaged to prototype and field test a passive type FCC and an active FCC, respectively. In addition, a Project Advisory Group was assembled with experts from utility companies, national laboratories, regulatory boards, and other relevant organizations to guide the process.

The intended outcome of this project is to facilitate improved, safe and reliable operation of the power system by advancing the FCC technology as a cost-effective and environmentally-preferred option to breaker upgrades or system reconfiguration, and by evaluating the realistic potential of this technology to mitigate fault current levels at higher voltages in the electric system through real-world utility testing. The ultimate program goal is to enable the commercialization of FCC technology for the benefit of California and the United States.

CHAPTER 2:

Technology Survey

This chapter presents an overview of past research activities, recent advances, and emerging technologies of FCCs, and provides brief discussions about the operation principles and main features of several representative FCCs based on solid-state and saturable core concepts.

2.1 Solid-State FCC Technologies

The advancement in high-power semiconductor technologies such as new thyristors, high-power IGBTs, and emerging SiC devices, makes it possible to implement a commercially viable Solid-State FCC. In the following discussion, the solid-state FCC topologies are classified into three major groups: the Series Switch, the Bridge and the Resonant types.

2.1.1 Series Switch Type FCCs

The Series Switch type FCC, illustrated in Figure 4, is composed of a bidirectional controlled semiconductor switch, S_{ss}, and a bypass network. The bidirectional switch may be implemented with various semiconductor devices, whereas the bypass network can be a combination of several parallel branches: the normal-state bypass, S_{bp}; fault current bypass, Z_f; an overvoltage protection bypass, ZnO; and a snubber network. Depending on the FCC's fault response algorithm, the bypass network can be a simple one or sophisticated one.

The normal-state bypass is usually implemented by an electromechanical switch, the purpose of which is to provide a low resistance conduction path in order to avoid the semiconductor conduction losses and waveform distortion in the normal state.

Figure 4: Generic Topology of the Series Switch type FCC.

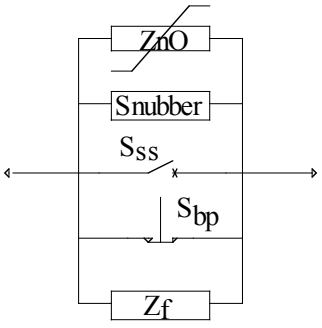

The fault current bypass is employed by the non-interruptive FCCs to restrict the fault current flowing in the power circuit and allow other protection schemes to take appropriate action during a fault. The fault current bypass can be implemented with either resistive or inductive components. The inductive bypass is the preferred solution due to its reduced thermal management requirement. The interrupting FCCs do not need fault current bypass. Some schemes just turn off the switches to interrupt the current, while other designs control the semiconductor switches to modulate the fault current and keep it within the acceptable limits.

While the fault current bypass is optional, the overvoltage protection bypass is a must, which is usually implemented by a high-voltage and high-power zinc oxide (ZnO) varistor or arrester. As the semiconductor switch is commanded to turn off, the varistor provides an alternate current path, while limiting the voltage across the semiconductor switch and absorbing some of the energy stored in the line inductance. In the case where the semiconductor switch is a composite one, the varistors can also be placed across each individual semiconductor device to limit the voltage across the series-connected devices and prevent overvoltage breakdown due to turn-off or turn-on delays.

The snubber network is an important part of the solid-state FCC. The task of the snubber is to limit the voltage rise across the switch at the turn-off instant and keep the dv/dt below the maximum allowed value according to the manufacturer specifications.

The semiconductor switch in Figure 4 can be implemented by SCR [17], ETO [18], GTO [19], or IGBT [20], [21], [22].

2.1.2 Bridge Type FCCs

The bridge type FCCs are realized using a current-fed full bridge arrangement (see Figure 5 (a)). This topology is inherently suited to using diodes as line-commutated switches as well as advanced thyristors. The bridge type FCCs do not have a normal state bypass, may or may not have a fault current bypass, but they do need an overvoltage protection bypass.

In the normal state all the Bridge elements are "on," providing an unrestricted conduction path for the AC current (see Figure 5 (b)). The bridge type FCC relies on the insertion of a DC current source in series with the line, as illustrated in Figure 5 (c). A practical bridge type FCC uses reactors to emulate the current source action. If the bridge is implemented by thyristors or semi-controlled switches, AC current interruption or diversion to a fault current bypass is possible, as shown in Figure 5 (d).

Figure 5: (a) Generic Topology of the Bridge type FCC; (b) Normal state; (c) AC fault current limited by the DC current source; (d) AC fault current limited by the fault current bypass.

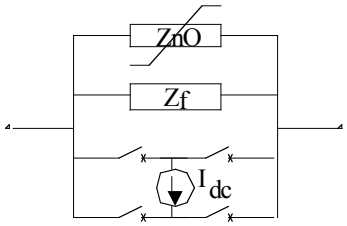

(a)

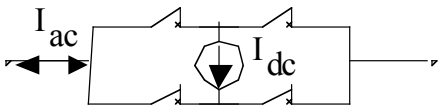

(b)

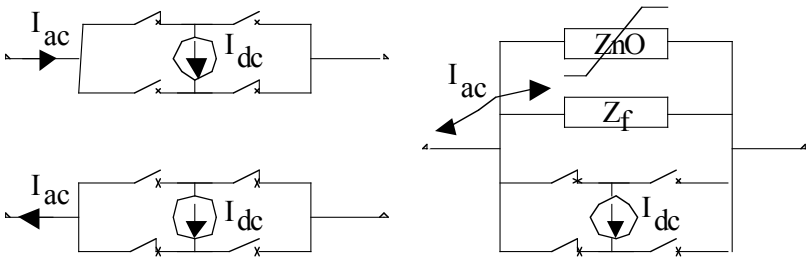

(c) **(d)**

Figure 6 shows an interesting rectifier bridge-type FCC, proposed in [23] and patented in the early 1980s, this circuit has evolved into many derivatives over the years.

Prior to the start-up, the DC bias supply connected in series with L_1 charges the inductor to the DC current to a level that is higher than the expected AC peak current. All bridge diodes are in full conduction and free-wheel the reactor current. Hence, the AC terminals of the bridge appear "short circuited" and present a low insertion impedance. The AC line current splits equally between the bridge legs. Depending on the line current polarity, one diode pair carries the summation current $\frac{1}{2}(I_{dc} + |i_{ac}|)$, whereas the other, differential current $\frac{1}{2}(I_{dc} - |i_{ac}|)$. The equivalent circuit for the normal state as well as the fault condition state are illustrated in Figures 6 (b) and (c). When a downstream short circuit fault occurs, the rising AC fault current exceeds the DC current level. Consequently, the diode pair for the difference current turns off when its current reaches zero. The diode pair for the summation current remain on and steers the line current through reactor L_1. Consequently, the fault current is limited by L_1 allowing the circuit breaker to take a protective action. Upon interruption, the current in the DC reactor freewheels through the bridge and the energy absorbed during the fault is, then, dissipated in the diodes and wiring resistance.

Figure 6: Single Reactor Rectifier Bridge FCC.

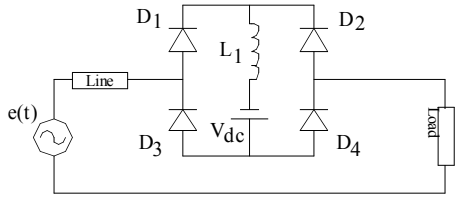

(a)

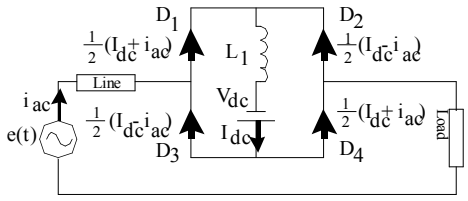

(b)

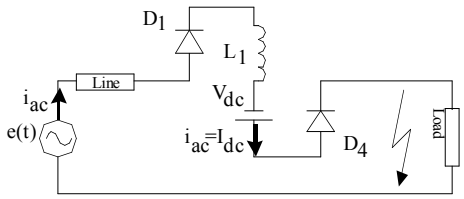

(c)

The advantage of this type of FCC is that neither controlled devices nor a control circuit are needed. Available power diodes have rather high blocking voltage and current ratings. The current rating of the diodes and limiting reactor L_1 is dictated by the peak fault current. Since the current limiting reactor L_1 is on the DC side of the rectifier, during a fault condition the inductor is subject to high DC voltage, which causes inductor current build-up and eventually saturates the inductor. Once the inductor is saturated, the current increases sharply and, thus, the FCC may lose its current limiting capability. Therefore, this type of FCC cannot sustain the fault condition indefinitely, rather it limits the fault current build-up rate, helps to safely ride through faults of short durations and, in the event of a major fault, it "buys a short time" for the circuit breaker to take action. Also, the diodes should be rated to withstand the full fault current magnitude. A clear disadvantage of this FCC is the rather significant conduction losses in normal state operation caused by the constantly flowing high DC current. To alleviate the conduction losses [23] used a superconductive coil as a DC reactor. For this reason the rectifier bridge FCC is sometimes referred to as a "superconductive" type; however, from the operational principle, the superconductive reactor is not a necessary feature.

Another example is shown for a three-phase rectifier type FCC described in [25] as shown in Figure 7. The FCC uses a full-bridge three-phase diode rectifier with a superconductive coil as a DC reactor at the secondary winding of the isolating transformer. The transformer's primary is inserted in series with the line to provide the FCC function. The distinct feature of the proposed FCC is the absence of a DC bias supply. The FCC relies on the rectified grid voltage to charge the DC reactor. Otherwise, the FCC operation principles are similar to that of Figure 6. The transformer isolation makes this FCC suitable for higher voltage applications. Alternatively, diodes with lower voltage ratings can be used.

Figure 7: Transformer isolated Three-Phase Rectifier Bridge FCC.

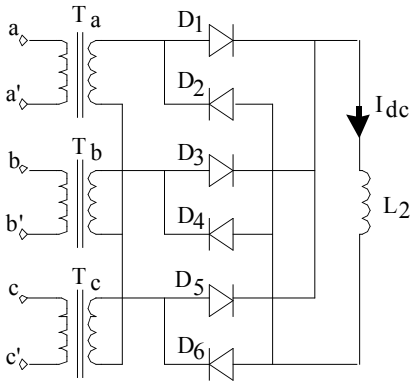

A single-phase SCR bridge-type FCC is shown in Figure 8 [26]. At start-up the SCRs are gated to charge the L_1 reactor with a DC current equal to or higher than a preset peak line current. Alternatively, the charging may be accomplished by using an auxiliary DC supply connected

across L_1. All the SCRs are then gated to remain in full conduction. When a downstream short circuit fault occurs, the rising AC fault current reaches the DC current level. Consequently, the SCR pair, who is carrying the differential current, turns off at zero current, whereas the SCR pair carrying the sum current, remains on and steers the line current through L_1 in order to limit the fault current. Meanwhile, the gate signals to SCRs T_1 and T_2 are removed so that the conducting SCRs extinguish at the zero crossing of the fault current. The gating of T_3 and T_4 remain on to provide a freewheeling path for the L_1 current. In the next half cycle, the fault current flows through the fault current bypass reactor L_2.

Figure 8: Two Reactor SCR Bridge FCC [26].

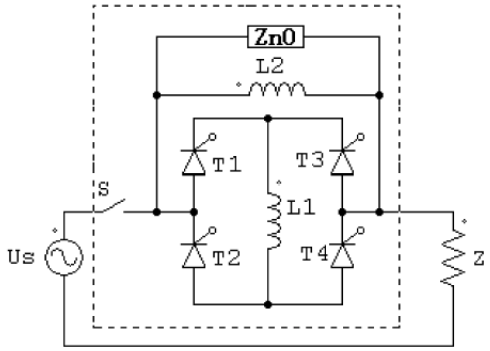

Due to the fact that the fault bypass inductor is subject to an AC voltage, there is no current build-up in the L_2 reactor. Consequently, this type of FCC can endure rather long faults. The fault current bypass reactor L_2 should have a greater current rating than the DC reactor L_1. The later should be designed to withstand only a half cycle of the line voltage. In practice the current in the AC reactor L_2 only lasts for a few cycles until the circuit breaker trips, therefore, L_2 can be designed with relatively small size. Also, since the fault current is diverted to the fault current bypass, the switch current stress is lower. Thus, this kind of FCC exhibits good reliability. In addition, since no cryogenics systems are required, both the initial and maintenance cost of this FCC are expected to be low.

The ZnO arrestor prevents over-voltage protection across the bridge and also provides a discharge path for the L_2 reactor at the opening instant of the circuit breaker.

Many other approaches are reported with half-controlled IGCT switches [27], [28] single switch IGCT bridge [29], [30] , transformer isolated GTO bridge [31], saturable DC reactor bridge [32], GTO bridge with emergency power source function [33], superconducting magnetic energy storage (SMES) system [34], switched-resistance bridge [35], etc.

2.1.3 Some Practical Difficulties of the Bridge-Type FCCs

In each of the circuits above, there exist equivalent resistances R_{dc} and R_{ac} representing the losses of the AC and DC circuits, respectively. These are always present and help dissipate the fault energy. The resistance R_{ac} incurs a power loss only during the fault period, whereas the resistance R_{dc} incurs the loss during the normal state operation as well as during the fault period. Due to the high DC reactor current the DC power loss can be very significant. This

lowers the FCC normal-state efficiency and poses an additional thermal management problem. By adopting a superconductive DC reactor, the DC losses can be significantly reduced, but at the cost of a cryogenic system which requires periodical maintenance.

Furthermore, for proper operation of the Bridge-type FCC, the DC inductor current has to be maintained above a preset peak AC current. Thus, in practice, the inductor has to be recharged in order to compensate for the current decay. Under this consideration, self charging is a prefer approach to the one using an external DC suply. By this approach, as the differential current ceases, one pair of devices turns off and the inductor is inserted into the line for recharging. Since this happens near the peak of the line voltage, the instantaneous voltage drop across the inductor "shaves the peak" of the line voltage and causes voltage distortion. The larger value of the DC inductor , the greater the distortion. Moreover, with a large DC inductor, the Bridge type FCC will have difficulty in accommodating a rapid load increase [35]. Figure 9 shows the line current, I_{ac}, and the DC reactor current, I_{dc}, during the load transient and the steady state conditions. The simulation was performed with PSIM software for the circuit shown in Fig. 19 for a 12kV line voltage and a 1kA load, summing DC reactor of 20mH with 0.1Ω stray resistance. Recharging of the DC reactor introduces a clearly noticeable distortion. The design tradeoff between the power quality in the normal state and fault current limiting performance is alleviated in the designs by having an AC by-pass inductor in addition to the DC reactor with a smaller value.

Better power quality can be obtained by using a DC bias supply, which pumps the DC reactor current above the peak AC line current. This bias supply has to provide a rather significant DC current at low voltage. Several proposals can be found in literature for bias supply implementation [26], [36], [38].

Figure 9: AC line and DC reactor currents of a Bridge type FCC.

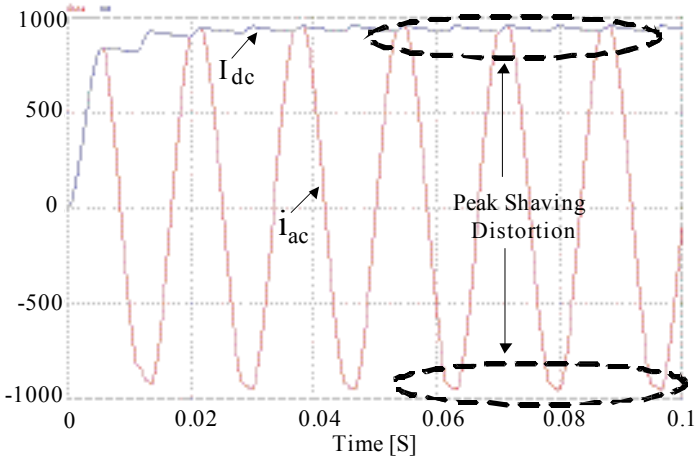

2.1.3 Resonant Type FCCs

Instead of having distinct normal state and fault current bypass elements, the resonant types of FCCs use switches to reconfigure their networks either into the normal state (NS) or into the fault condition (FC) sub-topologies (see Fig. 10). These FCCs employ series resonant circuit (also

called resonant tank) as their normal state bypass. To achieve a near zero series impedance, the resonant circuit is fine tuned to the line frequency. Under the fault conditions, the circuit is switched to the fault state sub-topology and, thus, is out of resonance. Therefore, a much higher impedance is presented to the line. Accordingly, the resonant FCCs can reduce the fault current but do not have interruption capability.

Though the normal state bypass is not a part of the bridge or resonant type FCC fault interruption schemes, some kind of bypass and clear switches should be a part of the FCC installation in order to maintain service in case of FCC malfunction to allow the FCC be taken off the line for maintenance.

Figure 10: Generic topology of the Resonant Type FCC.

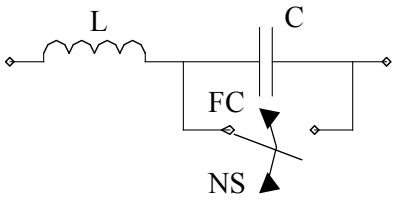

Several interesting FCCs based on resonant circuits and thyristor switches were suggested in [38]-[41]. The presented FCC topologies, see Fig. 11, are some representative circuits found in the literature sources. In the normal state the resonant circuit is tuned to the line frequency thus presents negligible impedance to the line. In an event of a fault, the thyristors are turned on either to introduce a short circuit or to connect an additional component to the resonant circuit, which takes the circuit out of resonance. Subsequently, the fault current is suppressed by the high impedance of the mistuned resonant tank.

Figure 11: Resonant FCCs.

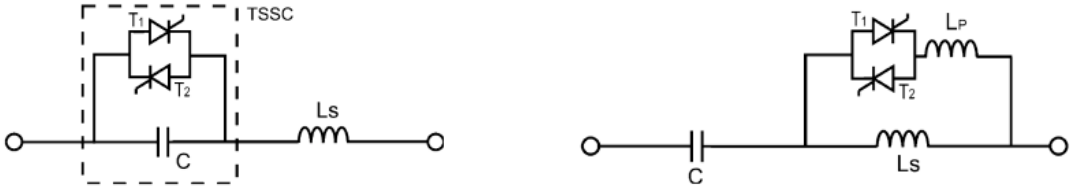

(a) **(b)**

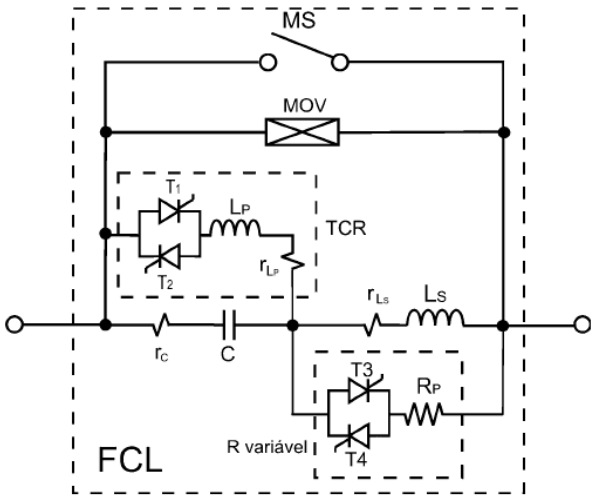

(c)

The advantage of a resonant FCC includes a better power quality and a desirable zero-voltage or zero-current switching operation. Another advantage is that the switches are activated in fault condition only and remain cut-off in the normal state. This contributes to a better efficiency and reliability and relaxes thermal management requirement. However, the resonant circuit may impose a higher peak voltage or current stresses on the semiconductor devices. Fault transients also create over-voltages or sags. Moreover, the capacitor bank size and cost are considerable and require precise tuning.

Another example of FCC proposed in [42] consists of a series inductor and a self-commutated voltage source inverter connected in series with the line by an isolating transformer (see Fig. 12 Not immediately recognized, however, is that this FCC may also be classified as a resonant type. In the normal state, the inverter is operated in a capacitive mode to compensate for the voltage drop across the series inductor. During a fault, the inverter is commanded to emulate a large inductor, therefore impeding the fault current.

Such FCCs can also be beneficially used in the normal state to improve the power quality of downstream voltage by compensating for line voltage distortion and voltage sags [43], [44].

The disadvantage of this approach is that the inverter has to process high current and operate at relatively high frequency using pulse width modulation (PWM) control. Also, conduction and switching losses are considerable. Moreover, the inverter's DC link capacitors have to be of a relatively large value to handle the large amplitude currents while maintaining a moderate DC bus voltage swing.

Figure 12: Inverter Based FCC.

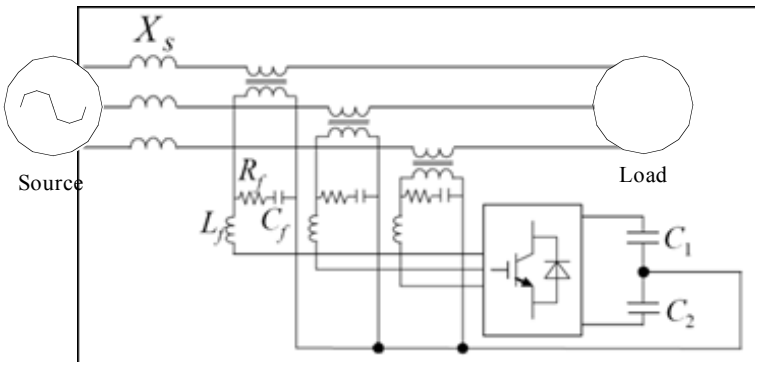

2.2 Saturable Core Fault Current Controller Technologies

Saturable core FCCs exploit the nonlinear characteristics of ferromagnetic materials in order to realize a variable inductance. In essence, such an FCC is just a coil wound around an iron core and connected in series with the protected load. In a normal state, the core is saturated by a dedicated bias circuit. The inductance of the saturated coil and, accordingly, the voltage drop across the coil terminals are negligible. Thus, the coil has no obvious effect on the system. In the event of a fault, the magnetic core is taken out of saturation, exhibiting a high inductance that limits the fault current. This basic principle of "passive" inductive switching can be employed in a variety of ways to realize a saturable core FCC. The designs mainly differ in the core shape, magnetic design, and core bias arrangement.

Many saturable core FCCs also incorporate superconducting technologies and thus are frequently referred to as superconducting. However, the key physical principle of saturable core FCC is the inherent mechanism of impedance change due to magnetic properties, whereas the superconducting part is the assisting technology which aims to enhance performance, such as higher currents, higher magnetic field intensity, reduced power loss, and more compact design, etc.

Saturable core FCC technology shares some commonality with other distribution equipment, such as transformers and power reactors and, to a certain degree, thus is a compatible addition. Particular mention should be made of their ruggedness and inherent ability to quickly react to fault without any detection circuitry. Furthermore, a saturable core FCC presents an inductive impedance to the line during the faulted state. The absorbed energy is stored in the magnetic field and mostly recycled back to the system, which reduces the power dissipation and alleviates the thermal management problems.

Several feasible ideas for implementation of a Saturable core FCC were proposed in literature. According to the reports, the major contributors to the cost of the magnetic FCC are the superconducting wire, the cryostat and the associated cooling, as well as the iron core and copper. One engineering challenge is to minimize the cost of the components in the design that makes the FCC an affordable and commercially viable device for distribution and transmission systems. Another engineering challenge is to minimize the voltage surge induced in the DC bias circuit during the fault. In the following sections, several concepts of saturable core FCCs are reviewed considering the aforementioned characteristics.

2.2.1 Saturable Core FCC by Raju et al.

A basic single-phase saturable core FCC device was patented in the early 1980s [45]. The fundamental structure of this type of FCC is illustrated in Figure 13.

Figure 13: Conceptual structure of saturable core FCC.

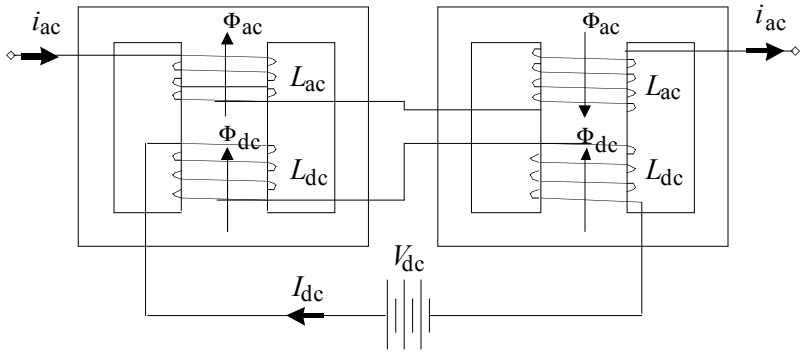

The FCC was constructed around two pairs of iron EE cores. Each EE core has two coils wound around the center limb. The AC coils were conventional copper coils connected in series differentially and inserted into the AC line in series with the protected load as shown in Figure 14. The DC bias coils were wound on top of the AC coils and fed by a low voltage, high current DC power supply. With superconducting (SC) wires, the DC coils impose zero resistance to the bias circuit. Hence, the bias current was limited only by the internal resistances of the power supply. This allowes attainment of high DC current, generation of a strong magnetic field and saturation of both cores efficiently.

Figure 14: Connection of a Saturable Core FCC.

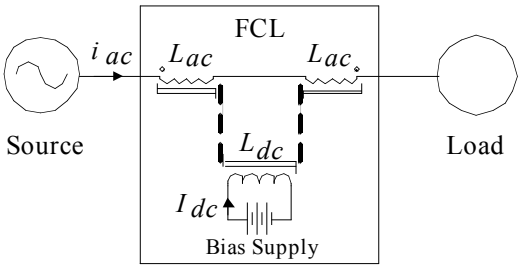

The principle of operation of this device is described here considering the magnetomotive force (mmf)-flux relationships. By regulating the DC coil current, the mmf-flux operating point of both cores is established in the vicinity of point B (see Figure 15). As the AC line current flows through the AC coils, the core operating point is shifted. Due to the differential connection of the AC coils, the AC-induced mmf in one core reinforces the DC mmf; whereas in the other core, the AC mmf weakens it. Therefore, the operating point of one core shifts into a deeper saturation, point A, whereas the operating point of the other core moves towards shallow saturation, at point C, closer to the hysteresis knee point. In the normal state both cores remain in saturation so that their combined inductance is low. When a fault occurs, the abnormal amplitude of the fault current is capable of driving the core with the counteracting mmf out of saturation into region C-D of the hysteresis curve. Here, the permeance of the desaturated core sharply increases, resulting in a considerable increase in coil inductance and, consequently, higher impedance, which limits the fault current. Depending on the AC line current polarity, the coils alternate in and out of saturation to limit the current in each half cycle.

Figure 15: Illustration of Saturable Core operating points.

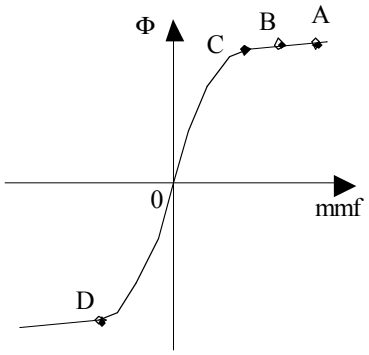

The FCC inductance may be characterized as function of the AC current amplitude as shown in Figure 16. The current threshold value, I_{knee}, corresponds to the operating point C whereas, the value I_{max} corresponds to the operating point D. As the current amplitude is increased above I_{max} the core enters reverse saturation region left of D. As a result, at current levels above I_{max}, FCC inductance falls back to the low value. Therefore, I_{knee} defines the highest normal current amplitude, above which the FCC current limiting commences, whereas, I_{max} defines the current level, above which the current limiting effect is lost.

The advantages of this approach include simple and symmetrical core design, ruggedness and fail-safe operation. However, the designer's choice of two E cores per phase, each with coils wound on the center limb, makes it difficult to implement a compact distribution-level three-phase FCC, since it requires a battery of six cores, stationed apart from each other with a safe clearance. Aside from its bulky size, the cryogenics design is challenging. The original design used a quite bulky liquid nitrogen cryostat to chill the superconducting DC coils. FCCs of higher power rating may have larger dimensions so that each core may have to be provided with a dedicated cryostat and superconducting DC coil.. Another problem with this magnetic design is the transformer coupling between the AC and DC coils in the faulted condition. The high voltage across the AC coil may induce a large voltage in the DC coil and cause destruction to the DC power supply. As a protective measure, a resistor in series with the DC coil was used, causing high losses in the bias circuit.

Figure 16: Saturable Core FCC inductance as function of the current.

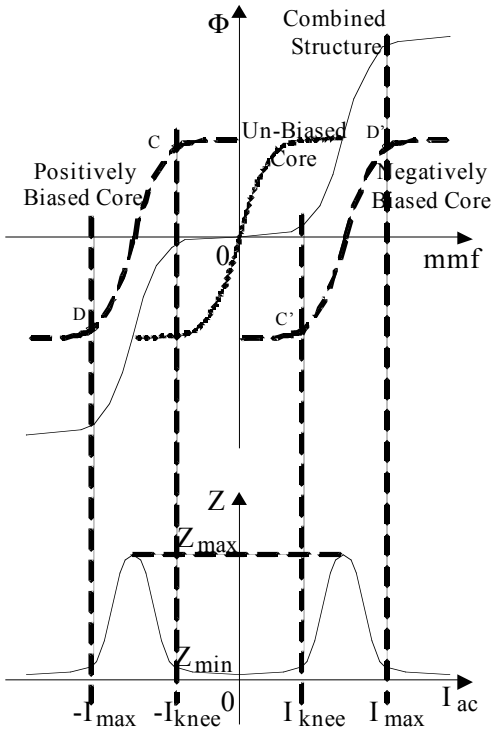

2.2.2 Saturable Reactor Limiter for Current by Oberbeck et al.

A saturable reactor limiter for current proposed in [46] actually preceded that of [45]. The structure of a bipolar, single-phase FCC is shown in Figure 17. The FCC is constructed using a core with four limbs. The first limb is gapped. The DC bias coil is wound on the second limb. The AC coils are wound on the third and fourth limbs and are connected in electrical opposition in series with the protective load. The DC bias current of the DC coil induces a DC flux which drives the core into saturation. In a normal state the AC current is insufficient to desaturate the core so the AC coil inductance is low. Under the fault condition, the high fault current generates mmf of sufficient intensity to overcome the DC bias mmf and desaturate the AC limb carrying counteracting mmf. The increased AC coil inductance during the fault condition limits the fault current.

The major advantage of this magnetic structure is that in the faulted state the AC flux desaturates one limb and then flows through the gapped limb rather than through the strongly saturated DC coil limb. In consequence, the AC flux is diverted from the DC coil. This results in significant reduction of the coupling of the AC coil to the DC coil. Therefore, under fault conditions, this FCC has a reduced voltage surge in the DC winding.

Figure 17: Saturable Reactor Limiter for Current [18].

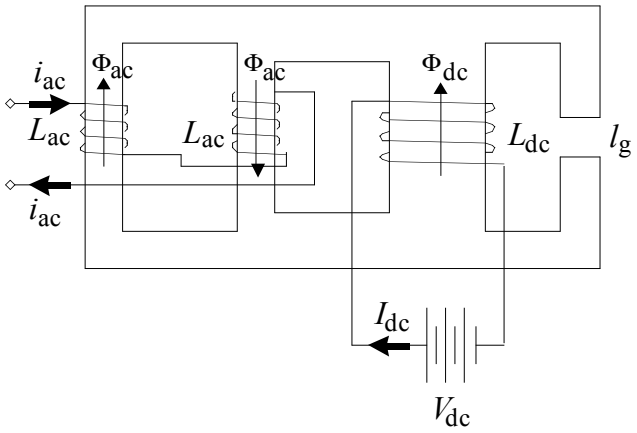

The major disadvantage, however, is the significant power loss of the bias circuit, since an ordinary DC coil was used. The resulting DC coil temperature rise restricts the bias current level and, accordingly, the attainable mmf. Furthermore, assuming that the AC coil limbs and the gapped limb are of the same cross-section, in order to keep the AC limbs in deep saturation, with same flux density, the cross-section of the horizontal segments, between the DC limb and the AC limb, is required to be twice the cross-section of the AC limb, whereas the cross-section of the DC limb must be two, and up to three, times the cross-section of the AC limb. As a result, the FCC has a complicated core structure that is difficult to build. Thus, the achieved DC-AC coil decoupling comes at the cost of additional core volume and weight as well as production complexity and cost.

No suggestion was made in the article regarding how to construct a three-phase FCC. One possible solution is to put together three single-phase units. Another, seemingly possible, solution is to extend the magnetic core so that two additional pairs of AC limbs could be fitted for each phase. In the latter case, only a single bias DC coil is needed; however, the core structure becomes even more complicated.

Another disadvantage that can result from the asymmetry of the core is unequal I_{knee}, I_{max} and Z_{max} values for the positive and negative current paths.

2.2.3 Magnetic-controlled Switcher Type Fault Current Limiter by Pan et al.

A single-phase FCC shown in Figure 18 was proposed in [47]. This FCC was constructed with a EE cores having the AC coils wound on the outer limbs with smaller cross section than the rest of the core. The DC bias coil was wound on the central limb. Another added feature is the inductor L_{dc} in series with the DC bias supply. Owing to these two features the operation principle is different from that of the aforementioned FCCs.

The FCC is connected to the line as in Figure 14. In the normal state the outer limbs are biased to saturation, whereas the rest of the core remains in the linear region. This takes place due to the lesser cross-section of the outer limbs. As a result of the saturation of the outer limbs, the inductance of the AC coils and, accordingly, their impedance is very low so that the normal power flow is unobstructed.

Figure 18: Magnetic-controlled Switcher Type Fault Current Limiter.

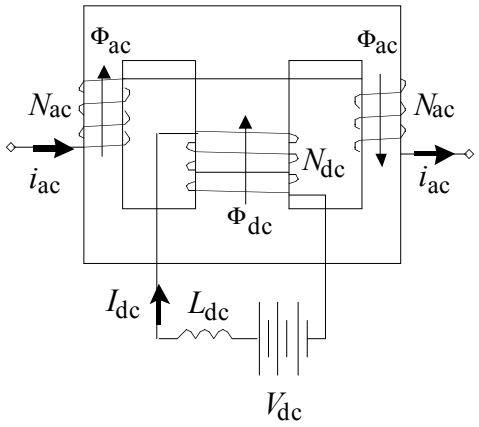

In the faulted state, the large amplitude of the fault current drives one outer limb into deeper saturation, whereas the other is desaturated. Consequently, a closed magnetic path with a high permeance is established providing high magnetic coupling between the desaturated AC coil and the DC coil. Thus, the magnetic structure starts operating as a linear transformer. First, the desaturated AC coil exhibits high inductance and starts acting as transformer primary. Second, by virtue of the transformer action, the impedance of the DC circuit is reflected to the line.

The advantage of selective saturation of the core segments is that the inductance of the DC coil remains relatively large and requires lower bias current to keep the AC limbs saturated. This feature allows an ordinary, i.e., non-superconducting, DC bias coil to be used. Thus, the production and maintenance cost of the auxiliary support systems can be lower. This advantage is offset by the added volume, weight and cost of the core as well as the DC-side inductor L_{dc}.

The fault impedance of this FCC is determined by the impedance of the inductor L_{dc}, reflected according to the turns-ratio of the AC and DC coils, in parallel with the inductance of the desaturated AC coil. The high impedance introduced into the line helps limit the fault current. However, since the reflected and magnetizing impedances appear in parallel, their equivalent impedance is lowered. Therefore, the effectiveness of the method is somewhat offset,so that it requires a higher number of turns of the AC coil. This results in a structure with larger window area, larger core, and higher copper weight. In addition, the higher normal state impedance and, accordingly, causes a higher voltage drop across the FCC terminals.

To saturate the FCC core, it requires an intense mmf, which is achieved by a sizeable number of turns of the non-superconducting DC coil. Therefore, the turns ratio between the DC and AC coils is considerable. As a result, very high voltage is induced in the DC coil under the fault condition. Thus, proper isolation is necessary for the DC coil which further increases the thickness and volume of the DC coil and consequently the window area of the core and the overall core size. Additional concerns are related to L_{dc}. Though the power supply current is limited by the DC inductor, L_{dc}, a high voltage at the DC bias circuit poses a safety issue. All of these are severe disadvantages.

2.2.4 Improved Saturable Core FCC with Magnetic Decoupling by Cvoric et al.

The Current Limiting Device proposed in [46] was further improved by [48] to achieve a better decoupling between the DC and AC coils. The idea here is to interchange the positions of the DC and AC coils shown in Figure 19. The bias coil is wound on an outer limb, whereas the AC coil is wound on a central limb. Otherwise the principle of operation is identical.

The advantage of this magnetic structure is that in the faulted state the AC flux flows through the desaturated gapped limb, positioned further away from the DC coil. Thus, the AC to DC coils coupling is weaker than that in the original structure of [46]. Therefore, this FCC has a greatly reduced voltage surge induced in the DC coil. Note that in the faulted state, the permeance of the AC coil magnetic path is determined mainly by the air gap. The shorter the air gap, the higher the permeance. Thus, the AC coil can be constructed with a lower number of turns, resulting in lower copper weight, lower normal state inductance, lower voltage drop and reduced conduction losses.

However, the need for an additional limb, the asymmetric core structure and the associated iron volume, and the cost remain the main disadvantages.

Another idea for implementing a reduced core volume FCC was presented in [49]. This single-phase FCC was constructed on a pair of EE cores having a deeply gapped middle limb.

Figure 19: Saturation Fault Current Limiter with the Magnetic Decoupling.

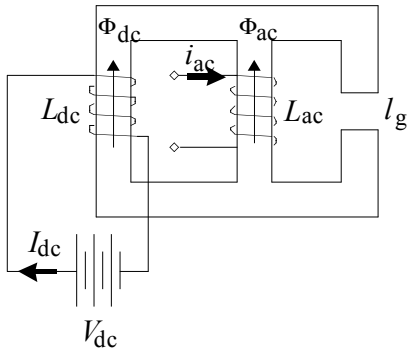

2.2.5 Saturable Core FCC with a Parallel PM Bias

The FCC bias circuit reported in [45] was realized by a superconducting DC coil to allow higher bias current and cut the DC bias losses. However, superconducting wire is one major factor contributing to the FCC cost. The cryostat and DC bias supply both require extensive maintenance and may adversely contibute to the overall system reliability.

A Permanent Magnet (PM) Bias circuit proposed by [50] and [51] can potentially alleviate these problems. Several other derivatives of this idea were also reported. A proof-of-concept laboratory prototype was reported in [51] to verify the idea. The PM biasing structure was installed as the center limb as shown in Figure 20. Since the PM flux is split between two parallel branches, this bias arrangement is referred to as the parallel PM bias. The advantages of the approach include lower cost, lower volume of the device, ruggedness, and higher reliability. The disadvantages of PM bias FCC are the lower field intensity and PM demagnetization.

Figure 20: A Parallel biased PM FCC [22].

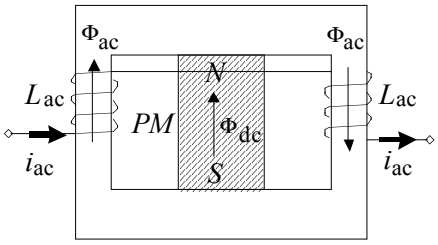

2.2.6 A Series Biased PM FCC

A single-phase 400V/63kA FCC using a different operating concept and magnetic design was experimentally demonstrated by [53]. The structure of a series PM biased FCC is shown in Figure 21 (a). In this design the PMs were inserted as segments of a "C" iron core.

Figure 21: A series biased PM FCC (a); in the normal state the PM material operating point circulates along the minor loop, whereas in the faulted state a major loop in the B-H plane is traced (b).

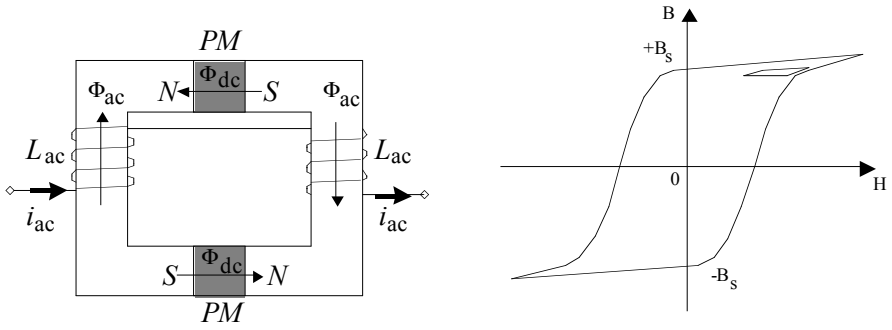

(a) **(b)**

The principle of operation of such a device exploits the hysteresis property of the PM material. In the normal state, due to the lower current amplitude, the magnetic field strength is decreased before the flux density reaches B_s, so the operation follows a minor loop (see Figure 21 (b)). Regardless of the polarity, a high fault current in the AC windings will cause large variations in magnetic field. Consequently, the material will trace the major loop. An operation following the minor loop incur low flux density variations and low losses, whereas greater flux variations occur and much energy is dissipated when it follows the major loop. Thus, in the faulted state, the FCC's inductance and the equivalent series resistance increase considerably. The design challenge of such an FCC is to minimize the losses and voltage drop across the FCC terminals in the normal state, while attaining a large voltage drop under the fault condition.

The advantages of a series PM FCC are that only one core is needed to implement a bipolar single-phase FCC, whereas a battery of three cores is needed for a three-phase FCC. Neither superconducting coil, nor cryostat, nor bias power supply are required. Implementation of the

idea results in a more compact, smaller size, lower weight, all passive, and more reliable FCC that, potentially, can operate in harsh weather conditions with minimum or no maintenance.

The disadvantages of the approach are that such an FCC has higher normal state voltage drop and power dissipation due to the PM's core hysteresis and eddy current losses. To minimize the eddy currents the PM was constructed by stacking several insulated disks. Another disadvantage of this FCC is that it cannot limit the first peak fault current. The reason for this is that the initial fault current surge may take the PM material from a point of normal saturation along the minor loop towards the deepest saturation point of the major loop lying in the same quadrant of the B-H curve (see Figure 21 (b)). Along such a trajectory the relative permeability is low. As a result, the FCC's AC coil inductance remains low, which may not clip the first peak of the fault current. Also, in consequence of the fault, the PM may need some time to cool down before resuming a normal state function.

Additional handling and mechanical construction problems will arise due to the natural tendency of the PMs to repel each other and attract other metal objects.

2.2.7 A Three-Material Passive dI/dt Limiter by Young et al.

Another idea of a PM-biased FCC was presented in [54]. The idea here was to employ a PM bias concept and to keep only some parts of the core segments saturated as shown in Figure 22.

The core of the device consists of four AC coils connected in series. Each coil is wound on a low saturation density core material segment and biased by a PM. Both high permeability and high saturation flux density core segments are placed at the corners so as to provide a closed magnetic path.

In the normal state, the PMs have sufficient intensity to saturate the low saturation density segments. With cores saturated, the inductance of the coils is low. The high saturation flux density material at the corners remains unsaturated, and it allows flux bending. As a result, the flux is confined to the device and the flux leakage is minimized. This results in a more uniform flux distribution in the saturated segments of the core. As the fault occurs, the larger current of an appropriate polarity induces an opposing mmf which reduces the flux density in the core. Consequently, the low saturation flux density segments are desaturated and the coil presents a higher inductance.

However, in view of the previously mentioned drawbacks of PM bias and a relatively large number of components and the complexity of this design, this FCC structure appears as a less attractive option.

Figure 22: A three-material passive dI/dt limiter.

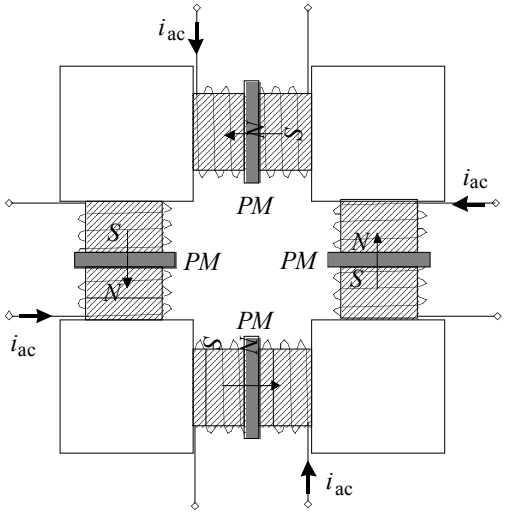

Another PM-biased FCC exploiting the same concept, but with a simplified design, was presented in [55]. An "EE" magnetic structure has a center limb made of a low saturation density material with a PM inserted in the midst of the limb. The rest of the core segments were of a high saturation density material. The AC coil is wound on the center limb as shown in Figure 23. With a reduced number of components, this design can be constructed more conveniently and, thus, it is better suited for implementing a practical device than the previous one. Yet, a common weakness of the series PM bias FCCs is that the resultant mmf always passes through the PM causing elevated losses and demagnetization of the PM core.

Figure 23: A three-material magnetic current limiter [27].

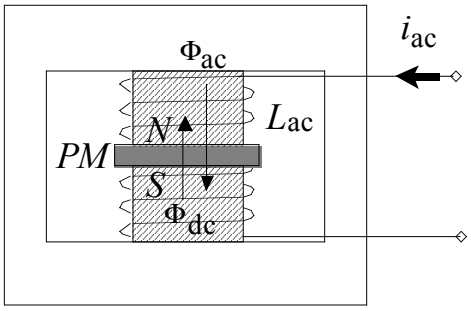

2.2.8 Saturated Open Core FCC by Rozenshtein et al.

The structure of the Saturated Open Core FCC [56] is shown in Figure 24. This FCC presents an original idea different from all of the above. The DC bias coil is wound on the narrow segment of a closed, strongly elongated "CC" type magnetic core. The AC coil is wound around the core so as to engulf both elongated segments of the core. Owing to this magnetic design the core provides a closed magnetic path for the DC bias flux; however, it appears as an open core for the AC coil.

The high permeability closed magnetic path can be easily saturated by moderate amplitude DC bias current. Notice that the "go" and "return" DC flux are flowing in opposing directions through the midst of the AC coil. Regardless of the AC current polarity, the induced AC flux reinforces the DC flux in one segment and counteracts the DC flux in the other segment of the core. In a normal state the AC flux is low, so all the segments of the core remain saturated and the AC coil acts as an air core inductor. As a result, the inductance of the AC coil is low. In the event of a fault, a large AC current is capable of desaturating the core segment carrying the counteracting flux. Thus, the AC coil appears as having a high permeability open core and, consequently, a larger inductance.

A clear advantage of this FCC is that only one magnetic core and one AC coil per phase are required. A three-phase FCC requires a bank of three cores, roughly half the size of the previously mentioned FCCs. A single DC coil may serve all three cores. Furthermore, making the DC coil superconducting helps improve the bias circuit performance and reduce losses. Such an approach enables decreasing the volume, weight and cost of the FCC and allows for a compact design with tunable limiting factors.

Another important advantage of this FCC is the decreased coupling between AC and the DC coils. This comes as a result of the orthogonal arrangement of the DC and AC coils.

Figure 24: A Saturated Open Core FCC.

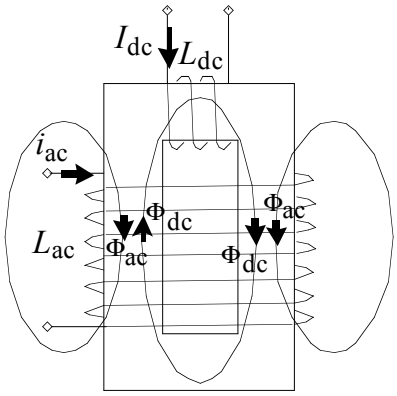

2.2.9 Bias Power Supply Issues

Low voltage, high current DC bias supply is required by most of the Saturated Core FCCs, the exception being the PM-biased FCCs. The bias circuit can be either a simple unregulated or phase-controlled rectifier bridge, or a switch-mode power supply. A clear advantage of the regulated supplies is the option to preset the fault current magnitude by readjusting the bias current.

A switched mode supply is the preferred solution due to its much higher efficiency. An example of the switched mode bias circuit is shown in Figure 25. The circuit can be recognized as an inverted Buck chopper fed by a three-phase rectifier [57]. Here, the superconducting DC coil is employed as the buck inductor. The large DC coil inductance helps in attaining low bias current ripples. The chopper is duty-cycle-controlled to provide precise regulation of the average DC coil current.

Figure 25: DC Magnetization System for a 35 kV, 90 MVA Superconducting Saturated Iron-Core Fault Current Limiter [28].

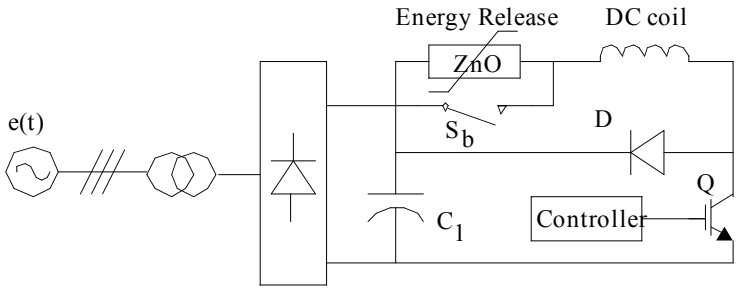

A serious concern, common to the DC biased Saturated Core FCCs, is the voltage surge across the DC bias coil [58]. The surge may occur as the AC coil comes out of saturation and as it establishes a linear operation regime in the core, which may induce a very high voltage surge on the DC coil. Since the number of turns of the DC coil is greater than that of the AC coil the problem is quite serious and may result in breaking the electrical insulation of the DC coil, damaging the bias supply, burning out the superconducting wire, and destroying the cryostat.

One possible solution to the problem was proposed in [45] using an ordinary series resistor. This, however, incurs a huge DC power loss. An energy release ZnO resistor installed in series with the DC coil was proposed by [57] as in Figure 25. In the normal state the energy released by the ZnO resistor is bypassed by a switch to help improving the efficiency of the bias circuit. As the fault occurs, the bypass is opened so the DC coil current is diverted to the ZnO arrestor which absorbs the energy while keeping a constant voltage across DC coil terminals. This helps protect the coil and bias supply circuitry from the induced voltage. The disadvantage of the approach is that fast active control of the bypass switch is required.

Another approach was proposed by [59], where a low turn number non-superconducting suppressive winding, L_{aux}, was wound on the DC bias limb and electrically connected in parallel with the superconductive bias winding, L_{dc}, as shown in Figure 26(a). In the normal state the DC bias current flows mainly through the superconducting winding due to its zero resistance. Under fault condition, however, the terminal voltage of the two parallel windings is determined by the low-turn number suppressive winding so that the surge voltage across the coil terminals is effectively reduced. The disadvantage of this approach is that though the resulting terminal voltage is low, still, through the transformer-like action, the AC induced voltage contributes to elevate the current in the bias circuit.

Figure 26: A parallel Overvoltage suppression winding configurations: parallel (a); shorted (b).

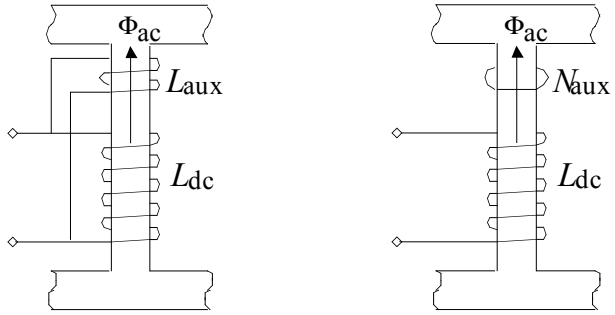

(a) **(b)**

An interesting idea was proposed in [46]. In order to protect the DC coil from the induced AC flux a shorted winding was added on the DC bias limb (see Fig 26(b)). The shorted winding has no effect on DC operation, however it reacts on the AC flux. A current is established in the short which, by the Lenz law, creates a counteracting flux and reduces the undesirable AC flux in the DC limb. This appears a good solution to the problem. However, [46] provides no report of experimental verification of the effectiveness or limitations of the proposed method.

2.3 Summary

This chapter surveyed Solid State and Saturable Core Fault Current Controller technologies for AC power systems and reported on recent research work done in this area. Notwithstanding the fact that the research and development of FCCs has been going on for many years, diversity of FCC concepts is still rather limited. Seemingly, much of the effort has been dedicated to optimization of components, improving the efficiency and reducing the cost of a limited number of basic ideas.

Experimental FCC systems described in this survey indicate continuing progress in this field. However, a practical, efficient, reliable and economically feasible device, suited to utility needs, has remained elusive.

The main challenge for the Solid State FCCs is related to the insufficient voltage and current ratings of existing semiconductor devices, which are much lower than needed for operation in transmission and distribution power systems. Thus, stacking is required, which gives rise to voltage sharing problems.

The difficulties with the Saturable Core FCCs are related to the magnetic coupling and, more importantly, to the high volume, weight of the devices. This challenges the commercial viability of these FCCs.

Nevertheless, innovation in FCC technologies is continuing. Two promising technologies, a saturable core, passive type of FCC by Zenergy Power and a solid state, active type FCC by EPRI/Silicon Power, were the focus of this project and thoroughly investigated for further development. The following chapters provide a detailed report on the results of these investigations.

CHAPTER 3:

EPRI/Silicon Power Fualt Current Controller Development

3.1 EPRI/Silicon Power Solid State Current Limiter Concept

EPRI/Silicon Power based their FCC on their Solid State Current Limiter (SSCL) design using the Super GTO (SGTO) thyristor technology [60], [61] with a modular approach. A Standard Building Block (SBB) was developed that can be stacked in series and in parallel to attain the desired voltage and current ratings. The power train of a single SBB is illustrated in Figure 27. SBB includes a main SGTO switch, auxiliary commutation circuit, fault bypass current limiting inductor and an overvoltage bypass varistor/arrestor. The main SGTO switch is composed of anti-parallel connected SGTOs. The commutation circuit consists of auxiliary SGTO switch and a series resonant commutation network.

In the normal state the main GTO switches are gated "on" to carry the line current with only a negligible voltage drop across the switches. In the event of a fault, the auxiliary circuit is activated in order to provide low stress turn off of the main switches. The high switching speed and superior di/dt capability of the auxiliary SGTO allows the commutation circuit to apply a high amplitude, short duration resonant current pulse to the conducting main switch in order to reduce the current of the main switch to zero at the turn off instant. Thus, a reliable turn off of the main GTO switches is obtained which significantly reduces the switching losses of the main switches. After the main switches turn off, the commutation capacitor resonates with the line inductance and provides a soft dv/dt transient across the main switches. The switch voltage is allowed to rise until it is clamped by the varistor at 4kV. The varistor then sees the full fault current. However, with 4kV across the current limiting inductor, only a few tenths of a millisecond is sufficient for the current limiting inductor to take over the current and the varistor becomes inactive. Henceforth, the fault current is limited by the inserted current limiting inductor. PSCAD software was used to simulate the SSCL. Principal waveforms of the simulated circuit are shown in Figure 28.

Figure 27: SSCL Schematic.

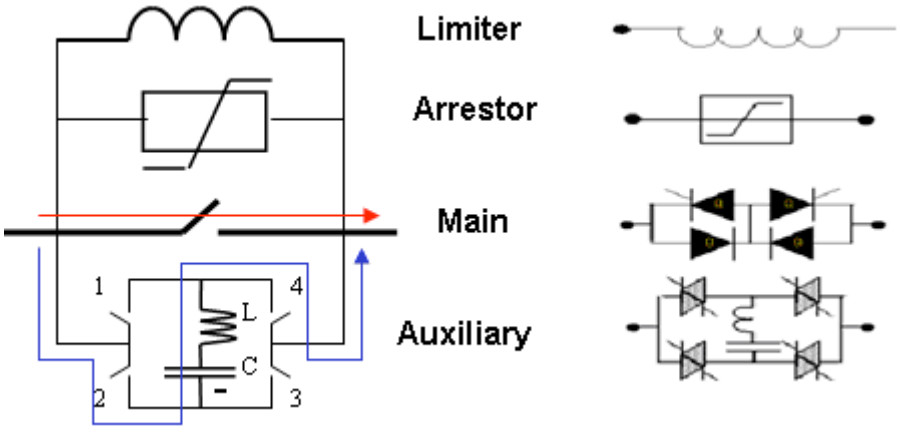

Figure 28: Simulated waveforms of the SSCL circuit.

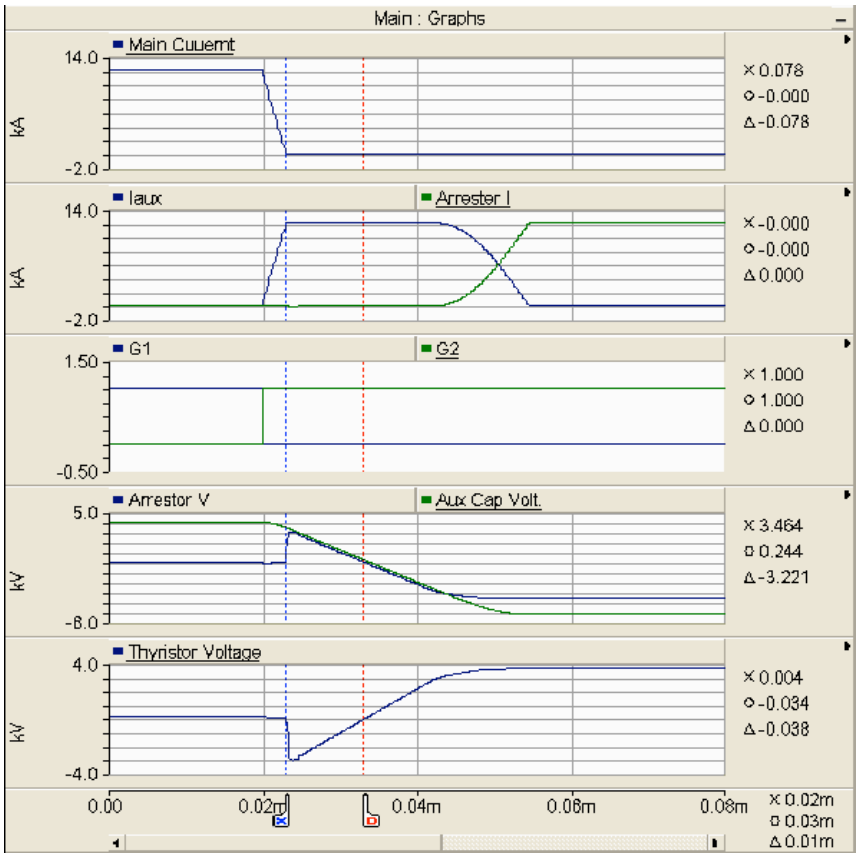

3.2 SSCL Design

3.2.1 Standard Building Block and Standard Power Stack

In order to facilitate manufacturing and to reduce the maintainability and the ownership cost of the unit, a modular approach with standard building blocks (SBB) is used. Figure 29 shows the SBB design. One SBB contains the complete circuitry represented in Figure 27, including the main switches, auxiliary switches, varistors and the CLR in addition to the control boards. Each of these building blocks is a complete SSCL switch rated up to 2kA and about 5kV blocking resembling a fully functional SSCL. The number of series levels required is determined by the breakdown voltage of the main switch modules and the arrestor voltage. The current limiting reactor (CLR) is chosen based on the fault current requirement of a particular unit.

Ten SBBs will be connected in series to form a standard power stack (SPS) for a complete single-phase 15kV, 1200A unit. A prospective view of an SPS with 10 levels in series is shown in Figure 29. The CLR chosen for the required 9kA let-through current rating is 142μH.

Figure 29: Standard Building Block (left), Standard Power Stack (right).

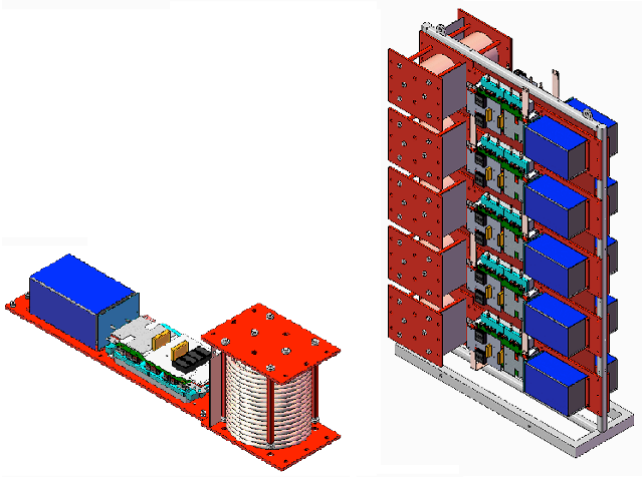

3.2.2 Final assembly

To manufacture a complete distribution level SSCL, a multiple of the SPSs are packaged into a three-phase unit as shown in Figure 30. The housing encloses the power modules, current limiting reactors, bus bars and manifolds. They will be assembled in a tank that has cover-mounted primary and secondary bushings and a provision to connect directly to the overhead utility power lines. The tank will be made of 3/8" steel and will have sufficient mechanical strength to withstand environmental conditions for the expected service duration. The tank includes accessories such as liquid level gauge, liquid temperature gauge, pressure vacuum gauges, pressure-relief device, control cabinet mounting, and cooling radiators.

Figure 30: A view of the SSCL Assembly and its accessories.

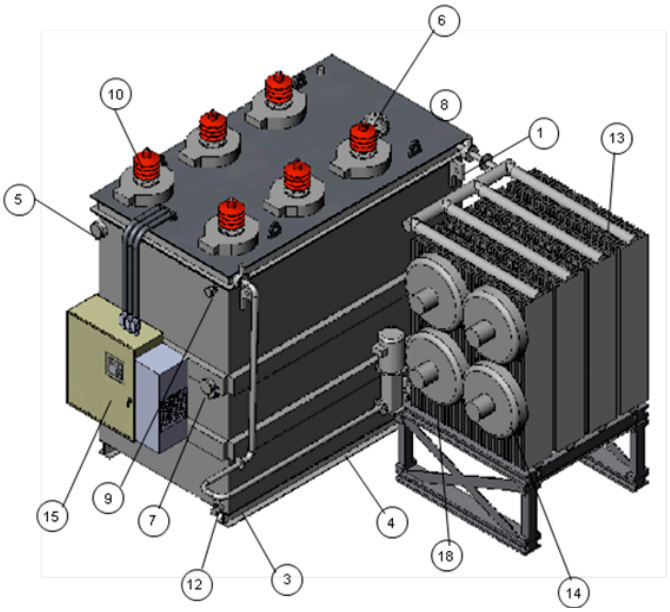

1. Lifting Hooks for Complete Unit
2. Lifting Hooks for Tank Cover
3. Tank Grounding Provisions
4. Transformer Base
5. Liquid Level Gauge
6. Pressure Relief Device
7. Dial Type Thermometer
8. Gas Relay
9. Pressure Gauge with Bleed Valve
10. Bushing
11. Drain Valve
12. Filler Valve
13. Radiator/Heat Exchanger Assembly
14. Cooling Fans
15. Control Cabinet
16. Inert Gas Cabinet (Nitrogen)
17. Current Transformer
18. Oil Circulation Pump
19. Shut-off/Isolation (valves)

3.2.3 Thermal Design

The 15kV 1200A SSCL is designed for outdoor substation use and follows the IEEE Standard for Standard General Requirements for Liquid-Immersed Distribution, Power, and Regulating Transformers (C57.12.00). The overall package is similar to a standard substation transformer tank with an external radiator bank. Immersing the system in a mineral oil dielectric fluid provides a high degree of electrical protection. The radiator bank is connected to a series of cold plates that are located directly underneath the power electronics devices. The cold plates provide highly efficient, directional cooling with a reduced coolant flow rate and pump size. The coolant chosen for the system is the same mineral oil as for the bulk tank. This reduces the chance of incompatible fluids mixing. The tank design is such that all of the power electronics will be immersed in Crosstrans 206 mineral oil as a dielectric. The same type of fluid will flow in a closed circuit to cool the power electronics devices via the cold plates. The radiator bank will provide cooling of the tank by use of forced air cooling from external fans.

3.2.4 Controls Design

The SSCL is designed to operate primarily from a remote operator interface. It also has the ability to be operated locally. The controls can provide ON/OFF controls, equipment protection, display and monitoring of operating parameters, a fault log, access protection, e-Tagout, and safety padlocking, among others. The SSCL controls will provide a trip free feature where any close signal will not inhibit the SSCL from opening upon command.

The control hardware is divided into two groups as shown in Figure 31. First the device level, incorporating all device level controls like gate drives, sensing and device protection. Above that is the system level mater controller, consisting of all system level controls like display, data acquisition, Local Operator Interface or human-mchine –interface (HMI), supervisory controls, data storage and retrieval. The communication between the two tiers is via fiber optic cables, which provide galvanic isolation and noise-immunity; both are critical for proper functioning of the controls. The system controller is built around a Schweitzer controller. The selection of this particular controller technology is based on the performance requirement, complexity, reliability, and cost.

Figure 31: SSCL Control Architecture.

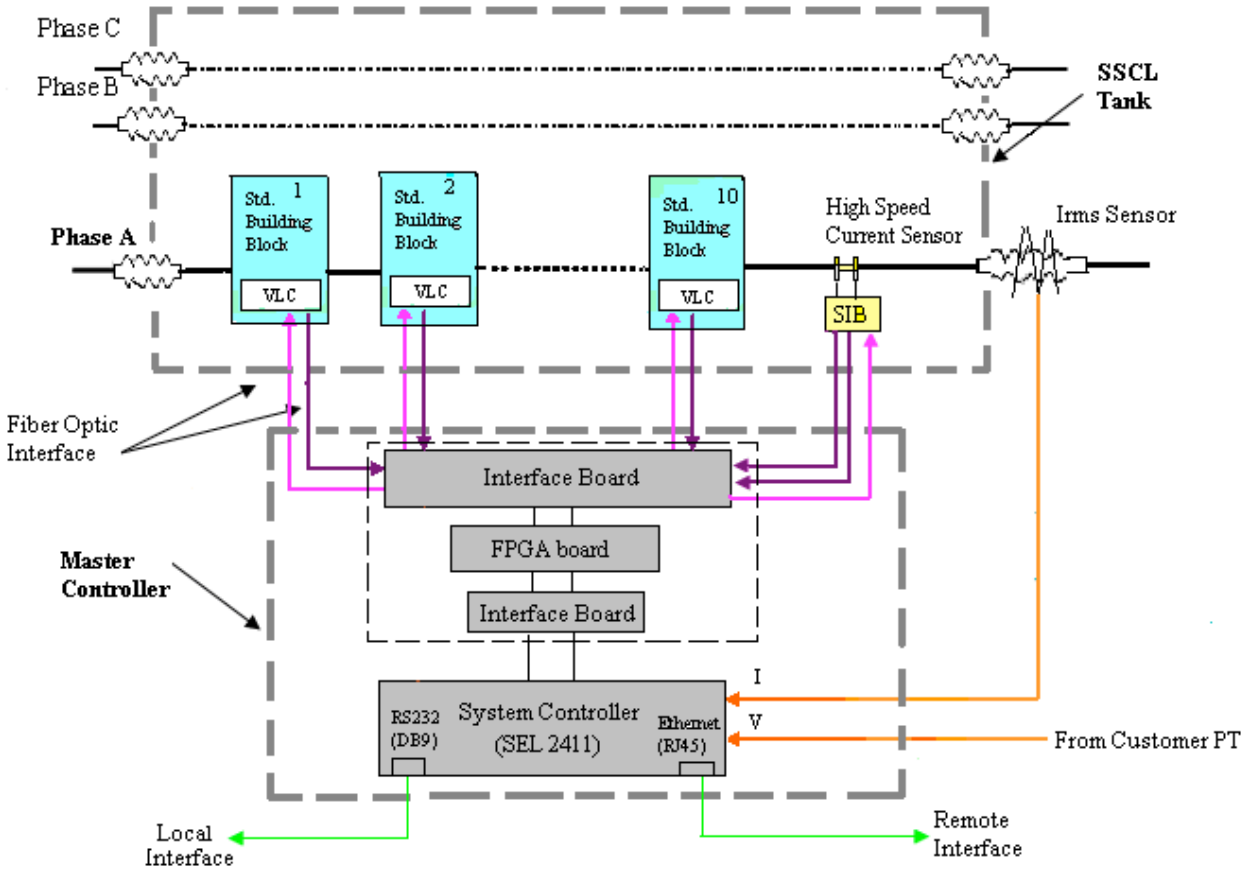

The Schweitzer system controller is an off-the-shelf controller (see Figure 32), which can provide manual ON/OFF controls, equipment protection, display and monitoring of operating parameters, local and remote interface and access protection. It also facilitates the IEC-61850 standard protocol communication. The monitoring functions are performed by using the inputs from the CT's and PT's.

Figure 32: Industrial Panel Mount Controller.

- Utility Grade
- Schweitzer (SEL) make, Model #2411
- Microprocessor based
- LCD Display
- Touch Pad
- **IEC 61850 Protocol Compliant**
- Designed for Indoor/ Outdoor use
- Type tested to sections of C37.90, IEC 60255, IEC 60068 and IEC 61000 standards

3.2.5 SSCL Design Changes

The design of the SSCL has evolved over the course of the project. Some of these design changes were required for the operation of the system. Others were to accommodate a particular mode of operation or to use a specific mechanism to fulfill a given role. The main areas affected by these design changes were the thermal management system and the control boards. These design changes, and other material cost changes, led to an overrun in the estimated material budget for construction of the SSCL. Details of these design changes are provided below.

A. Thermal Management System

The original design for the SSCL envisaged the SGTO modules being mounted on heat sinks with dielectric oil being forced over the fins of the heat sinks before returning to an external radiator system to exchange heat with the ambient air. Simulation showed that in this design the SGTO modules would have been operating at different temperatures and experienced different stresses at the two ends of the stack, a less than optimal situation.

The design was therefore adjusted to locate the SGTO modules on cold plates containing a serpentine path in their interior. Oil can be pumped into the individual cold plates to remove the heat generated by the SGTO modules. With the new design the SGTO modules all see the same temperature differential and each SGTO module experiences the same stress, improving the reliability of the system.

The change to the cold plates also reduces the volume of oil required for the closed circuit cooling system and allows the possibility of directing cooling fluid from the manifold to the current limiting inductors.

B. Electrical and Control System

The original concept proposed using a single control board for the standard building block, combining both power and controls. As the project progressed, the decision was made to place the control and power functions on separate boards to provide better noise immunity. This in turn led to custom designs for the microcontroller based VLC board, the floating power supply board and the capacitor trickle charge board. This separation allows a less complex design for the individual boards. The floating power supply board components now include EMCO high voltage power supplies, which are rare and expensive components. The EMCO power supplies are required to maintain the charge on the commutation capacitor. The VLC board communicates with the upstream FPGA board by fiber optics, which also helps boost noise immunity.

The high speed current sensor design also underwent some modifications. The initial design performed well in a certain measurement range but the response exhibited a non-linear behavior outside of that range. The design was modified to improve the response across the entire measurement range.

The control cabinet design also evolved to accommodate the new control components. The features included in the control cabinet now include the FPGA board, the master SEL controller, the required control power circuits and relays, fan and pump starters and fiber-optics interface board.

C. SGTO Modules

The SGTO modules required for the SSCL have overcome some manufacturing issues during the course of the project. Some of the SGTOs exhibited cracking and chipping. The cracking was due to the sawing process used to dice the silicon wafers and produce the individual SGTO die. The saw was hitting small pieces of nickel on the top and bottom of the wafer and this led to cracks. A layer of protective material has been added to stop the nickel build up and now the cracks are not seen. The yield has improved. The protective layer also boosts the voltage capability of the SGTOs.

At present, the design of the auxiliary module includes two diodes in series, to handle the expected current and voltage conditions. There is the possibility of removing the second diode in the future but this cannot be verified without further testing.

D. Material Cost Changes

The estimated material cost for the new design has a significant increase (more than double), due to design changes (whether driven by changes in project requirements or necessary changes compared with the proposal to meet the functional requirements of the unit) and also due to material cost changes.

3.3 SBB Testing

Testing of the critical building block components such as the current limiting inductor has been undertaken. The control boards and auxiliary power supply components have been tested in the laboratory. The standard building block tests have verified the ability of the SGTO modules to turn off in the required time and to block the necessary voltage. A series of tests were conducted to demonstrate the maximum current that a single SGTO module could interrupt. It was found that a single SGTO module was capable of interrupting over 6.5kA in a matter of microseconds. Exact time taken is a function of the auxiliary circuit, not the SGTO module itself. It should be noted that the 6.5kA per module is well in excess of the value required for operation of the SSCL in the proposed design. A second series of tests measured the current sharing between modules in the same standard building block. The current sharing was observed to agree to within 5%.

Figure 33: Single building block module current interruption: fastest time (upper left), largest current (upper right); and current sharing (lower) during fault operation.

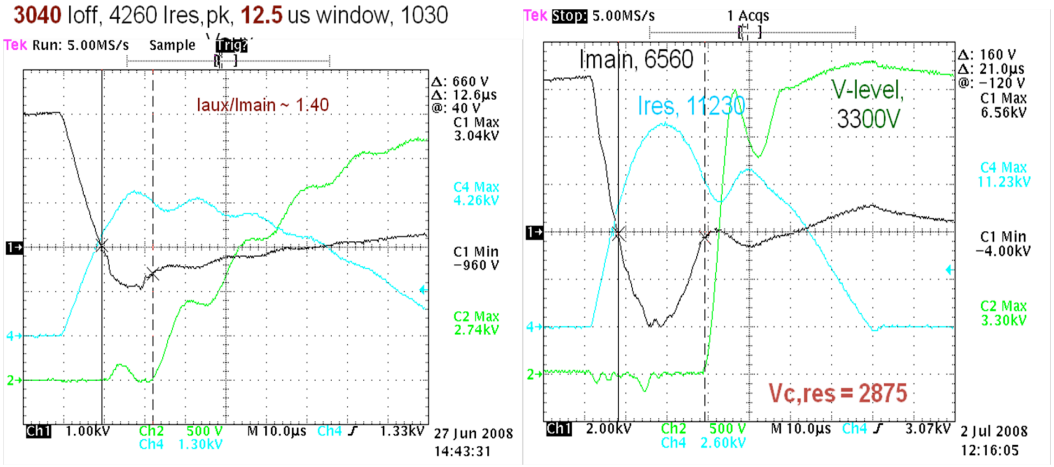

Test Results

Module current sharing

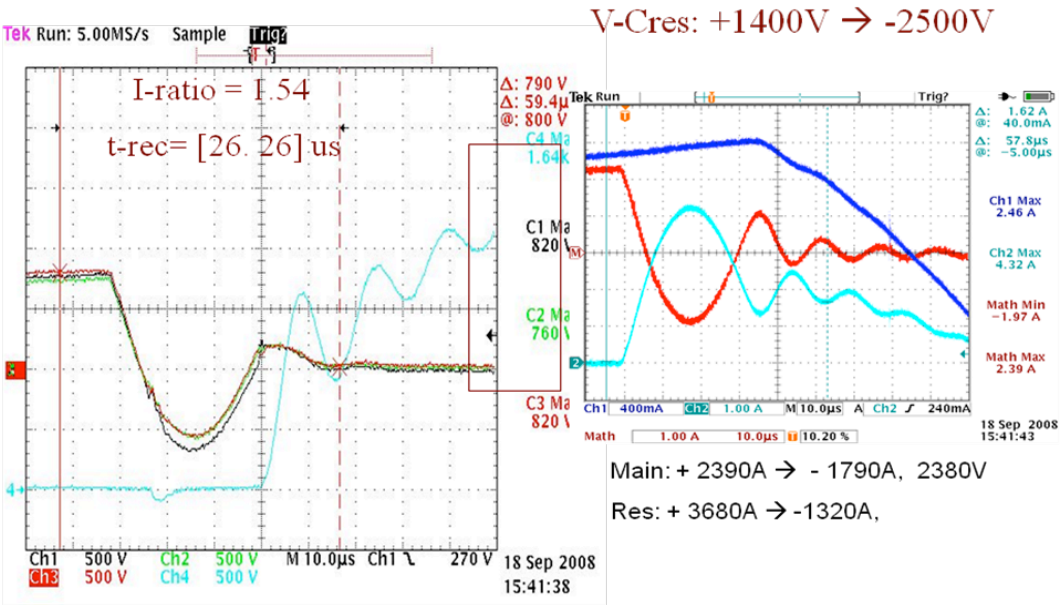

3.4 Summary

The Solid-State Current Limiter (SSCL) design presented here is the result of pioneering work in the high-power electronics equipment industry. The SSCL employs a modular and scalable design, applicable to a range of voltage classes. Such an SSCL can provide a solution to the rapidly rising available fault currents seen in utility systems. The advantages of the emerging EPRI/SiliconPower SSCL approach are immediate recovery after fault, no voltage or current distortion, no cryogenics, low losses and reduced size and weight. In addition, this type of FCC can be designed for interruptive capability as well as management of excess fault current.

Some major technical issues have been resolved and the detailed design of the system has been completed. The design of the standard building block, control system, power stack and tank were all finalized.

The main technical issues encountered have been related to the thermal management system and the SGTO modules. The thermal management system now features a forced oil system, passing through cold plates under the SGTO devices, with an external radiator system. The SSCL thermal management design, centered on the use of cold plates, has been verified by simulation done at the Novatherm Lab of Villanova University.

The results of the hardware design and elemental testing are promising and, so far, encouraging. The SGTO module and standard building block testing has demonstrated several important functional requirements, including current interruption and module-to-module current sharing. Control board testing has demonstrated the key algorithm functional requirements.

A summary of the tests that have been completed so far is as follows: SGTO module current interruption test; Standard Building Block topology demonstration; Standard Building Block control boards and gate drive functionality test; Standard Building Block power supply test; auxiliary power supply inverter and transformer test; and current limiting reactor (CLR) testing. The tests have provided valuable feedback to the design of the system so far and have enhanced the robustness of the design.

The future scope of work for this project would include the construction of the standard building blocks and the manufacture and testing of the SSCL. The possible future steps for the 15kV, 1200A, three-phase SSCL could include SBB construction and testing at Silicon Power, power stack assembly, assembly of full size SSCL, testing at an independent high voltage lab and field demonstration at utility site.

CHAPTER 4:

Zenergy Power First Generation FCC—the "Spider" HTS FCL Development

4.1 Zenergy Power HTS FCL Concept

The Zenergy Power FCC is based on their High-Temperature Superconducting Fault Current Limiter (HTS FCL) approach using the Saturable Core Reactor concept, following the ideas of [45], [62] and [63]. The proposed HTSFCC is for three-phase power systems. Each phase of the proposed HTSFCL is constructed around a dual iron core with three coils wound around each limb as shown in Fig. 34. The DC bias coil is wound around the combined center limb. A pair of AC coils is wound on the outer legs of the cores. The idea is similar to that of [45], however, here, the AC coils are implemented using CC cores rather than EE cores as in [45]. This has the advantage of having a single DC bias coil to be shared by the two cores.

Figure 34: Conceptual structure of ZynergyPower single-phase Saturable Reactor FCL.

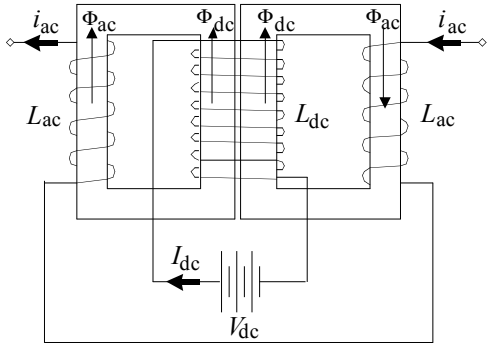

Similarly to the saturable reactor FCCs described in the previous chapter, the AC coils are connected in series, differentially, and are inserted into the AC line in series with the load as shown in Figure 14. The mmf-flux operating point of all the cores is established by the DC coil in the vicinity of point B (see Figure 15). As the AC line current flows through the AC coils, the core operating point is shifted. Due to the differential connection of the AC coils, the AC-induced mmf in one core reinforces the DC mmf, whereas in the other core it weakens the bias mmf. Therefore, the operating point of one core shifts into a deeper saturation (point A), whereas the operating point of the other core moves towards shallow saturation, at point C, closer to the hysteresis knee point. evertheless, in the normal state the cores is designed to remain in saturation so that their impose a low impedance. When a fault occurs, the high amplitude of the fault current drives one of the cores out of saturation into the steep region of the hysteresis curve. The unsaturated AC coil is capable of supporting a large voltage across its terminals, and thus limits the fault current. Depending on the AC line current polarity, the coils alternate in and out of saturation to reduce the current in each half cycle.

4.2 First Generation "Spider" HTS FCC Design and Prototyping

A three-phase prototype incorporates three pairs of single-phase FCLs in a spider-like structure featuring a hexagonal iron core with a thick central limb as shown in Figure 35. Here, the three pairs of AC coils are wound on the outer legs of the cores using non-superconducting conventional copper coils. Each pair of the AC coils are connected in series, differentially, and inserted into the appropriate phase. The DC coil is made of first generation High Temperature Superconducting (HTS) wire wound around the center limb. The HTS coil forms a strong electromagnet fed by a low voltage, high current DC power supply. The HTS coil provides an efficient method of saturating all six cores with minimum DC power losses.

It is worth noting that during normal operation the cores operate almost symmetrically, so that the AC flux in the center leg is mostly canceled out. As a result, there is no AC voltage induced in the DC coil. During the fault, however, the cores operate asymmetrically, with one or more of the cores partially desaturated. Therefore, in a practical device, coupling between the AC and DC coils can be a problem. However, the Zenergy Power design ensures that the coupling is only a few percent and, therefore, of no significant consequence. This reduces the risk of high voltage shock to the DC coil and power supply.

Figure 35: Physical structure (a) and a cutaway diagram (b) of the three-phase Zenergy Power Saturated Core Reactor HTSFCL. Note the DC coil and its cryostat on the middle leg and the AC coils wound on the outer limbs.

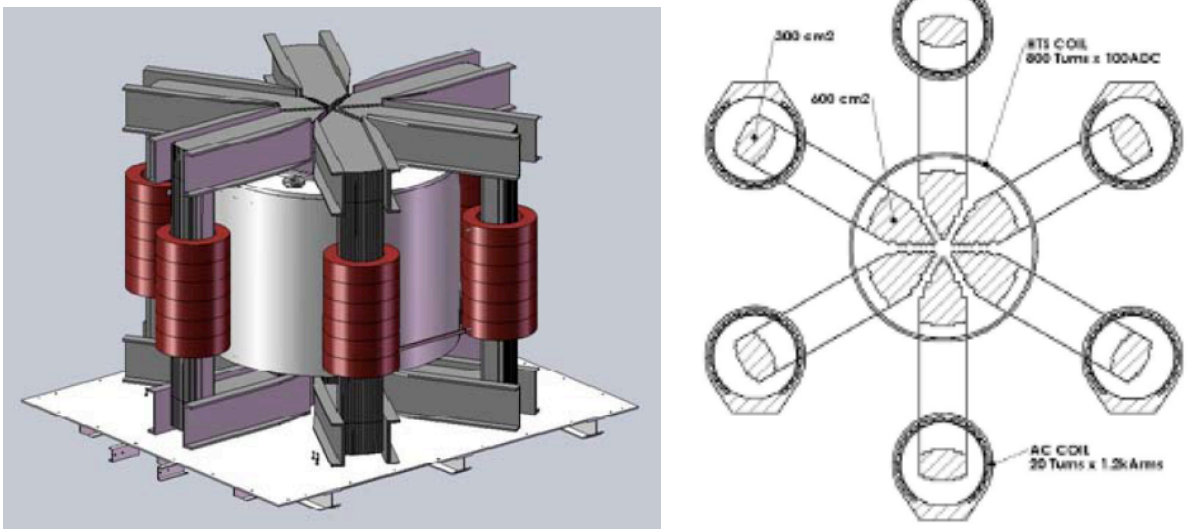

(a) **(b)**

A full-size three-phase distribution level FCL prototype was constructed. The prototype FCL employs cast-epoxy AC coils and a closed-loop cryogenic cooling system that uses sub-cooled liquid nitrogen at approximately 68°K to increase the working current of the DC HTS bias magnetic coil to maximize the DC magnetic bias flux. The basic design parameters of the prototype FCL are shown in Table 1. The cutaway views of the distribution level three-phase HTS FCL assembly are shown in Figure 36. The view of the internal structure and physical view of the experimental prototype HTS FCL unit are shown in Figure 37.

The prototype FCL was designed for a modest fault current limiting capability and was intended to limit a 23 kA RMS potential steady-state fault current by 20%. During the design, a

great emphasis was placed on accurately modeling and predicting the performance of the FCL and its associated electrical waveforms, simulation analysis of different line conditions, and predicting the interaction of the FCL with other power system components.

Table 1: Design Parameters and Main features of the prototype FCL.

Line Voltage	12.47kV
Maximum load current	800 A (3phase 60 Hz)
Voltage drop at max. load	<1% (70 V rms)
Prospective fault current	23 kA rms symetrical
Asymmetry X/R	21.6
Fault limiting capability	20%
Fault type	3 phase to ground
Fault duration	30 cycles
Recovery time	Instantaneous
Iron Core Weight (lbs)	52K
Cost of Iron @ $3.00/lb	$ 156K
Size	19' x 19'

Figure 36: Cutaway views of the distribution level three-phase HTS FCL assembly.

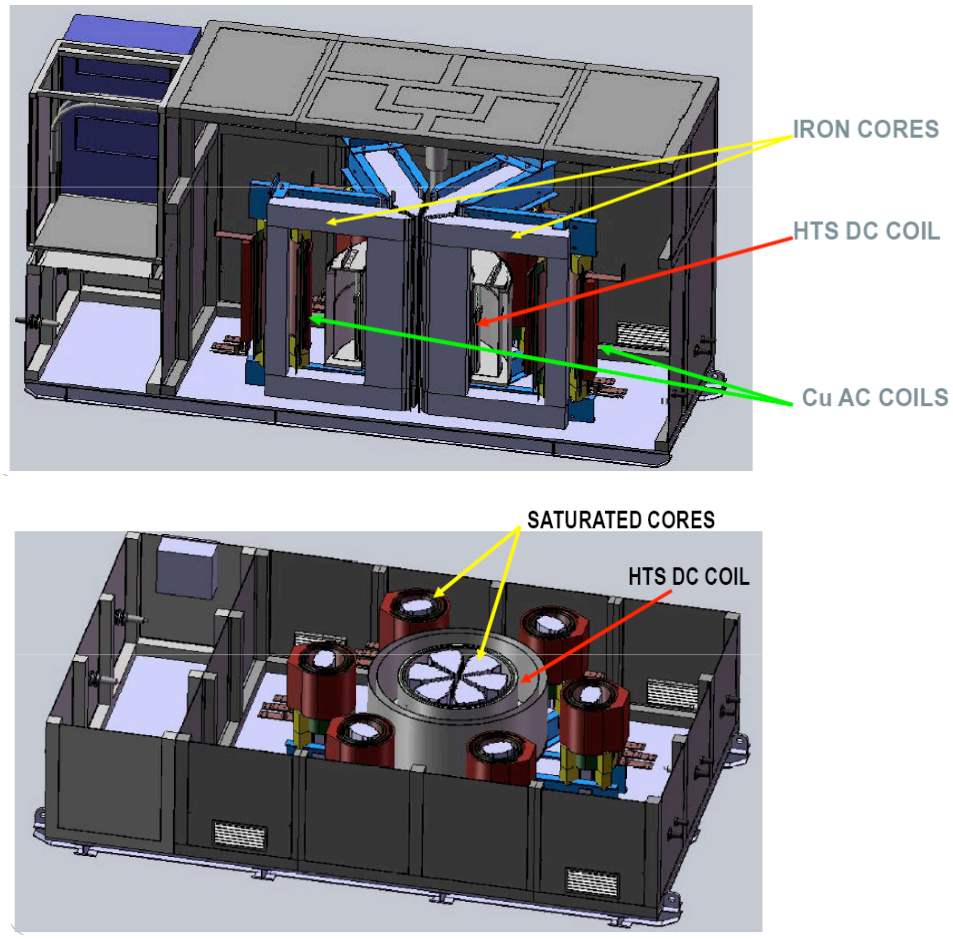

Figure 37: Experimental FCL prototype built by Zenergy Power Inc. (a) Main components of HTS FCL; (b) physical view.

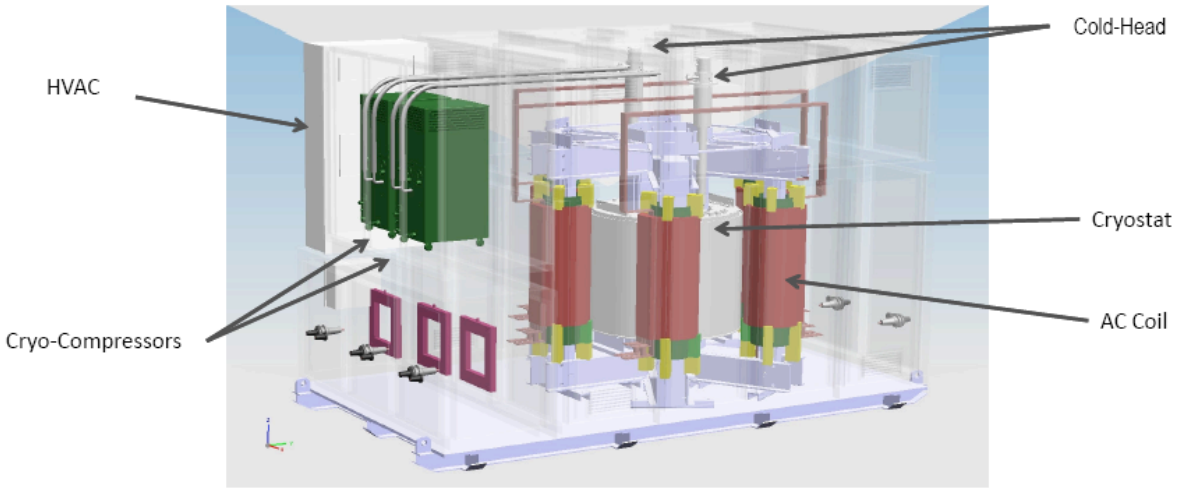

(a)

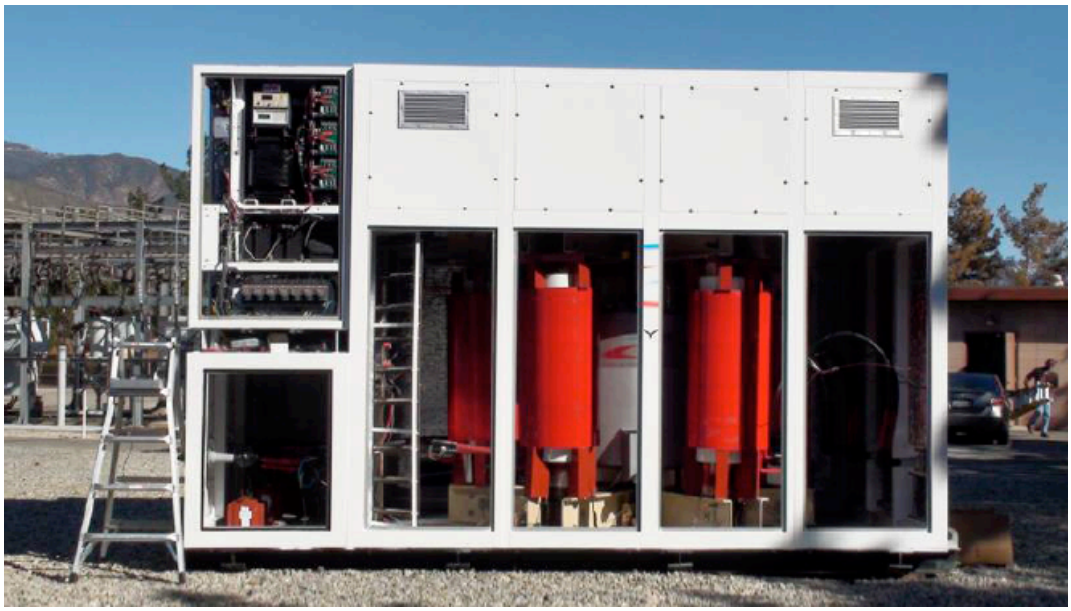

(b)

4.3 HTSFCL Modeling

4.3.1 Nonlinear Inductance Model

Saturable core HTSFCLs consist of a set of coils wound around one or more ferromagnetic cores. A superconducting magnet is coupled to the core region in such a way that the DC magnetization force can saturate the magnetic material. In the Zenergy Power FCL, each AC phase consists of two coils connected in series and wound around two core regions. The windings are oriented such that, in one core, positive AC current counteracts (bucks) the superconducting DC bias, while in the other core, negative AC current assists (boosts) the superconducting DC bias.

The nonlinear model that describes the behavior of the device is based on the physical principle described in a previous chapter and was derived in [64]. The core material has a B-H curve that can be approximated by an inverse tangent function as follows:

$$B(i_{ac}) = \frac{-2B_{sat}}{1+\tan^{-1}\left(K\pi - \frac{\pi}{2}\right)}\left[1+\tan^{-1}\left(K\frac{\pi}{I_{max}}(I_{max}-i_{ac})-\frac{\pi}{2}\right)\right]+2B_{sat} \quad (1)$$

Here, i_{ac} is the instantaneous AC line current, I_{max} is the line current that takes to fully saturate the cores, at which point the average magnetic field is B_{sat}, and parameter K determines the range of line currents where the magnetic state of the cores are actively changing from saturate to unsaturated. The equation is scaled in such a way that B = 0 at bias point, i.e. with $i_{ac} = 0$, and the majority of the change in field occurs just before $i_{ac} = I_{max}$. The induced voltage, or back emf, across this section of the FCL is $V = \tilde{L}\,\partial i/\partial t$, where $\tilde{L}$ is the differential inductance defined as:

$$\tilde{L} = n_{ac} A_{core} \frac{\partial B(i_{ac})}{\partial i_{ac}} \quad (2)$$

Here, n_{ac} is the number of turns in the AC coil, which carries the line current, and A_{core} is the cross-sectional area of the paramagnetic core material. In some cases, this model is improved by imposing two additional conditions. First, $\tilde{L}$ must be greater than or equal to an additional parameter called L_{air}. This value represents the insertion impedance as an equivalent air-core inductance. Furthermore, if i_{ac} is greater than I_{max}, then $\tilde{L}$ is constrained to be L_{air}. This accounts for the fact that, when the line current is very large, the FCL's magnetic core is reverse saturated and the impedance is once again approximately equal to the insertion impedance of an equivalent air-core inductor. The equations above provide a general framework for describing the behavior of an FCL in an electric circuit. This framework requires four input parameters: I_{max}, B_{sat}, K, and L_{air}. As described in the following sections, finite element methods (FEM) were used in simulations to calculate the average magnetic flux for various static values of DC and line currents. A least squares fitting procedure was used to determine the above parameters. To validate the model, PSCAD electrical simulation software was used to implement the FCL nonlinear inductance model and the simulation results were compared to the experimental results from the extensive tests performed on the 15kV FCL device.

4.3.2 Finite Element Model and Analysis

A. Finite Element Model

Precise finite element model (FEM) results require a number of inputs, including physical geometry, accurate descriptions of the electromagnetic properties of each material, and the current densities in the superconducting and AC coils. Calculations were performed using the ANSYS FEM code. The geometric parameters were either input directly from mechanical CAD drawings or by command files. Because the designs have many elements, calculation speed is a significant constraint. In most cases the models make use of geometric symmetries to improve the calculation speed. The B-H curve for the magnetic material was estimated from measured data shown in Figure 38. All calculations were performed under the static approximation. This assertion is justified by the fact that physical devices do not display significant hysteretic behavior.

Figure 38: Magnetization Curve of M-6 Steel used in the FEM model.

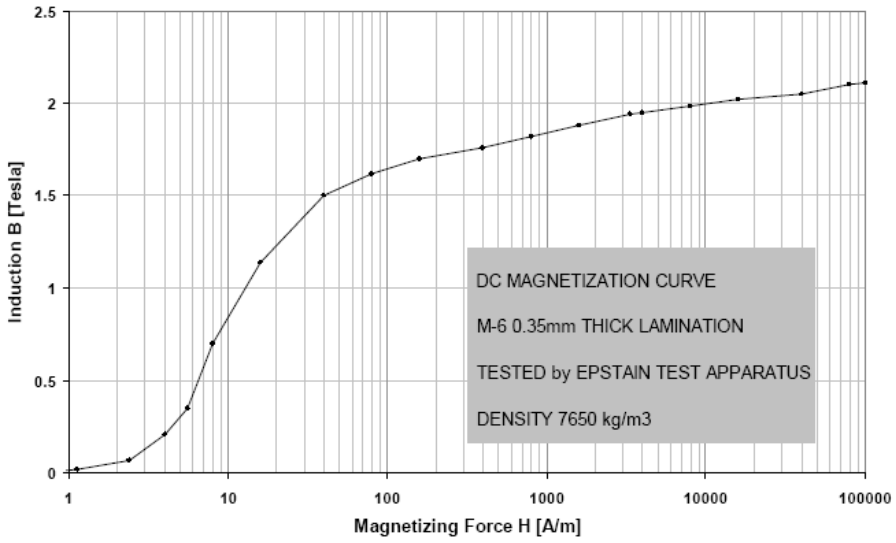

The LMATRIX subroutine of ANSYS provides the differential inductance matrix for the number of coils present in the model, and the total flux linkage in each coil, under a given set of current density conditions. The FEM provides graphical outputs that allow easy visualization of geometric properties (see Figure 39). The (grey) iron cores serve as flux links between the (blue) superconducting magnet in the center of the device and the (orange) AC coils. This three-phase device has six AC coils in total; one boosting coil and one bucking coil for each phase at any given time.

Graphical outputs also provide insight for future designs, which allows analysis of magnetic field densities in each region (see Figure 40). After using the graphical outputs to verify the model is working well, either the flux or the inductance outputs can be used to calculate the parameters for the nonlinear inductor model.

Figure 39: Finite element model of a 15kV three-phase FCL.

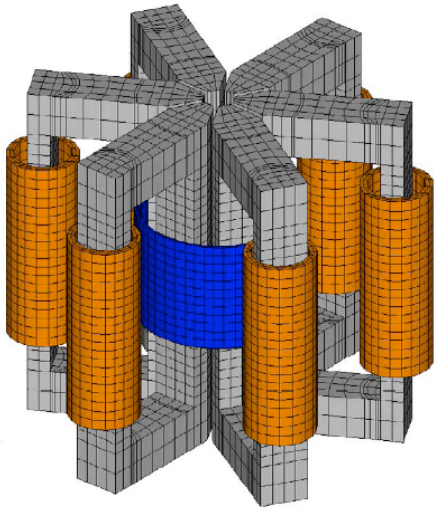

Figure 40: Total flux density due to DC Magnetization at 80,000 Amp-turns.

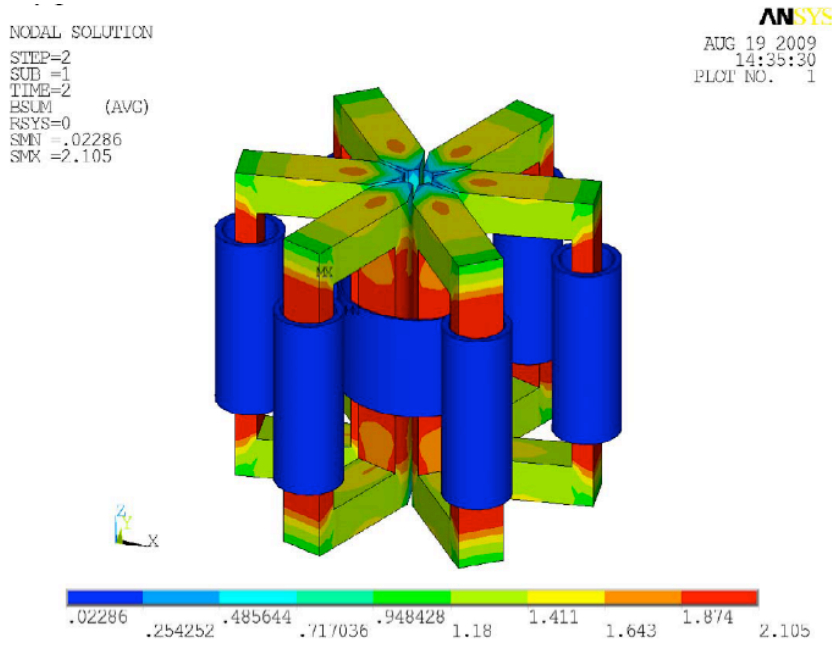

B. FEM Analysis

FEM analysis allows modeling the devices prior to their construction. First, a series of flux or inductance values over a range of AC and DC currents were calculated. The data points shown in Figure 41 were calculated for a superconducting bias current of 100 amps, and 800 turns, resulting in 80,000 amp-turns. The process can be repeated for other superconducting DC bias points if necessary. Figure 41(a) shows the average magnetic field linking the boosting and the bucking coils. The values were calculated from flux values, $\Phi(i_{ac})$, with the equation:

$$B_{ansys} = \Phi(i_{ac}) / n_{ac} A_{core} \qquad (3)$$

In this case, n_{ac} = 20 turns and A_{core} = 300 cm^2. Figure 41 (b) shows the sum of these magnetic fields. The inductance values shown in Figure 41 (c) were calculated from Figure 41 (b) with the relation:

$$\tilde{L} = n_{ac} A_{core} B(i_{ac}) / i_{ac} \qquad (4)$$

The dotted red lines in Figure 41 (b) show the model described above applied to both the boosting and bucking cores. A similar fit was obtained for the inductance values shown in Figure 41 (c). This inductance is related to the differential inductance by

$$L = \frac{1}{i_{ac}} \int_0^{i_{ac}} \tilde{L}(i)\,di \qquad (5)$$

which was performed numerically to account for the conditional statements applied to our differentially-defined inductance when $i_{ac} > I_{max}$ and $L \sim < L_{air}$. Next, the best-fit values from the inductance fit were used to compare this model to the measured behavior of the FCL device.

Figure 41: FEM simulated results and model fitting. (a) Average flux density through the AC coils for various AC current values when 80,000 amp-turns are applied to the superconducting magnet. (b) The sum of the two average B-fields shown in figure a. The dotted line is a best fit to the non-linear model in section 2 with B_{sat} = 2.09 Tesla, L_{air} = 33.6 µH, I_{max} = 4.38 kA, and K = 3.73. (c) The FEM generated inductance. The dotted line represents the same model with best-fit parameters B_{sat} = 2.11 Tesla, L_{air} = 36.2 µH, I_{max} = 4.28 kA, and K= 4.48.

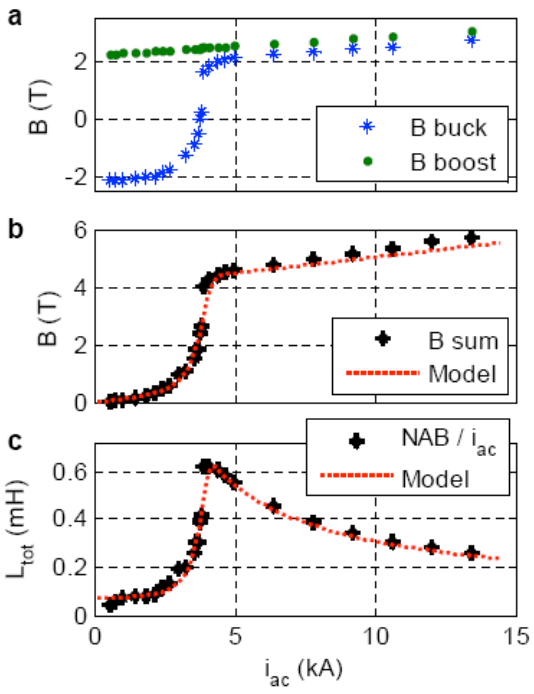

4.3.3 Experimental Model Validation

Short circuit tests of Zenergy's 15kV FCL took place at Powertech Laboratories in British Columbia, Canada. The three-phase FCL was connected to the test source voltage as shown in

Figure 42, and an auxiliary breaker provided the fault current by closing the three-phase-to-ground fault at the appropriate point-on-wave. Source resistance and reactance were selected to provide the necessary prospective fault current levels with the required asymmetry factor.

Figure 42: High-power short-circuit FCL test set up.

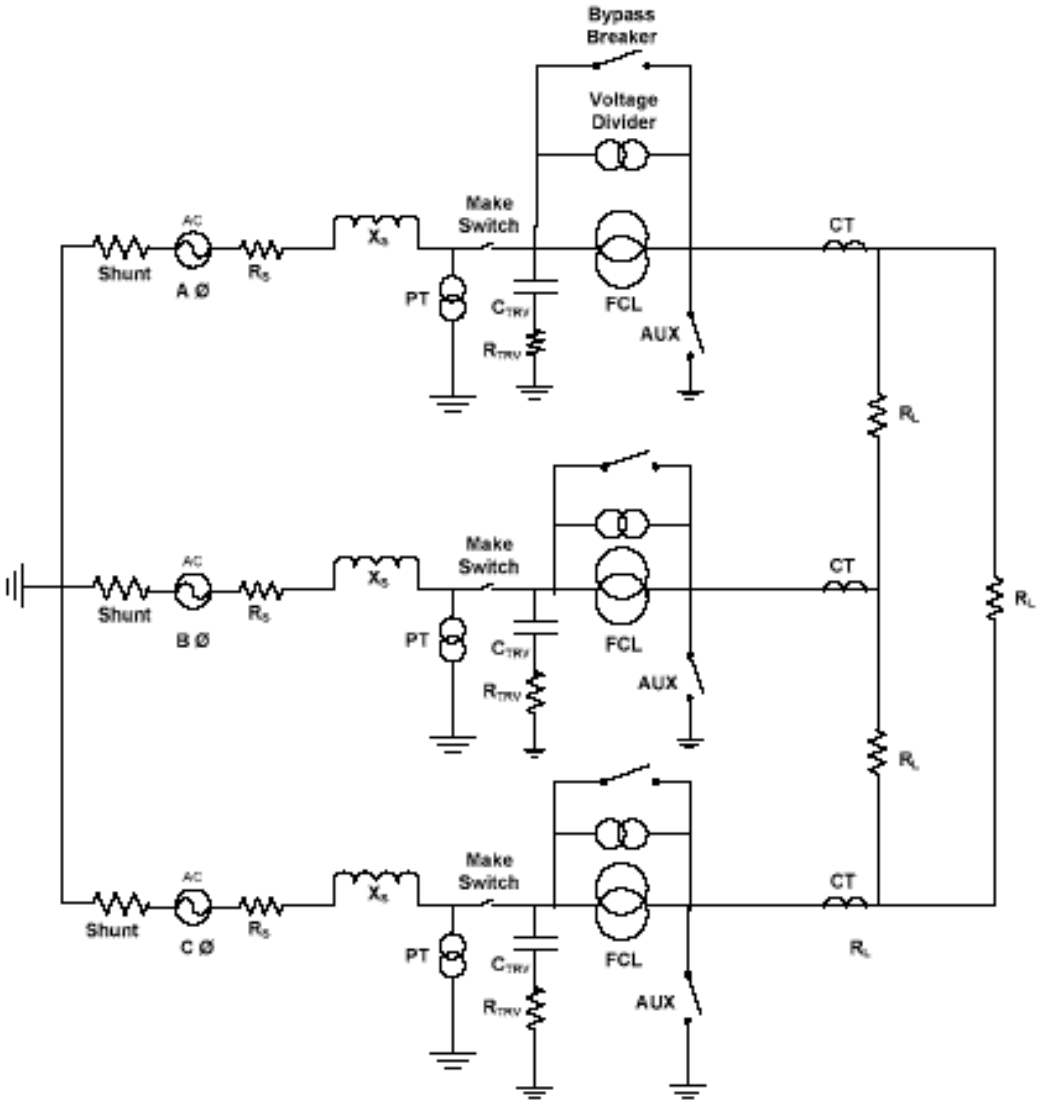

Figure 43 shows two cycles of load current followed by the first two cycles under faulted conditions. Figures 43(a) and (b) show a 6.5 kV line-to-line system with a 3 kA rms and a 12.5kA rms prospective fault, respectively. Figure 43(c) shows a 13.1kV line-to-ground system with a 20 kA rms prospective fault. All tests were performed with an X_S/R_S ratio greater than 20. The symmetrical fault limiting performance of the model is provided in Figures 44 and 45.

Figure 43: Measured and modeled current as a function of time. a) A 6.5 kV line to line system with two 830A rms load cycles followed by a 3kA rms prospective fault. The symmetrical part of the fault current was limited by 17%. b) The same system with two 825 Arms load periods followed by a 12.5kA rms prospective fault. The FCL limited 30% of the symmetrical prospective fault current. c) A 13.1 kV line-to-line system, with two 780A rms load cycles followed by a 23kA rms prospective fault where the FCL limited 20% of the symmetrical current. The dotted red lines use the parameters derived from FEM modeling.

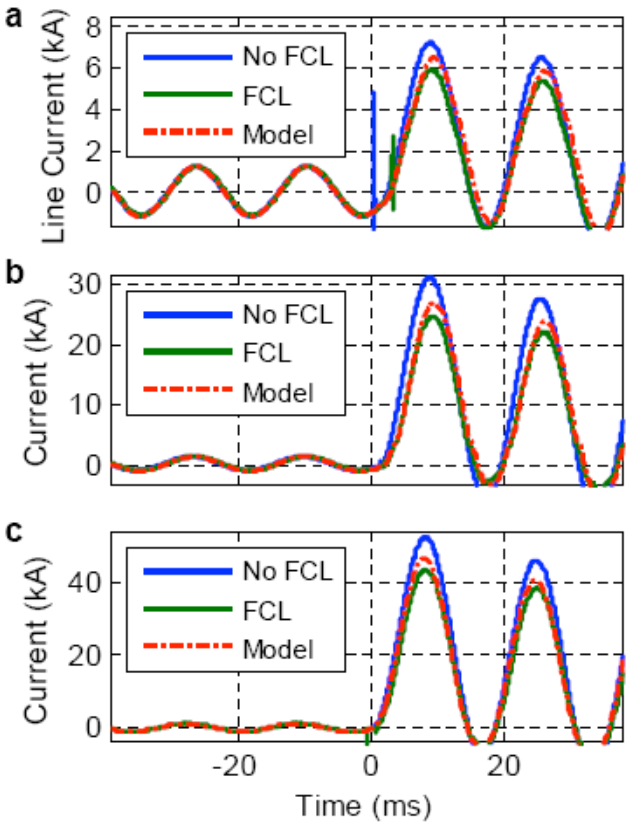

The experimental results were analyzed using a simplified lump-sum circuit that consists of a voltage source, the nonlinear voltage FCL model, and a time-dependent load resistor. The idealized source has the voltages listed above and a source impedance of 0.8 mH and 14 mΩ. The FCL includes the current-dependent inductance described above, along with a resistance of 1 mΩ. The simplified model's load impedance was chosen to generate the correct current during the loading cycles. This impedance was switched to zero during the fault cycles.

It was found that the nonlinear FCL voltage model quantitatively reproduced the measured results. The FEM analysis provides a concrete method for estimating the model parameters for the saturated core FCL design. The estimated parameters were used for the modeled results shown in Figures 43 and 44. Figure 44 shows the symmetrical fault current after 21 cycles of continuous operation. At this point, the estimated parameters provide excellent predictions for overall fault current reduction. The qualitative features of the FCL voltage response are also estimated well as shown in Figure 44(b). Figure 44(c) shows the average magnetic field defined by the measured flux change (i.e., the integrated bushing-to-bushing measured voltage with respect to time) divided by $n_{ac}A_{core}$. While the qualitative features of the magnetic field are reproduced by the model, the quantitative agreement is not precise. In order to increase the

accuracy of the model the input parameters were adjusted to match the measured response. Figure 45 demonstrates the qualitative agreement that is possible after the model updating.

Figure 44: Measured and modeled current (a) and voltage (b) as a function of time for a 12.5 kA rms symmetrical prospective fault after 21 cycles or 350 ms. (c) Average magnetic field as computed from the integral of the measured FCL back emf with respect to time.

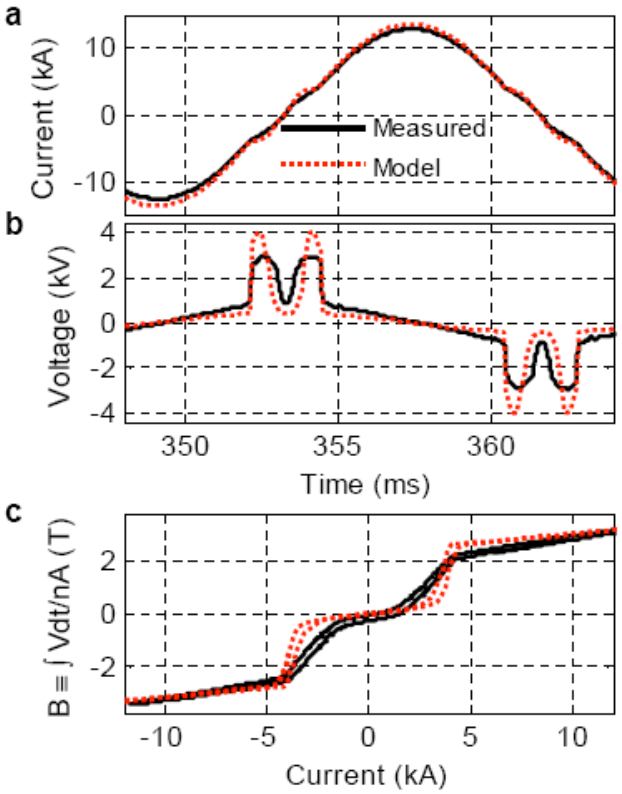

Figure 45: Measured and modeled current, voltage, and integrated B-field under the same conditions shown in Figure 44. We found excellent agreement between the model and measured values with the following input parameters. B_{sat} = 1.8 T, L_{air} = 70 μH, I_{max} = 4.3 kA, and K = 1.5.

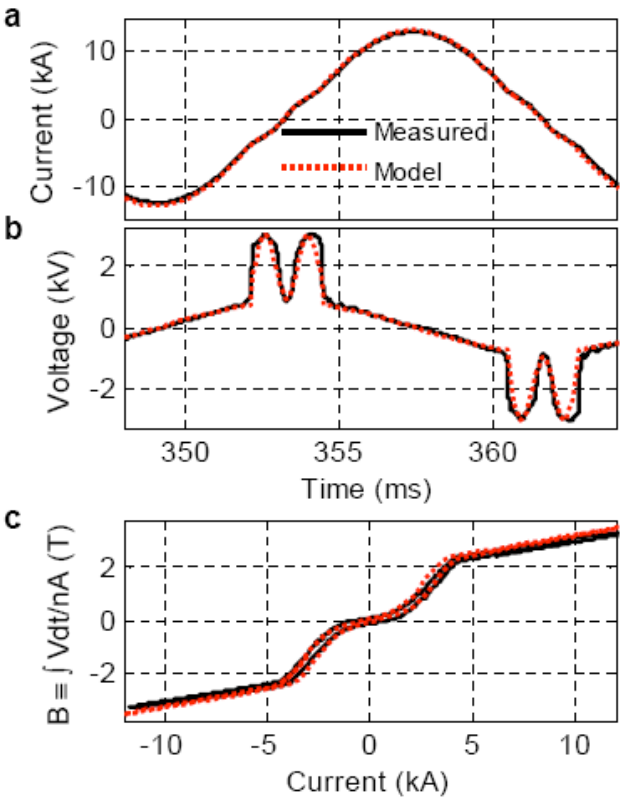

4.4 Summary

This chapter reported on the recent development of a Saturable Core FCL by Zenergy Power. Successful controlled and field testing of the FCL proved the technological feasibility of the device. The FCL described here was built, laboratory tested and underwent field testing by the Southern California Edison Co. from March 2009 to October, 2010. Although the design was still not optimized at this stage, the FCL prototype provided an extensive "learning experience".

This prototype FCL has the advantages of a passive design, the ability of limiting the first peak fault current, automatic recovery under load and fail-safe operation. Moreover, the DC bias magnet showcased an excellent application of superconducting technology, where the superconductor experienced no quenching, and thus no recovery time. In addition, the adiabatic operating regime of the HTS coil presents a relatively small heat load to the cryocoolers.

The state-of-the-art HTS technologies use liquid nitrogen and provide significant advantages over their low-temperature liquid helium counterparts, since the liquid nitrogen systems are less complex compared to the liquid helium systems. These offer significant savings in cryogenic equipment costs and a reduction in operational costs. Furthermore, in the Znergy Power design, only one HTS DC coil is needed, albeit a relatively large diameter. An additional advantage of this FCL design is the placement of the HTS coil on the center limb, which gives a sufficient electrostatic clearance to the high voltage AC coils wound on the outer limbs. The isolated high-voltage and cryogenic systems lead to a simplified high-voltage design.

A systematic approach to modeling of the electrical behavior of the saturated-core HTS FCL was also developed. The physically-derived model was supported by FEM electromagnetic simulations as well as circuit analysis, and then fine-tuned to match the experimental results. The nonlinear FCL modeling, with the FEM-updated parameters, provided an excellent tool for predicting the overall fault current reduction of a saturated core HTS fault current limiter. The FCL model was used by ZenergyPower in designing a superior "second generation" 15kV FCL with the objective of developing a transmission level FCL in the near term.

CHAPTER 5:

Zenergy Power HTS FCL Laboratory Testing

5.1 Standards

At the time of this writing, there are no official regulations or standards in place for testing of FCLs. The testing procedure for the prototype FCL was developed under a joint effort of NEETRAC, SCE and Zenergy Power, and University of California, Irvine (UCI). The procedure was derived from the existing IEEE Standard C57.16-1996: Requirements, Terminology, and Test Code for Dry-Type Air-Core Series-Connected Reactors, and IEEE Standard C57.12.01-2005: General Requirements for Dry-Type Distribution and Power Transformers Including Those with Solid-Cast and/or Resin-Encapsulated Windings.

The prototype was shipped to BC Hydro's Powertech Laboratory in Surrey, BC, Canada for laboratory testing. The laboratory testing of the FCL prototype was performed in three categories: basic pre-connection tests, normal state performance, and fault condition testing. FCL testing criteria are summarized in Table 2.

Table 2: Zenergy FCL testing criteria protocol.

#	Test	Reference
1	Winding Resistance	IEEE Std C57.16-1996
2	Impedance	IEEE Std C57.16-1996
3	Total Losses	IEEE Std C57.16-1996
4	Temperature Rise	IEEE Std C57.16-1996
5	Applied Voltage	IEEE Std C57.16-1996
6	Insulation Power Factor	IEEE Std C57-12.01-2005
7	Insulation Resistance Measurement	IEEE Std C57-12.01-2005
8	Fault Current Tests	Engineering Spec. ZP-ES-08-05
9	Turn-to-Turn	IEEE Std C57-12.01-2005
10	Lightning Impulse @110KV	IEEE Std C57-12.01-2005
11	Chopped Wave Impulse	IEEE Std C57-12.01-2005
12	Audible Sound	Engineering Spec. ZP-ES-08-05
13	Partial Discharge	IEEE Std C57.16-1996
14	Seismic Verification by analysis	IEEE Std 693

5.2 Pre-connection Testing

A series of the pre-connection dielectric and high-voltage tests were designed to verify the integrity of insulation of the device, bushings and support, and also to measure the AC coil resistance.

During the pre-connection testing, the FCL prototype was exposed to a series of high voltage lightning impulse tests. These were meant to ensure that the device can cope with the adverse conditions on distribution grid, in a manner similar to other existing distribution equipment.

The Partial Discharge test is designed to test the insulation of the device. To conduct the test both terminals of each phase of the FCL were shorted. Then, each phase was connected to 11.3 kV line to ground (L-G) for 10 seconds. The voltage was then reduced to 9.5 kV, held for 60 seconds and then the partial discharge was measured. After the first partial discharge test, each phase was energized at the applied potential test level of 34kV for 60 seconds. The voltage was then reduced to 9.5kV, held for 60 seconds and then the partial discharge level was measured again. Partial discharge levels at 9.5 kV fell below the recommended 100pC value in the three phases; the FCL passed the test.

The objective of the Lightning Full Impulse test is to simulate a traveling wave due to lightning strikes. This test is a good indicator of quality of insulation, design and manufacture. With the terminals of each phase under test connected together, each phase was subjected to one reduced full wave and three full waves of positive polarity, with a crest voltage of 110 kV for the full waves. Initially, the FCL had flashovers. Reconfiguration of the connecting cables and added insulation sleeves resolved the problem and all three phases withstood the lightning impulse tests.

The goal of the Chopped Wave Impulse test is to emulate a sudden flashover of line insulation. A chopped wave imposes a high rate of change in voltage and generates oscillations which result in high internal voltage stress. Thus, the Chopped Wave Impulse test is more challenging. To conduct the test both terminals of each phase of the FCL were shorted. Then, high-voltage impulses were applied to each phase of the FCL in the following order: one reduced full wave, one full wave, one reduced chopped wave, two chopped waves, followed by two full waves, with a crest voltage of 110 kV for the full waves and 120 kV for the chopped waves. Initially, phases A and B passed the test, but phase C failed. The FCL passed the repeated testing after reconfiguration of the connectors and additional insulation was added.

The goal of the Turn-to-Turn test is to detect inter-turn insulation breakdown. The turn-to-turn test consisted of a series of high frequency, exponentially decaying voltages between the terminals of each winding. The turn-to-turn test was performed by repeatedly charging a capacitor and discharging it through sphere gaps into each terminal of the FCL, which generated ringing. Other terminals of the FCL were grounded during the tests. The turn-to-turn test was done by applying one reduced and three full wave impulses of positive polarity to each terminal of the fault current limiter. The peak of the full waveform was 95 kV. The discharge waveforms were oscillating at the same frequency and damping, which meant that no inter-turn fault occurred, and the FCL had passed the test.

The purpose of the Applied Voltage test is to ensure that the device can withstand the required power frequency voltage from the bushing to ground. This test also stresses the insulation in between the different windings. During the test a potential test level of 34 kV was applied for 60 seconds on the reactor's supporting structure, including insulators. The FCL passed this test.

5.3 Normal State Performance Testing

The sequence of the normal state performance tests were designed to measure the steady-state voltage drop, impedance, and power losses, and to verify the thermal design.

The FCL was connected to three-phase bus voltage of 12.4kV and loaded as shown in Figure 42. The test was conducted under a set of predetermined load currents. The load power factor was close to 0.9. The voltage drop across each phase was measured and insertion impedance of the FCL was found. The FCL passed this test with less than a 1% drop in the nominal voltage.

In the normal state the voltage drop across the FCL terminals remains low, so the terminal voltage distortion has a negligible effect on line currents and the power quality remains good. As shown in Figure 46, the full load currents appear of a satisfactory quality.

Figure 46: Experimental waveform of the FCL's full load current in the normal state.

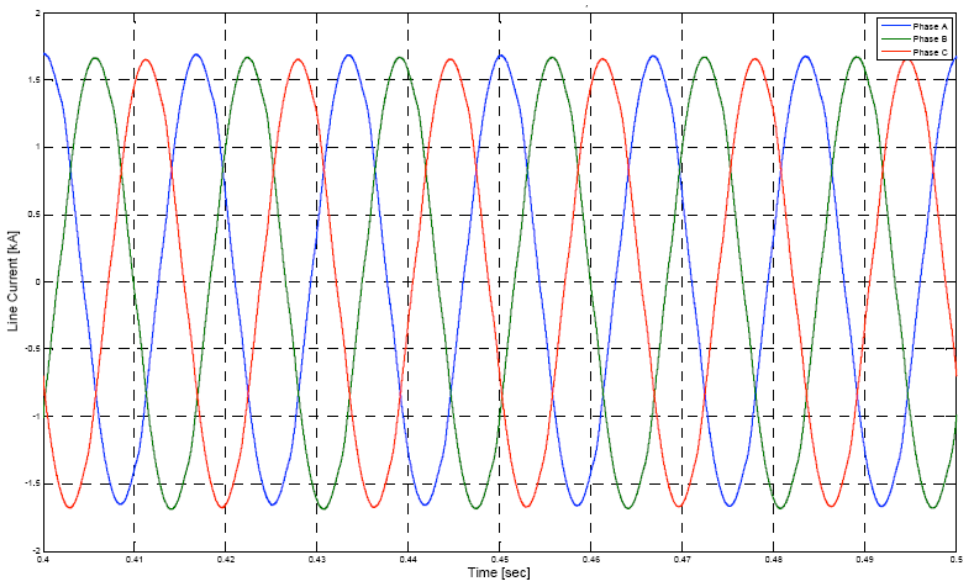

The FCL insertion impedance and rms voltage drop across a single-phase of the experimental prototype under different load current conditions and different DC bias currents are shown in Figures 47(a) and (b). Both the FCL insertion impedance and the voltage drop have a nonlinear dependence on the load current and increase as the FCL prepares to assume the current limiting function.

The FCL's power losses are caused primarily by the AC coil resistance. Figure 48 shows the normal state power losses of the FCL measured as a function of the load current.

The temperature rise test was conducted according to the test setup in Figure 42. Temperature was measured on the AC coils with thermocouples on different parts of the AC coils. Load current was increased until the nominal current of 750A rms was reached. The test was conducted for nearly 18 hours. The measured temperature of the hottest thermocouple on the AC coil during the temperature rise test was compared to the analytical thermal model in Figure 49. The thermal time constant was found to be equal to 3 hours. A final temperature rise of 35°C above the ambient 22°C was recorded.

Figure 47: (a) Measured FCL impedance [Ω] and (b) measured voltage drop [%] relative to source voltage across a single-phase of the experimental prototype under different normal state load

current conditions and DC bias current.

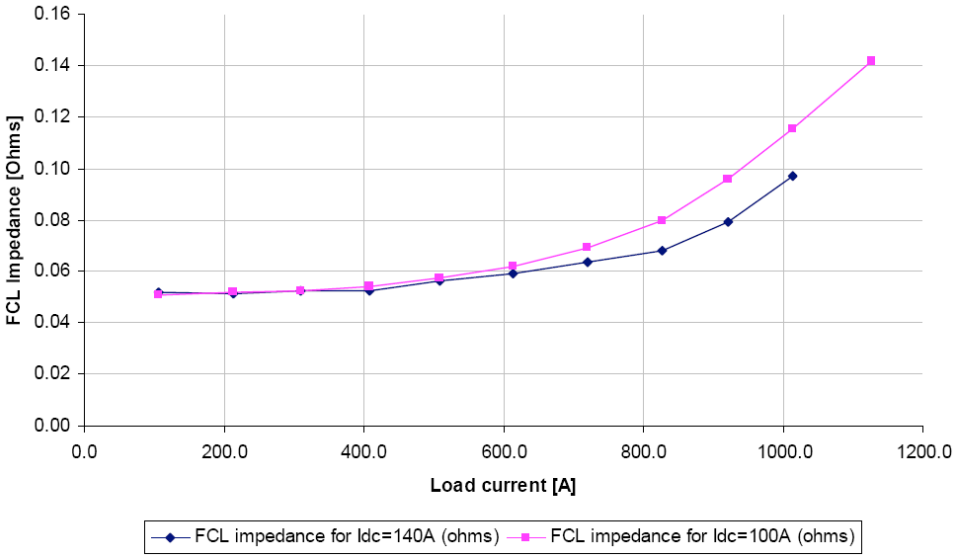

(a)

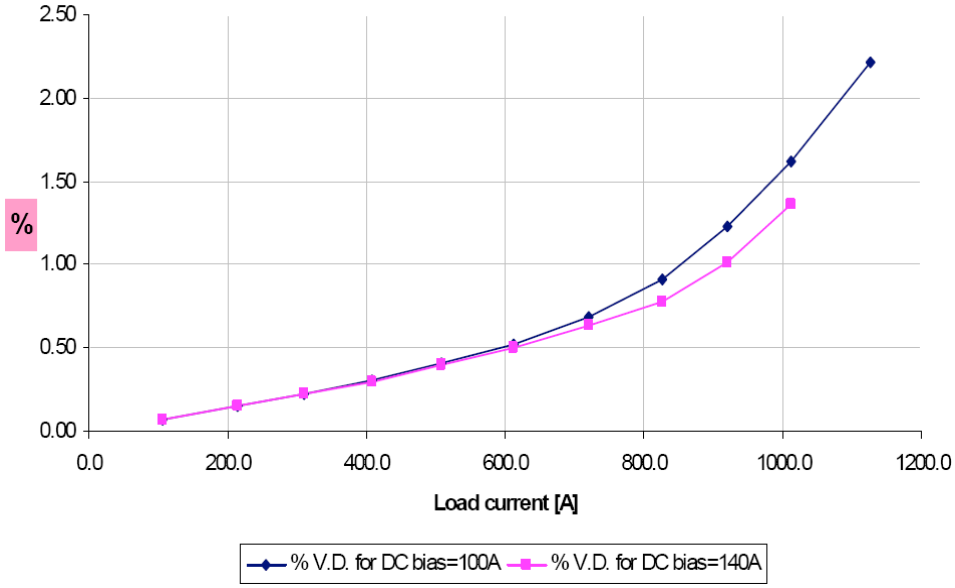

(b)

Figure 48: Measured normal state FCL power loss [%] relative to source power under different normal state load current conditions.

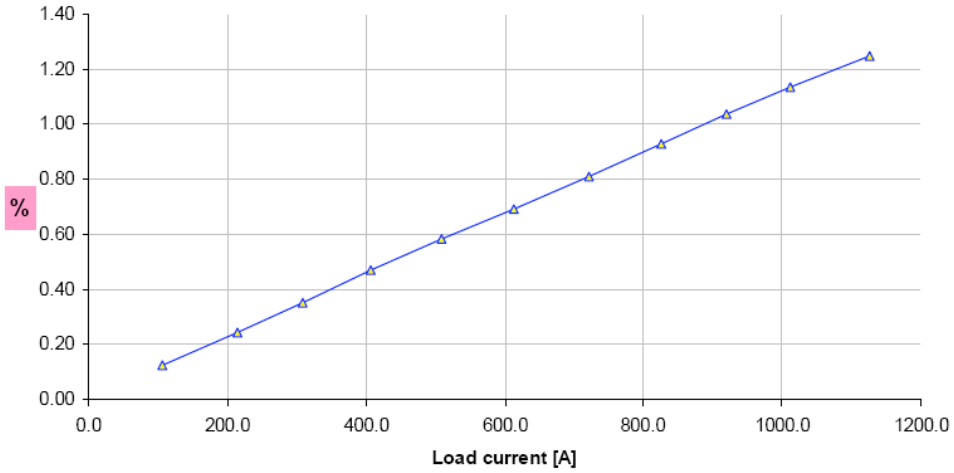

The non-linear core characteristic makes the FCL a nonlinear device with sharply varying insertion impedance, X_{ins}. The insertion impedance depends on the core magnetic properties, AC coil number of turn and the DC bias mmf. The experimentally-measured impedance of a single pair of AC coils as a function of DC bias is showed in Figure 50. The measurement was performed at low AC current level. The dashed arrow shows the minimum DC bias mmf required to saturate the core and keep the FCL in the low impedance state.

The FCL insertion impedance, Z_{ins}, depends on the AC current magnitude. Generally, the insertion impedance increases with the magnitude of the AC current. Therefore, the DC bias mmf was optimized to attain the largest insertion impedance change in response to the increase in the AC current.

Figure 49: Measured temperature on AC coil during temperature rise test with 750Arms load current per phase.

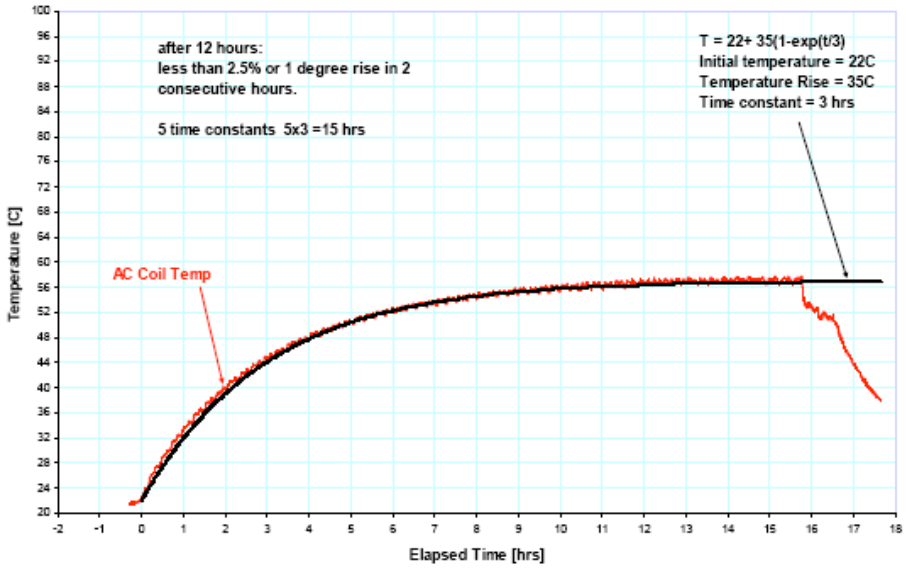

Figure 50: FCL insertion impedance, as function of DC bias mmf.

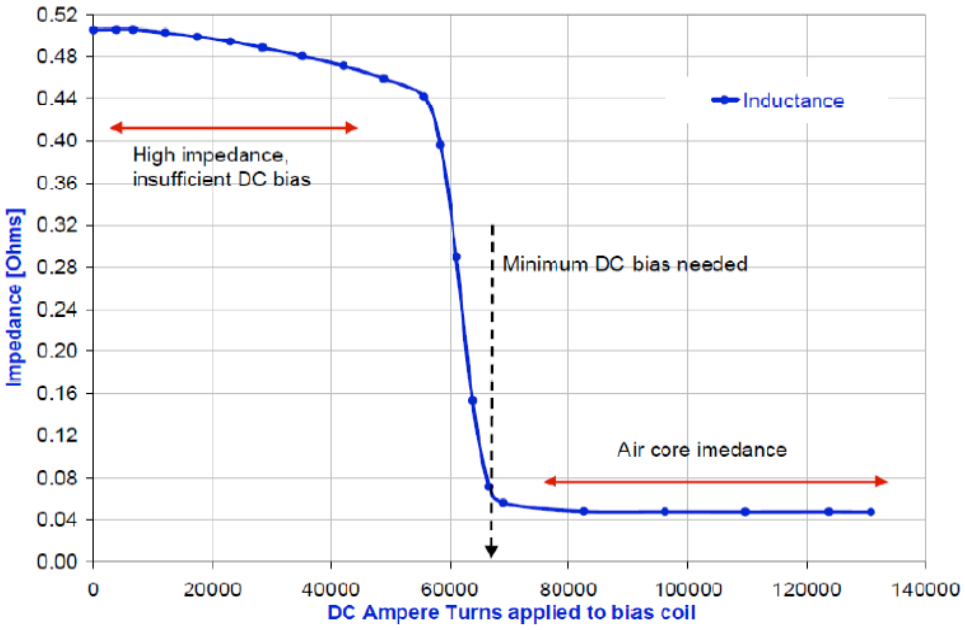

5.4 Fault Condition Testing

The objective of the fault condition testing was to evaluate the fault current limiting capabilities of the FCL under laboratory conditions.

5.4.1 Single-fault Test

The prototype FCL was subjected to a series of faults with different prospective fault current levels. Experimental results of a 23kA prospective fault current are shown in Figure 51. Figure 51(a) shows the comparison of the prospective (no FCL) current magnitude and the clipped, that is, limited by FCL, AC line currents during the fault experiment. Clearly, the FCL is able to successfully limit the first peak of the fault current in addition to the limiting of the successive peaks. Figure 51(b) shows the exploded view of FCL terminal voltage during the fault.

A comparison of the predicted (by the FCL's simulation model) and the measured percent of fault current clipping versus prospective fault current level is shown in Figure 52. The prototype FCL achieved 20% clipping of 20kA prospective fault current.

The measured bus voltage under fault condition with the FCL bypassed and with the FCL active is shown in Figures 53(a) and (b), respectively. Comparison of the waveforms clearly shows that due to the FCL's protective clipping the upstream bus voltage sag was significantly limited.

Figure 51: Experimental results of FCL clipping the 23kA fault: (a) comparison of a prospective fault current and clipped FCL current; (b) exploded view of FCL terminal voltage.

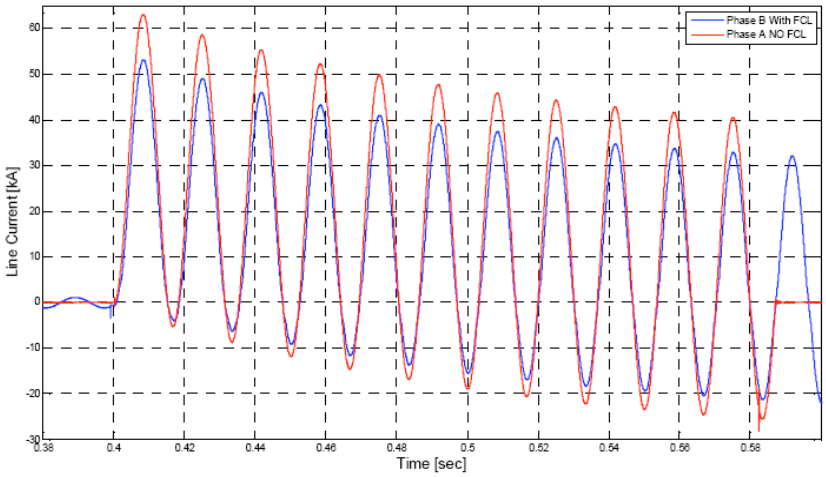

(a)

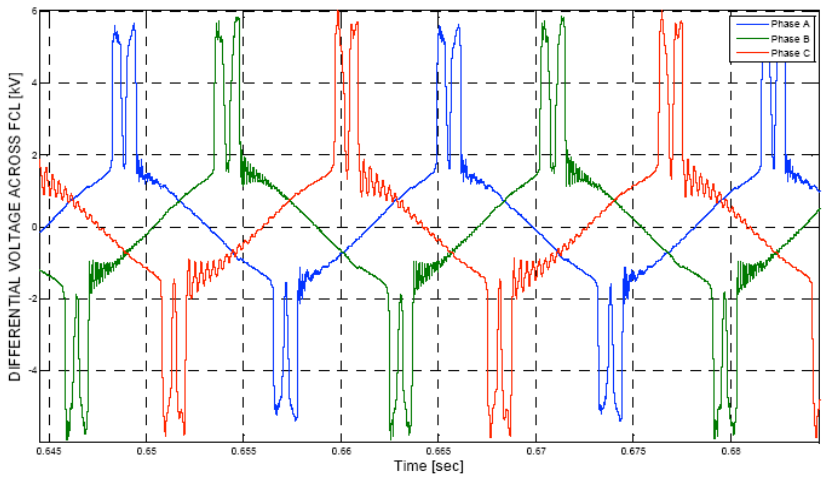

(b)

Figure 52: Percent of fault current clipping vs. prospective fault level.

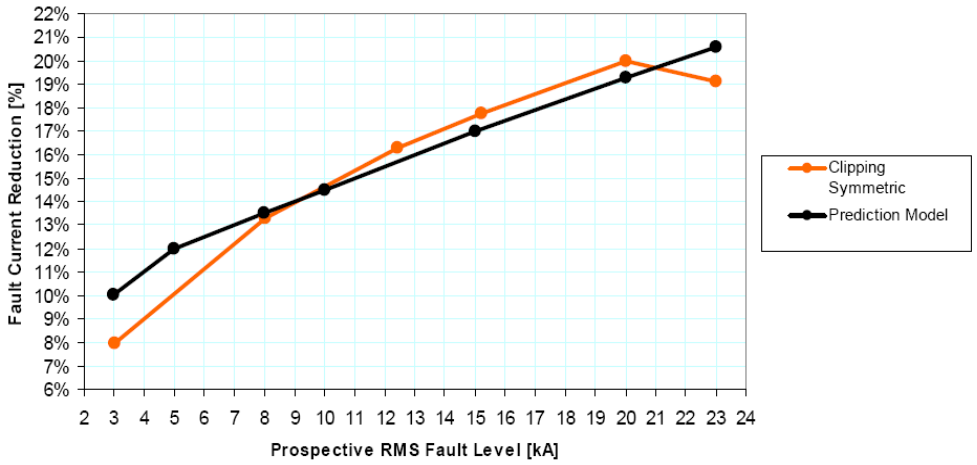

Figure 53: Experimental bus voltage sag under a 20kA fault condition: (a) with FCL bypassed; (b) with active FCL.

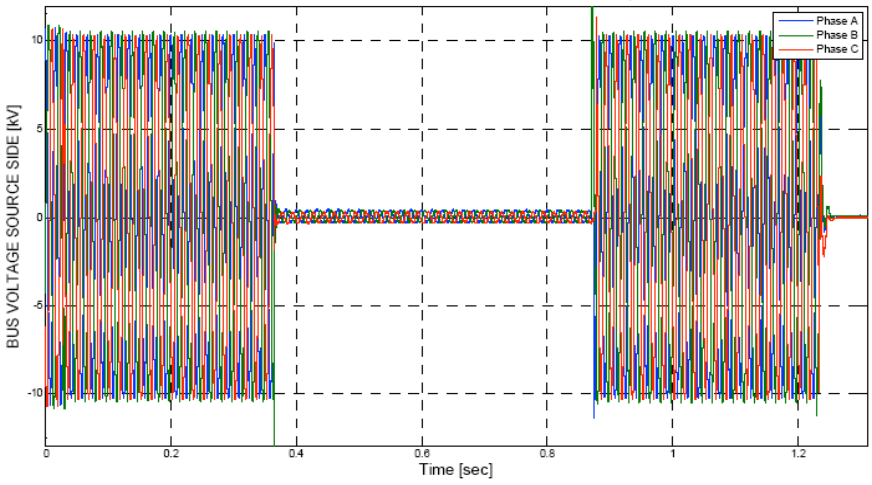

(a)

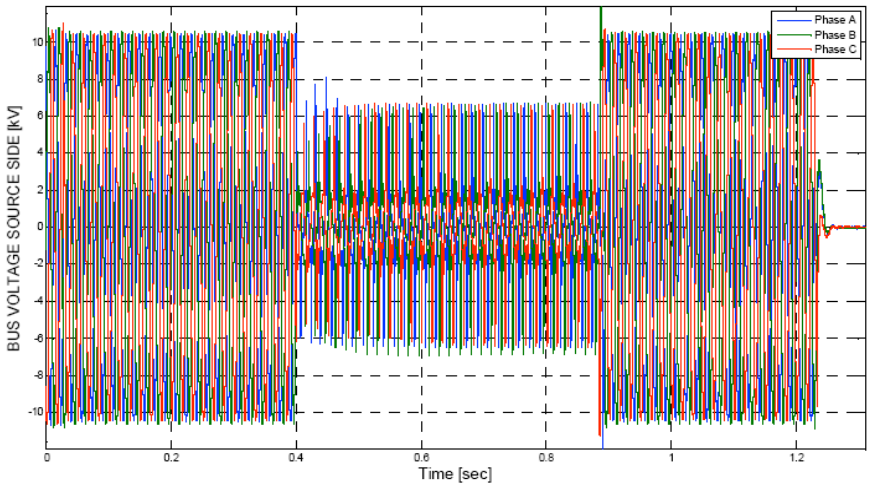

(b)

5.4.2 Double-fault Sequence

The prototype FCL also withstood a 20kA, double-fault sequence lasting for 20 cycles within a two-second time interval. The FCL succeeded in limiting both faults. Inspection of the experimental FCL current and voltage waveforms, shown in Figures 54(a) and (b) respectively, reveals that on clearance of the fault the prototype FCL had successfully recovered under load.

Figure 54: Experimental waveforms of a 20kA symmetric double fault 2 seconds apart: (a) FCL current; (b) FCL voltage.

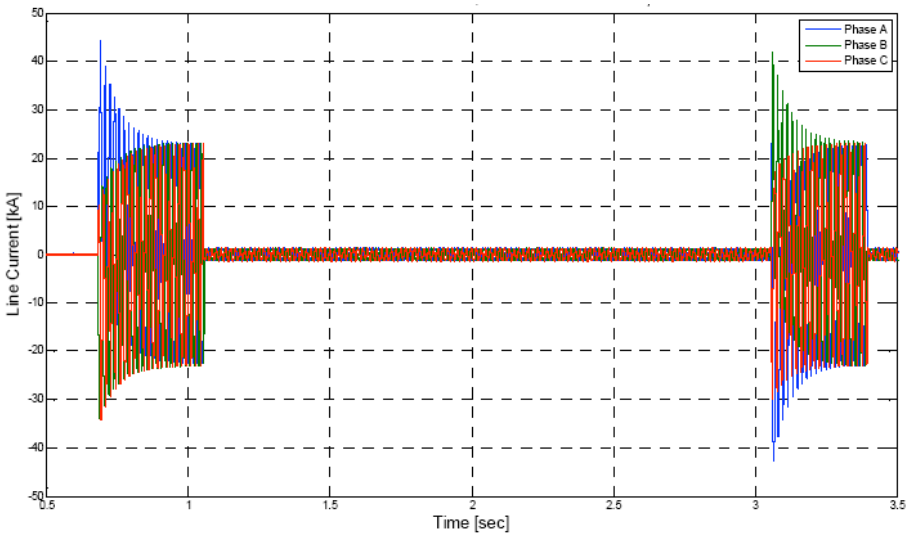

(a)

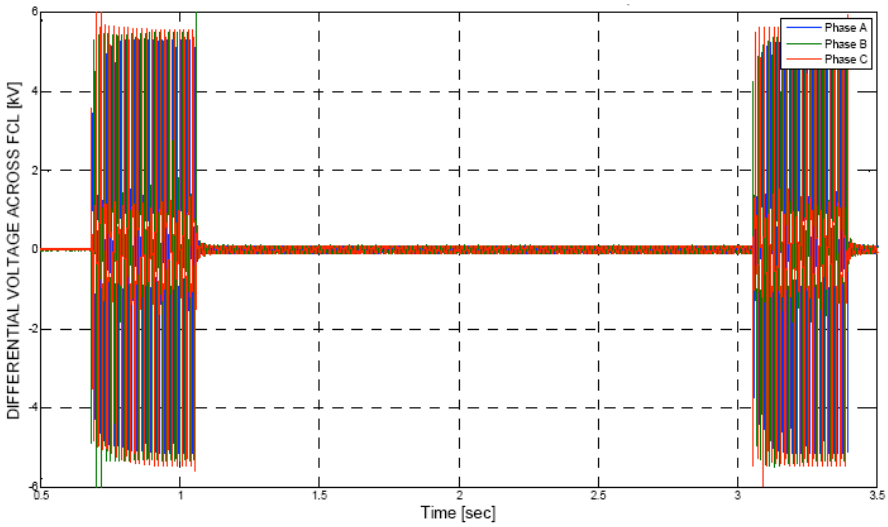

(b)

5.4.3 Endurance Test

The prototype FCL was also subjected to an endurance test and withstood a 20kA extra-long duration fault for 1.25 seconds , which is 82 cycles long. The FCL successfully clipped the fault without damage to itself. The experimental waveforms of the fault current during the endurance test are shown in Figure 55 and show no signs of abnormal activity.

Figure 55: Endurance test: experimental FCL current during the 20kA symmetric, 1.25 seconds, extra long fault.

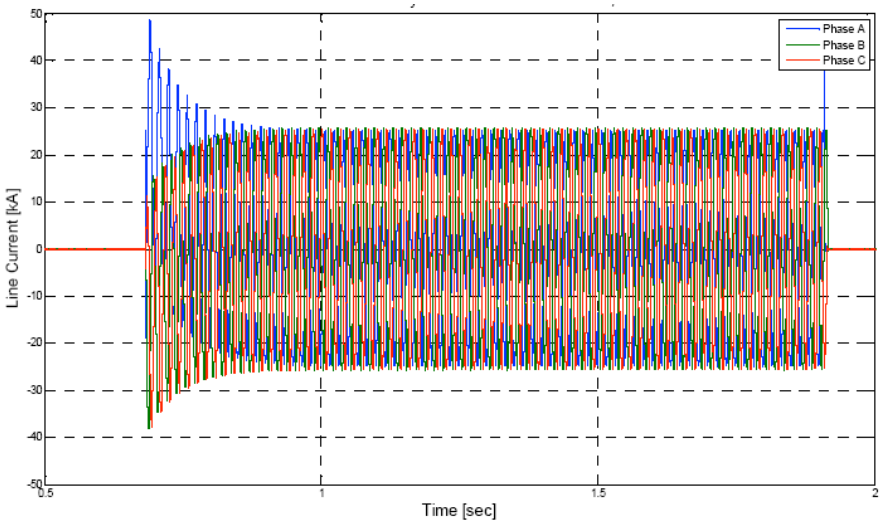

5.4.4 AC to DC Coil Coupling Test

One of the major concerns in implementing the Saturable Core FCL is the AC voltage that may be induced by the AC coil current in the DC coil. High voltage induced across the HTS DC coil may, potentially, destroy both the DC coil and the bias power supply and, therefore, should be controlled.

During normal operation the cores operate almost symmetrically, so that the AC flux in the center leg is mostly canceled out. As a result, the AC voltage induced in the DC coil is negligible. During the fault, however, the cores operate asymmetrically, with one of the cores at times out of saturation. By a proper geometry of the coils the coupling was minimized. Still, in a practical device some residual coupling, about 5%, between the AC and DC coils was observed as shown in Figure 56. As can be seen, higher DC bias results in lower coupling between the AC and DC coils. This reduces the risk of high voltage shock to the DC coil and power supply.

Figure 56: Test results showing the coupling of the AC-to-DC coils in the normal state and under fault conditions.

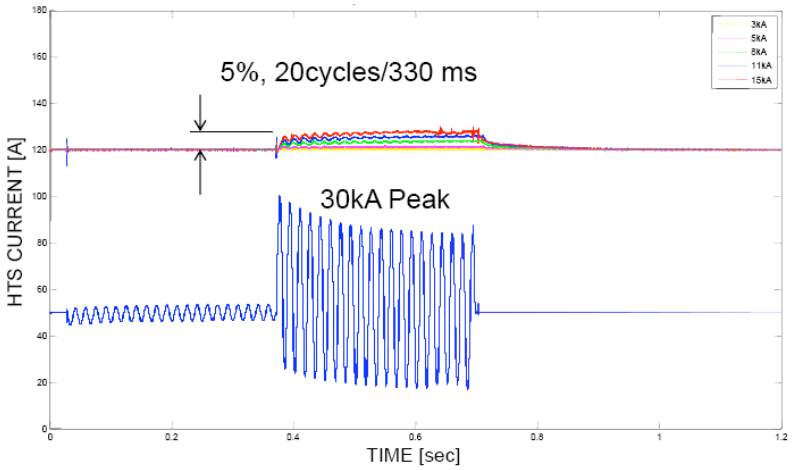

5.5 Summary

The prototype HTS FCL went through a series of rigorous laboratory tests in BC Hydro's Powertech Laboratory in Surrey, BC, Canada. A total of 65 separate tests were performed, including 32 full-power fault tests with first peak fault current levels up to 59 kA at the rated voltage. Fault tests included individual fault events of 20-30 cycles duration, as well as multiple fault events in rapid sequence (to simulate automatic re-closer operation) and extended fault events of up to 82 cycles duration, simulating primary protection failure scenarios.

The experimental FCL prototype has passed all the pre-connection, normal state and fault condition testing procedures. The prototype FCL proved to have low normal-state insertion impedance, was able to withstood real fault conditions, endured long duration faults, tolerated the resulting magneto-mechanical forces and thermal stresses with no damage and demonstrated instantaneous recovery under load.

Successful laboratory testing of the prototype Zenergy Power FCL earned its acceptance to be connected to a commercial circuit with commercial, industrial and residential loads.

CHAPTER 6:

Zenergy Power FCL Field Testing at SCE

The experimental FCL prototype was installed by Southern California Edison Co. (SCE) in the Avanti "Circuit of the Future" and was in operation from March 2009 until October 2010 for field testing and data collection. The installation was part of SCE's program for performance evaluation as well as for gaining experience with novel "smart grid" equipment. The prototype FCL was integrated into the utility SCADA system and operated in real time to provide protection to the distribution circuit. This comprehensive field demonstration was the first instance of an HTS FCL being used in commercial service in the US electric grid.

6.1 Setup and Metering

6.1.1 Avanti "Circuit of the Future"

The Avanti Circuit, shown in Figure 57, is a 12.47kV feeder serving residential, commercial and light-industry customers in San Bernardino, California. The Avanti Circuit is specially commissioned and instrumented to assess new "smart grid" technologies. The Avanti Circuit main feeder is about 7 miles long and composed of about 20% overhead and 80% underground construction.

Figure 57: Diagram of the Avanti "Circuit of the Future."

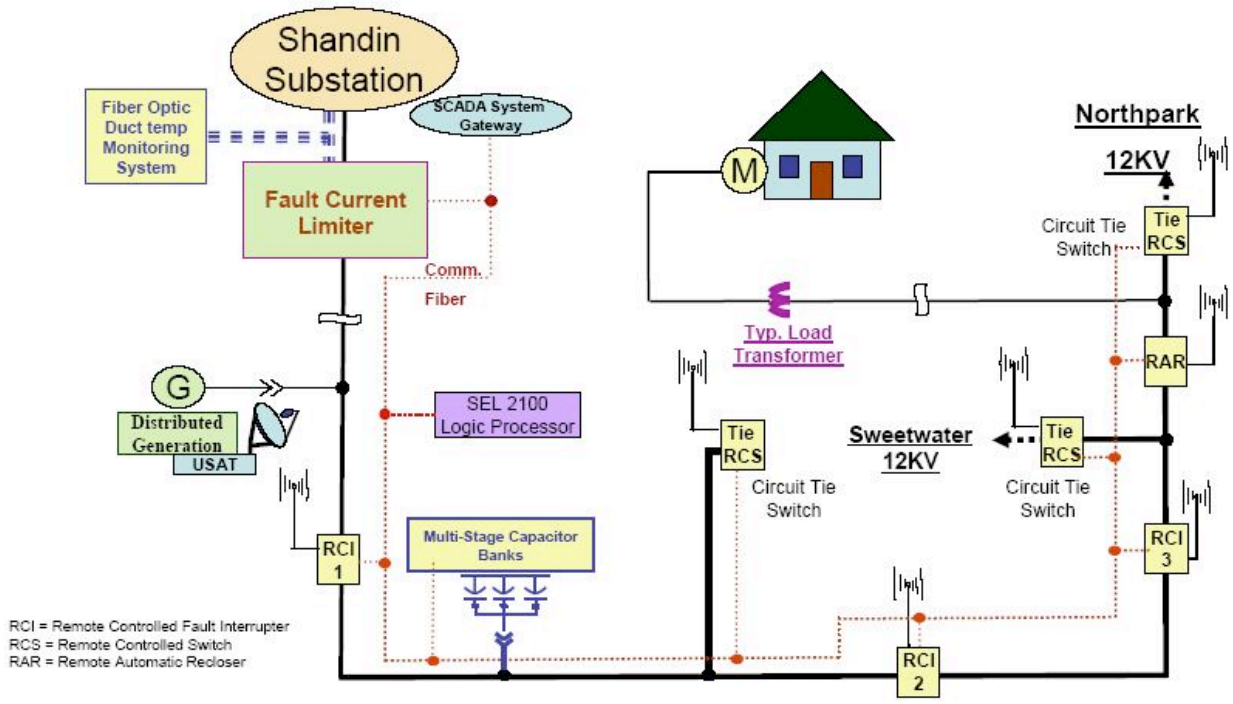

The experimental FCL prototype (Figure 58) was installed inside the Shandin substation fence line (Figure 59), immediately beyond the main feeder circuit breaker. The FCL was connected in series between the feeder loads and the 12 kV side of the substation's transformer bank. The FCL was also equipped with a bypass switch.

The purpose of the installation was to demonstrate the FCL's functions and gain operational and maintenance experience under real-world conditions [66], [67]. The operating environment at the substation is a severe, southwest US desert environment with hot, dry, dusty, high-wind conditions. Summer daytime temperatures were frequently well in excess of 40°C. Additionally, a residential neighborhood located nearby imposed a very restrictive ambient noise requirement.

Figure 58: View of the Zenergy Power Medium Voltage distribution-level three-phase Saturated Core FCL operating at Southern California Edison in Avanti Circuit of the Future.

Figure 59: FCL Installation in Avanti Circuit of the Future. Shandin Substation, San Bernardino, California, March 2009.

6.1.2 Metering

Figure 60 shows the schematics of the Shandin substation and installation of data recorders 1 and 2. Data recorder 1 is installed in the control room. Data recorder 2 is installed in the immediate proximity of the Zenergy Power FCL.

Data recorders are of the PX5 Drantez type with the following basic characteristics:

- Data volume: 1Gbit memory card (upgraded to 2Gbit).
- Data rate: 256 samples per cycle (60Hz line).
- Recording: Depends on setting, is triggered by current level, adjustable.
- Available recording time: depending on number and duration of recorded events.

These recorders have four independent channels. Three channels were monitoring the line currents and one channel was unused.

Figure 60: Location of the data recorders.

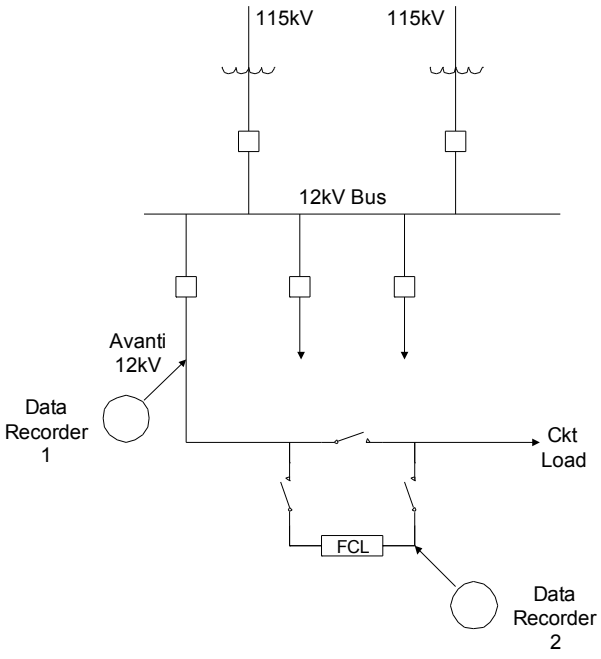

6.2 FCL Key Technical Events

6.2.1 Pre-Installation Events

A. Controller assembly and software testing – May 2008

This development task performed by Zenergy in preparation for the field prototype's implementation was a critical milestone. The basic monitoring and control software necessary to operate the FCL as designed was thoroughly tested and debugged in the lab prior to sending the FCL to the demonstration site. From this initial testing, the most important conclusions, derived in consultation with SCE's Advanced Engineering Group, were that redundant and fail-safe hardware and software designs as well as secure telecommunications were necessary.

B. Seismic analysis per IEEE Standard 693 – June 2008

Seismic modal analysis of the FCL unit was performed by Zenergy to determine any structural requirements to withstand a 0.5g zero-period acceleration, and to provide necessary information for SCE to design the anchorage, and stress release for the electrical connection according to the reaction forces. Finite element modeling and spectrum analysis up to 40 Hz with 2% damping indicated that the iron core of the AC coils required extra supports to limit stresses and deflections to within the allowable values, per IEEE Standard 693.

SCE's Civil Engineering Group was consulted to determine the best option for the physical installation of the FCL. One option considered for the foundation was to use railroad ties over the existing crushed gravel in the substation's yard. Another alternative was to build a traditional concrete foundation to ensure that the FCL would remain level in this seismically active area. The civil engineering team's recommendation was to set the FCL on compacted and leveled crushed gravel without any additional support because the FCL's enclosure is welded to steel I-beam skids.

C. FCL assembled and continuity and temperature rise tests performed – September 2008.

As there were no industry-accepted standards for FCL testing, NEETRAC, in close collaboration with several of its member utilities, including SCE, cooperated with Zenergy Power to develop a detailed FCL test program based on IEEE and CIGRE standards for transformers and reactors. The FCL was rated at 15kV, 1,200A rms, 110kV BIL, and designed to limit a 23kA rms symmetric prospective fault by at least 20%, with less than 1% voltage drop at maximum load current in the normal state. The FCL was first subjected to heat runs at a load current of 750A and full DC bias current to verify the maximum temperature rise of the AC coils and the HV terminations. All measurements were within the limits specified in IEEE Standard C57.16-1996.

D. High power and high voltage testing completed at BC Hydro – September 2008.

Prior to high-power testing, continuity and insulation resistance measurements were performed to verify that no movement of the device's components occurred during shipping. Source and load side bushing terminations were measured separately. A comprehensive battery of high-power tests was then conducted at BC Hydro's Powertech Laboratories. A total of 65 separate tests were performed, including 32 full-power fault tests with first peak fault current levels up to 59kA, all at rated voltage. Fault tests included individual fault events of 20-30 cycles duration, as well as multiple fault events in rapid sequence (to simulate automatic re-closer operation) and extended fault events of up to 82 cycles duration, simulating primary protection failure scenarios. The FCL measured performance agreed closely with the engineering calculations in all cases.

The FCL was then tested under full lightning impulse tests at Powertech's HV laboratory. Under the first round of tests, flashovers occurred between the HV jumper cables connecting the AC coils. All jumpers were replaced and re-arranged with more separation. Other HV

insulation enhancements made in order to pass the more severe chopped impulse tests included: application of heat shrink insulation over the exposed terminations; larger lugs and wall openings; molding mastic rubber to cavities, sharp objects, and connectors; and solid connection of all ground leads to a common ground point.

E. High Voltage testing performed by SCE's Westminster HV Lab – December 2008

HV acceptance testing was also conducted by SCE at its laboratories in Westminster, California, as follows:

- One reduced (1.2 x 50μs) full wave – 50% or 55kV peak wave
- One full (1.2 x 50μs) wave – 100% or 110kV peak wave
- One reduced chopped wave – 50% or 60kV peak wave (chopped at 2 μs)
- Two full chopped waves – 100% or 120kV peak waves
- Two full (1.2 x 50μs) waves (within 10 min after the last chopped wave)

All of the above and partial discharge tests were successfully passed by the FCL per IEEE Standard C57-12.01-2005.

F. Cold-head replacement – February 2009

One of the two cold heads of the helium refrigeration sub-system was replaced as a routine preventive maintenance task that was due. From this experience it was learned that this hardware needs better accessibility.

6.2.2 Post-Installation Events

A. The FCL was energized on the Avanti Circuit of the Future – March 9, 2009

On-site commissioning tests by SCE were successfully passed. These tests consisted of coil resistance, power factor, and megger measurements of all phases. These measurements were performed as a safety and reliability check every time work was conducted in the HV compartment to verify that the HV insulation had not been disturbed.

The change of the FCL's insertion inductance as a function of the DC bias current was also measured by SCE when HTS DC magnet bias system was first energized and de-energized.

B. Damped resonance event triggered by controller memory overflow – March 16, 2009.

The FCL experienced a loss of DC bias current, caused by a reset of the Programmable Automation Controller that was triggered by a RAM overflow. This shutdown occurred at a time when the Avanti Circuit's load current was approximately 120A. The FCL remained in the circuit for approximately 45-50 minutes, producing an initial 300V line voltage rise, followed by a 400V line voltage drop on the 12 kV circuit bus. During this period, two large automatic capacitor banks operated to regulate the voltage on the circuit according to their programmed limits. The combination of the FCL's high inductance due to the absence of DC bias current and the high shunt capacitance caused an intermittent damped resonance condition. The FCL was bypassed after 50 minutes and the circuit returned to normal operations. The FCL remained bypassed and was operating in the standby mode until December 9, 2009 after an automatic bypass was installed.

In more detail the event occurred as follows. At 10:10 am the DC bias current source shut off, initiating the feeder's voltage rise. At 10:13 am, three minutes into the event, the system voltage had risen above the upper dead-band limit (12.45 kV) of the 1.8 MVAR capacitor bank. After 60

seconds above the dead-band limit the 1.8 MVAR capacitor opened. Without a capacitor bank, the system voltage dropped to about 11.65 kV at 10:14 am. At approximately 10:17 am the 1.2 MVAR capacitor bank switched in, due to the system voltage being below the lower limit of the dead-band for three minutes. This action caused the feeder to re-enter a resonance condition. As a result the voltage increased to 12.4 kV. The feeder voltage remained at 12.4 kV until the FCL was manually bypassed at approximately 11:35 am. After the FCL was bypassed, the system voltage dropped to approximately 12.2 kV, which was approximately the same voltage as before the event. There were no negative consequences, but as a result of this event, SCE installed an automatic bypass switch and set in its automatic mode whenever the FCL was in service.

C. HVAC shutdown due to excessive ambient temperature – June 2009

An ambient temperature of 108°F was reached at the site in June 2009. The refrigeration systems of the device had operated almost continuously since its installation. During a hot summer week, the FCL experienced venting of the cryogenics fluid and required replenishment of the liquid nitrogen due to a shutdown of the compressor compartment air conditioning unit.

The solution was to upgrade the 3 ton HVAC to a 5 ton unit rated at 125°F ambient working temperature. An extension to the existing compressors' enclosure was added to provide sufficient air flow to the three faces of the heat-exchanger coils. A shade structure for the 5 ton HVAC and the compressors enclosure was also built to protect the FCL from the direct sun explosure. No changes were needed for the station's power and light supply and there were no more HVAC interruptions through the summer, which had even hotter days than before.

D. Controller upgraded, including watchdog function – June 2009

During the outage taken to install the higher rated HVAC unit, the controller was also upgraded. A more robust industrial-grade controller was installed with software and communications to perform the monitoring and control functions being performed by the original controller but with higher reliability to withstand the harsh environment found at Shandin Substation.

At this time a watchdog function was also added at the request of SCE to bypass the FCL in the event of loss of any of the critical control functions or loss of auxiliary and/or backup power.

E. Helium leak detected and fixed – June 2009

A slow helium leak was detected by observing the pressure and temperature trends of the cooling system. This did not cause any malfunction or shutdowns, but the leak was located and corrective action was taken.

F. The FCL returned to the online mode after the automatic bypass was installed – December 9, 2009.

G. Multiple-fault event successfully managed by FCL – January 14, 2010

Ten months after installation, the FCL experienced its first in-service fault. Measured data by SCE and Zenergy Power confirmed that the event evolved from a phase-to-phase fault, to a three-phase fault, to a temporary recovery, to a phase-to-phase fault, to another three-phase fault, ending with an open line and clearing. This multi-fault event occurred over a three-second period. The sequence initiated when phases A and B of the overhead section of the Avanti Circuit came together during high wind conditions. This phase-to-phase fault lasted about 250 milliseconds, when Phase C also faulted, thus evolving into a three-phase fault, lasting about half a second. The air recovered its dielectric strength for about one second, but then the conductors of phases A and B again flashed over to each other for about three quarters of a second. The arc was about to be extinguished at this time, but again Phase C also flashed, resulting in a three-phase fault. The event ended about a quarter of a second later when Phase B

conductor separated and dropped to the ground, and the circuit's protection cleared this solid ground fault.

The FCL limited the fault current throughout the various faults and sent the corresponding monitoring and control signals as designed.

H. Nitrogen pressure stability problem fixed – February 2010

The cause of this problem was that the cold-head heaters' power changed in steps that were too big, causing overshoot in the system's temperature control. As with the slow leak problem, this was detected through long-term observations.

An improvement with finer resolution of the power increments to the heater elements and a feedback loop stabilized the pressure and temperature and solved the problem.

This problem did not have any negative impact on the operation of the FCL, but the associated engineering and maintenance needed to fix the problem inspired the option of using dry cooling in future FCL's.

I. Shutdowns due to loss of wall power caused by transmission system fault – March 2010.

The FCL experienced three outages of substation auxiliary power due to faults on the high-voltage side of the substation or on the transmission lines. In one of these events where auxiliary power was lost, a fault on the 115kV high-voltage side caused a voltage dip and a two-minute outage on the 12kV side of the substation.

As required by SCE, the FCL's controller immediately issued a bypass command, sent out alerts to SCE and to Zenergy, and initiated an orderly shutdown of the DC bias current and cooling systems. It sent the correct alarms and bypass commands to SCE. Upon resuming AC power, the cooling system compressor was restarted and the cryogenic parameters returned to normal, with the HTS coil ready to be re-energized.

The FCL is now equipped with a DC uninterruptible power supply, which allowed it to ride through these types of outages without downtime.

J. Shutdown due to shorted terminal block – August 2010

This event initiated tripping of the auxiliary power from the substation's light and power panel. The FCL's controller again safely bypassed the unit, alerted SCE of the event, and shutdown the unit as designed.

The problem was caused by a loose connection at one of the supply cables on the terminal block where the auxiliary power to the FCL is received. A higher rated terminal was installed and the proper torque value to use was included in the installation manual.

K. Decommissioning of the Avanti FCL per agreement with SCE announced by Zenergy – October 2010.

The Zenergy FCL was removed from service on December 16, 2010, after having successfully completed its intended period of field testing.

6.3 Analysis of Major Events

6.3.1 DC Bias Current Loss Event, March 16, 2009

A. General Overview

A loss of bias event is a severe failure of the FCL and therefore was analyzed in detail in order to study the implication of such an event on the power system [68].

The Avanti Circuit is a 12kV distribution feeder. There are four shunt capacitor banks installed on the Avanti Circuit for voltage support. At the time of the event, two of the four capacitor banks were disabled. The capacitor banks remaining in service (see Figure 61), are rated at 1.2 MVAR and 1.8 MVAR. Both banks are connected in an ungrounded wye configuration and are capable of switching automatically. Prior to the event the 1.8 MVAR bank was closed, and the 1.2 MVAR bank was open.

Figure 61: Diagram of the Avanti Circuit relevant to the resonance event.

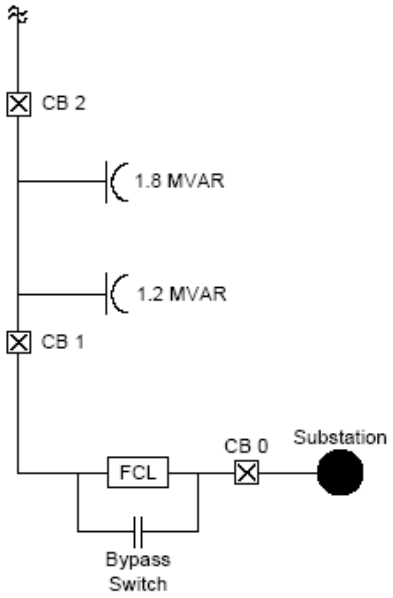

The switchable capacitor banks operate on a time-biased voltage control. The switched capacitor banks open or close if the measured voltage is outside of a programmed dead-band for a set duration. The capacitor banks also were set to perform an emergency open or close if the voltage is measured at 130 V or 110 V (on a 120 V base), respectively, for five seconds. The 1.8 MVAR capacitor bank was programmed to open on 124.5 V and close on 120.0 V (on a 120 V secondary base), and had a delay of 60 seconds. The 1.2 MVAR bank was programmed to open on 125.0 V and close at 121.0 V (on a 120 V secondary base) and had a delay of 180 seconds. It is important to note that the capacitor controls are set with a five minute delay before a capacitor bank can perform another open or close operation. Data was sampled at CB 1 and CB 2 where SEL-351 relays from the Avanti Circuit's advanced protection scheme were monitoring and reporting A-B phase voltage, and phase current every 5 seconds.

B. Description of the Event

Prior to DC bias current loss on March 16, 2009, the FCL was operating normally. The FCL's inductance is not a constant number even during normal operating conditions, but is a function of instantaneous AC current.

As shown in Figure 62, at 10:09 am the DC bias current source shut off, initiating the feeder's voltage rise. Current in the DC coil took approximately 5 minutes to decay to trace levels. Figure 63 shows the HTS coil's DC current (blue) and its voltage (red) during the event. The coil voltage dropped from predominantly resistive 120.0 mV to predominantly inductive -2.0 V, and decayed after several minutes as the HTS current settled to zero.

Figure 62: Recorded data: HTS coil current (blue) and coil voltage (red) during the event.

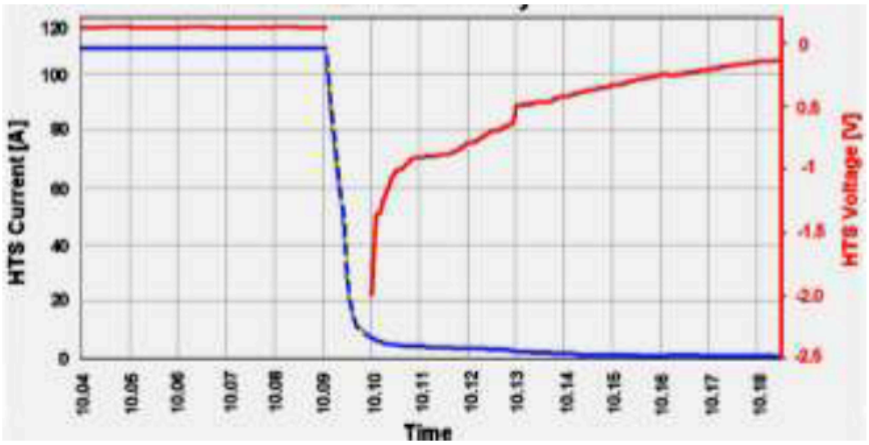

At 10:13 am, four minutes into the event, the system voltage had risen above the 1.8 MVAR capacitor bank's upper dead-band limit (12.45 kV). After 60 seconds above the dead band limit, the 1.8 MVAR capacitor opened. Without a capacitor bank, the system voltage dropped to about 11.65 kV at 10:14am. At approximately 10:17 am the 1.2 MVAR capacitor bank switched in due to the system voltage being below the dead-band lower limit for three minutes. This action caused the feeder to re-enter a resonance condition. As a result the voltage increased to 12.4 kV. The feeder voltage remained at 12.4 kV until the FCL was manually bypassed at approximately 11:35 am. A loud humming sound in the FCL was due to the high magnetostriction of the iron cores undergoing large flux variations. After the FCL was bypassed, the system voltage dropped to approximately 12.2 kV, which was approximately the same voltage as before the event.

Figure 64 shows the line-to-ground voltages, as measured by the three potential transformers installed at the load side of the FCL. The HTS current (black) also appears for reference. Both feeder voltage and feeder current as measured at the FCL agreed with SCE's field data.

Figure 63: Recorded data: Line-to-line voltage between A and B phase at CB 1 (a) from 10 minutes before the event to 25 minutes past the end of the event; (b) for the first 18 minutes of the event.

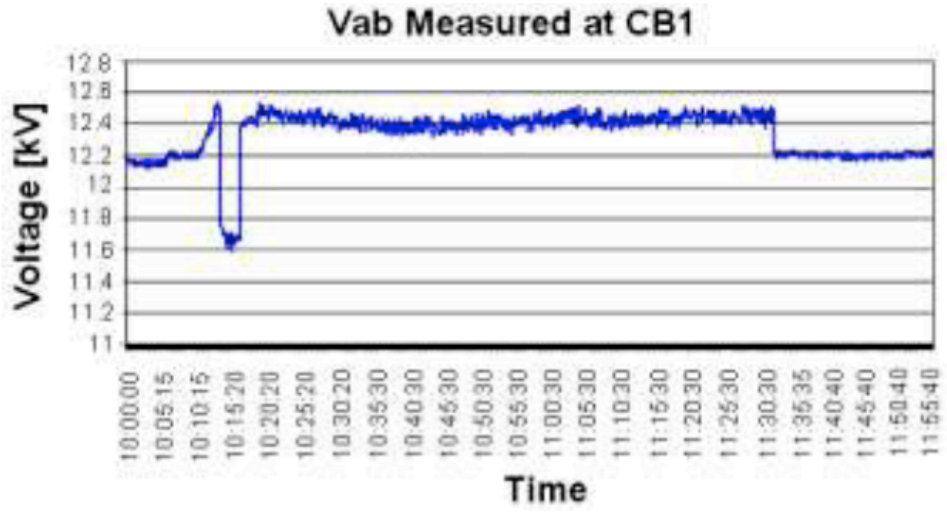

(a)

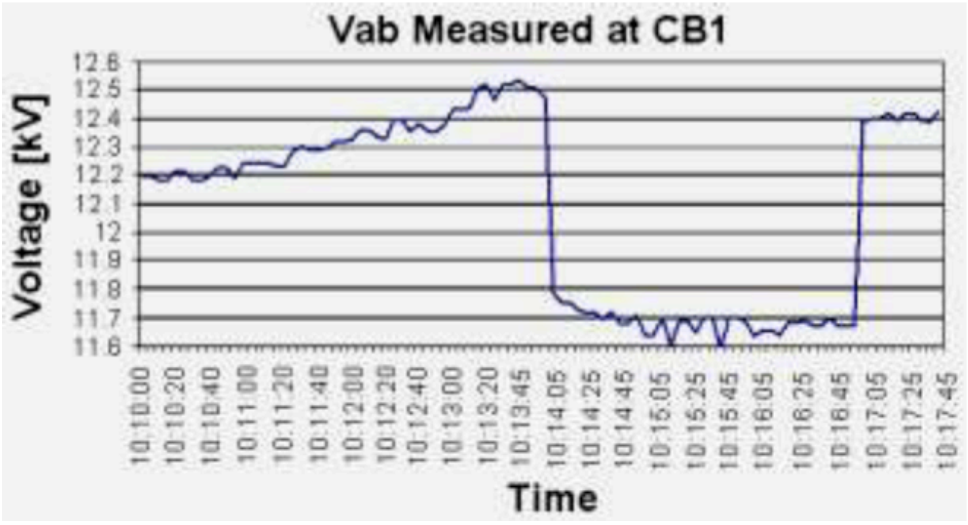

(b)

Figure 64: Recorded data: (a) HTS coil current (blue) and coil voltage (red); (b) HTS coil current (black) and line-ground voltage dynamics (blue-red-green) during the event.

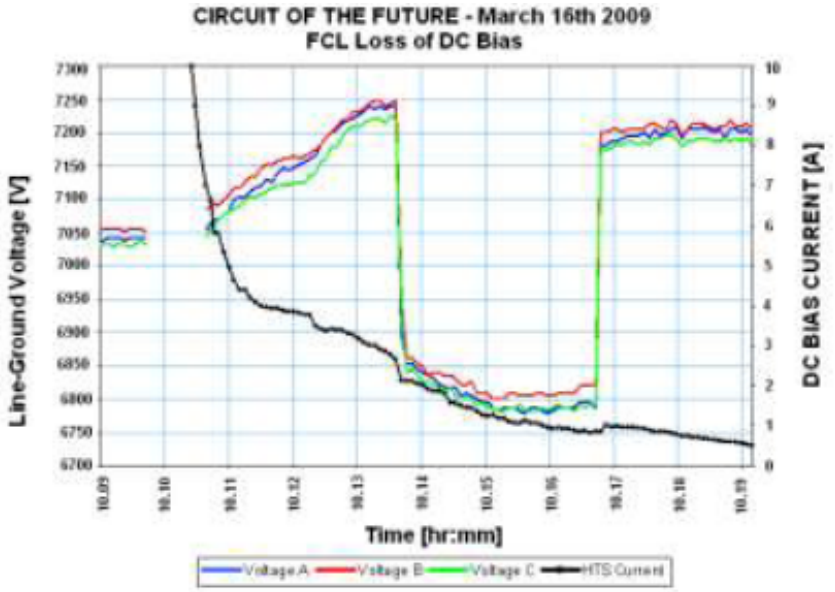

C. Observations

The measured bus voltage tended to increase due to resonance between the 1.8 MVAR capacitor and the increasing FCL inductance of de-saturation due to loss of the DC bias in the FCL. Note that the 1.8 MVAR capacitor bank switched out before the DC coil's current decayed to trace amounts. If the DC coil had decayed to trace amounts before the 1.8 MVAR capacitor bank opened, simulations show the line voltage would have risen to 12.65 kV. Simulations showed that, under normal system conditions, the voltage rise due to the 1.8 MVAR and the 1.2 MVAR capacitor banks would be about 0.2 kV and 0.12 kV, respectively. When the 1.8 MVAR bank opened, the resonance condition ceased and the system voltage dropped to 11.87 kV. This voltage drop from 12.2 kV was due to the FCL's voltage-drop under de-saturating conditions. This measurement allows comparison of the line voltage for the saturated FCL with that for the de-saturating FCL without a masking effect due to resonance. The line voltage decrement from 12.2 kV (saturated FCL) to 11.87 kV was caused by the FCL's voltage drop. Furthermore, the DC current was still decreasing, causing the FCL's voltage drop to increase, resulting in a further decrease to 11.65 kV.

D. Simulation Study of the event

The PSCAD model in Figure 65 was adapted to simulate FCL interaction with the Avanti Circuit during the DC bias current loss and the resulting resonance phenomenon. The event was simulated by estimating the transient decay of the DC bias current and calculating the transient increase of the FCL inductance. As the FCL's DC bias current collapses, simulated FCL inductance shows increasing swings riding upon a quasi-exponential rise, as shown in Figure 66. The steady increase in inductance occurs as the operating point of the FCL's core swings over to steep slopes in the B-H magnetization curve due to the DC bias current loss. The protuberance on the FCL inductance creates a resonance condition with the 1.8 MVA capacitor bank resulting in a rise in bus voltage.

Comparison of the simulated and measured line to ground voltages during the event is given in Figure 67. Good agreement of the simulated and measured results suggests that the Zenergy

Power FCL model is capable of closely reproducing the loss of DC bias current event and the resonance condition that followed.

Figure 65: Simplified PSCAD model of FCL installed in the Avanti Circuit.

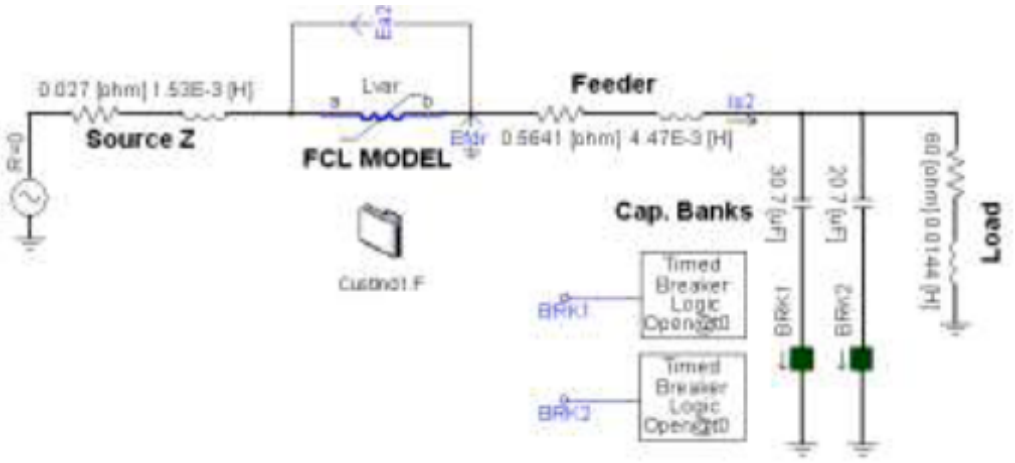

Figure 66: Simulated FCL rms inductance during the loss of DC bias event.

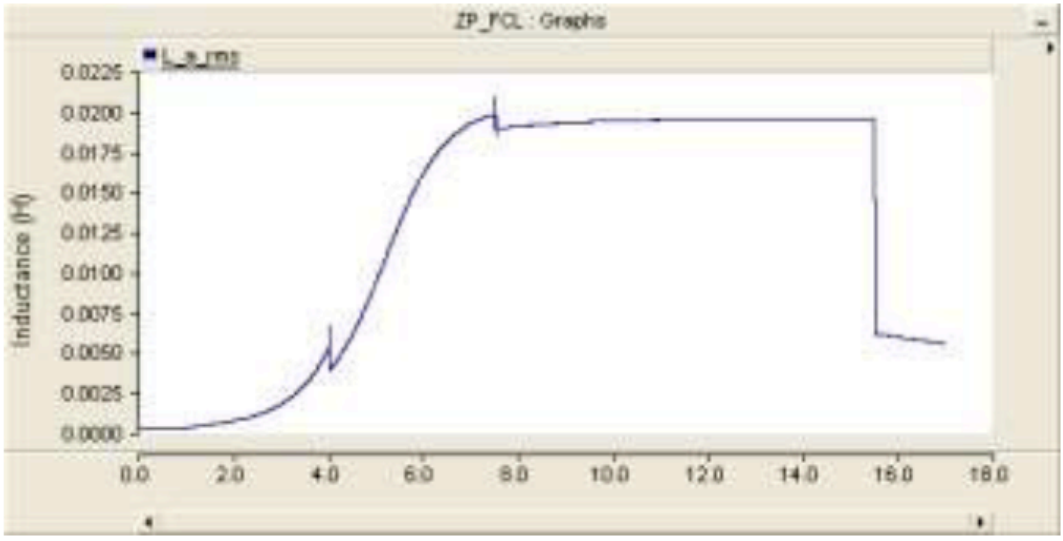

Figure 67: Comparison of simulated (blue trace) vs. measured line-to-ground voltage.

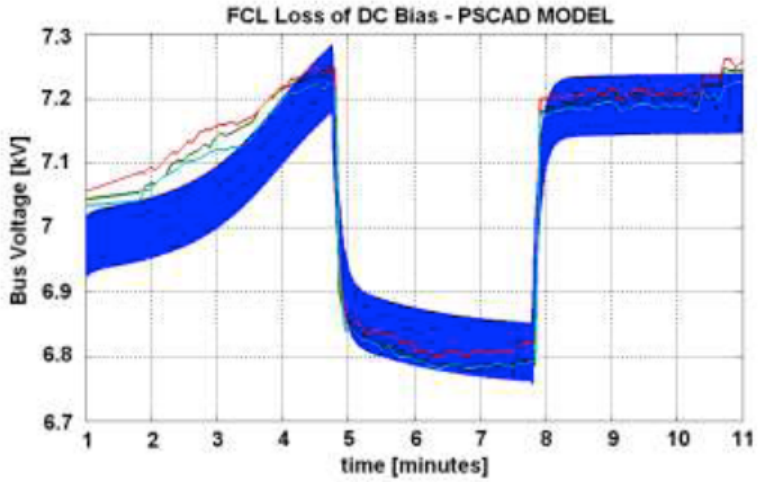

E. Recommendations for Resonance Suppression

i. Design

In the design process, simulation of the resonance should be conducted, including capacitor banks in the line where the FCL is to be installed at different loading conditions, to check for extraordinary events in the controller's logic. This entails an increased FCL inductance under de-saturation conditions.

ii. Operational

The ideal protection against resonance in this case is to immediately bypass the FCL. Given that the event evolves relatively slowly, an automated switch that can operate on the order of seconds is adequate.

Fixed capacitor banks should be carefully evaluated, and if they are integral to the FCL installation, operational planning should account for their presence. This measure is recommended,, because if the automated bypass switch would fail to close, the capacitor banks could be disconnected automatically. STATCON type of reactive conpensation should be a better alternative since it has the ability to regulate the circuit voltage within the design range. Lastly, base loading of the circuit should be increased, if operating conditions allow, as a more heavily loaded FCL is less likely to remain in a potential resonance condition.

6.3.2 Downstream Short Circuit Fault, Jan 14, 2010

A. Description of the Event

Prior to the fault event on January 14, 2010, the FCL was operating normally. The pre–event circuit load was approximately 100 A measured at the Avanti CB with system voltage approximately 12.1 kV near the fault. High winds were reported in the area of the overhead-line section of the 12kV Avanti Circuit located approximately 5.7 miles from Shandin Substation.

On January 14, 2010, at 9:58 am, the FCL experienced an in-grid fault. The voltage data recorded at the load side of the FCL is shown in Figure 68. The data suggests the following scenario. The event evolved from a phase-to-phase fault, to a three-phase fault, to a temporary recovery, to a phase-to-phase fault, to another three-phase fault, ending with an open line and clearing. This

very unusual, mostly symmetrical, multi-fault event occurred over a three-second period. Physically, the event was initiated by the overhead conductors of A and B phases slapping together during high wind conditions near the end of the Avanti Circuit. This phase-to-phase fault lasted about 250 milliseconds, when Phase C also faulted, thus evolving into a three-phase fault, lasting about half a second. The air insulation recovered its full dielectric strength for about one second, but then the conductors of phases A and B again arced to each other for about three quarters of a second. The arc was about to be extinguished at this time; however, Phase C also arced, becoming another three-phase fault. The event ended about a quarter of a second later when Phase B conductor separated and dropped to the ground, and the circuit was eventually cleared by system protection.

Figure 68: RMS voltages (upper screen) and currents (lower screen) measured downstream of FCL during the sequence of the multiphase fault event.

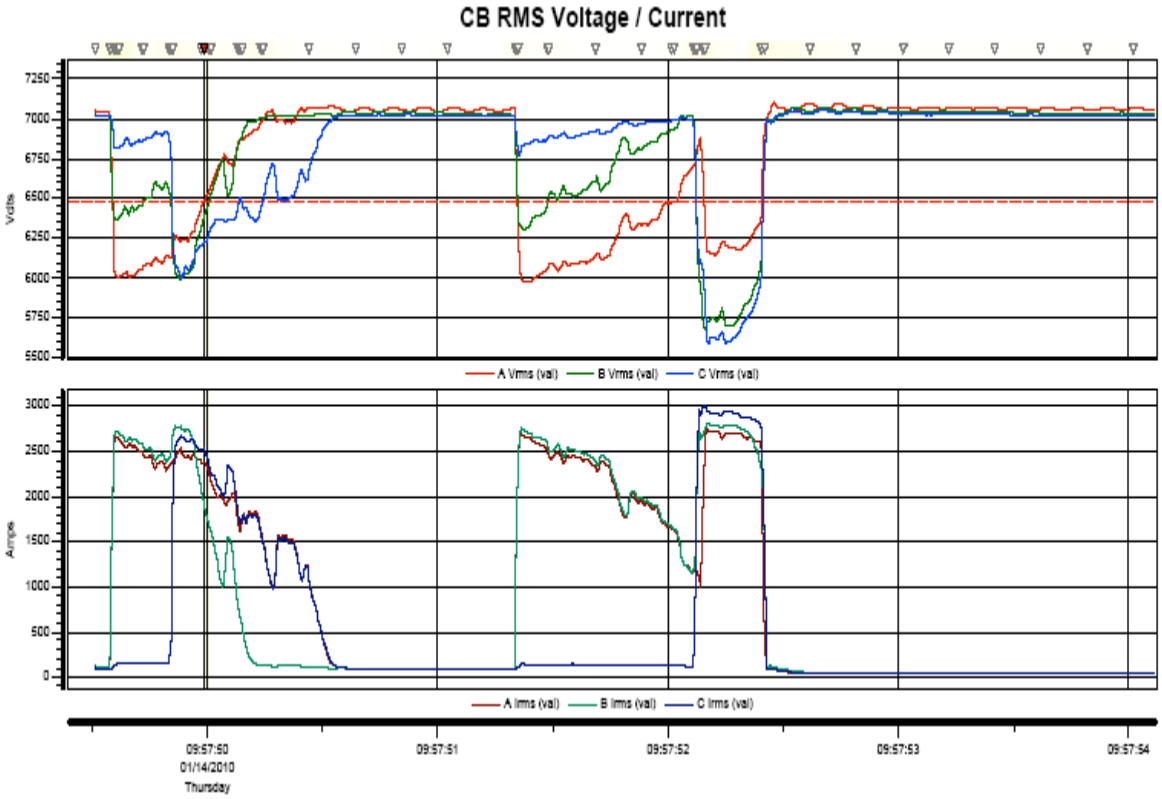

B. Simulation Study of the Event.

The FCL performance during the fault event was evaluated using the Zenergy Power FCL PSCAD simulation model previously described. As a first step, the FCL model performance was verified by comparison with realistic test results obtained during the FCL's laboratory testing. The comparison of both simulated and real fault current clipping vs. the prospective fault current is shown in Figure 52. This comparison shows that the accuracy of the simulation model is satisfactory.

As the next step, the FCL model was embedded into a PSCAD model of the Avanti Circuit to perform a full-circuit simulation of the event. To resolve the difficulty of establishing the exact arcing impedances during the fault, the fault scenario was approximated by several linear

segments of appropriate duration. Fault impedance for each segment was adjusted so as to generate the average fault current within the segment. PSCAD simulation results of the Avanti Circuit fault with the FCL bypassed are shown in Figure 69(a). Next, the FCL's bypass switch was opened and the FCL was introduced into the circuit, affecting the current flow. Since the FCL is a highly nonlinear device, during the normal state its impedance is very low; however, under fault conditions the FCL's inductance increases sharply. PSCAD simulation results of the fault event with the FCL in the circuit are shown in Figure 69(b).

Comparison of the fault current levels for both cases, that is, with the FCL bypassed and with the FCL active, is summarized in Table 3. Clearly, during this sequence of events, the FCL operated as designed and limited the fault current. However, the prototype FCL was designed for clipping 20kA fault current. Since the fault impedance was relatively high the fault current magnitude during the event was below 3kA. For such current levels, the experimental FCL provided partial clipping as designed (see Figure 69).

Table 3: Comparison of the fault current levels with active and bypassed FCL.

Segment	Active FCL	Bypassed FCL	% Clipping
F1	2554	2748	7.1%
F2	2782	2979	6.6%
F3	1568	1592	1.5%
F4	norm	norm	norm
F5	2643	2861	7.6%
F6	1968	2035	3.3%
F7	2782	2979	6.6%

Figure 69: PSCAD simulation results of multiphase fault: (a) FCL bypassed; (b) FCL active.

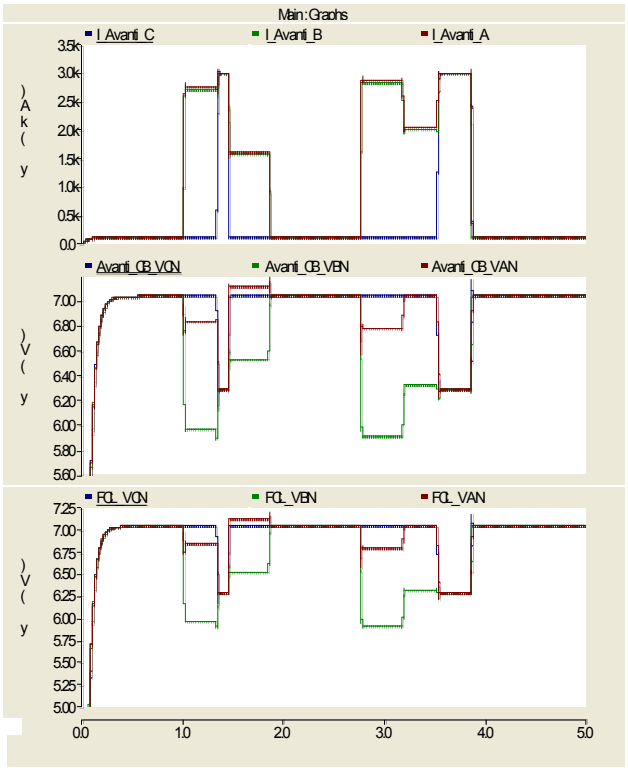

(a)

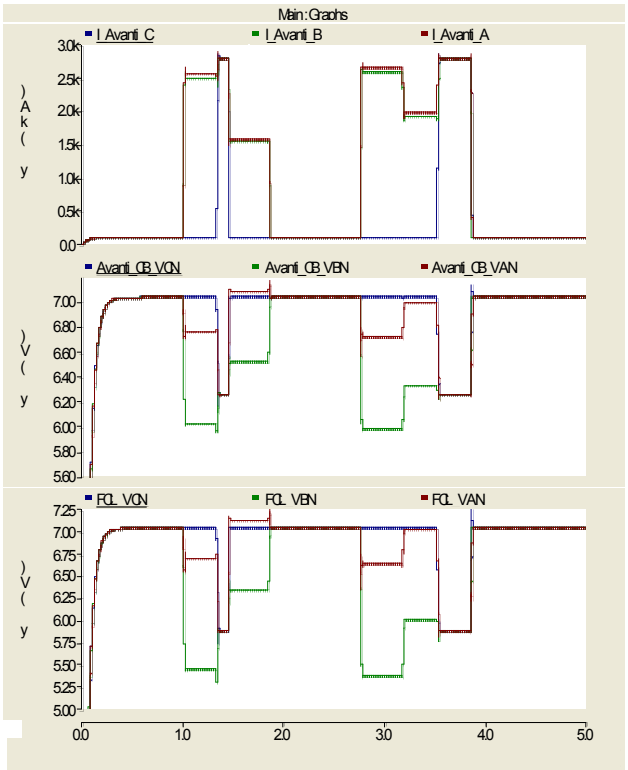

(b)

Another valuable observation was made regarding how the cryogenics and bias circuit responded during the fault. The measured performance is shown in Figure 70. The upper screen shows HTS magnet current and voltage; the lower screen shows the line currents. The fault instant can be recognized by the sudden decrease in load current due to the CB clearing the affected branch. There was no noticeable change in the DC bias and it was not affected by the fault current. No measurable effects on the cryogenics system, cold-head temperature or liquid nitrogen were observed either.

Figure 70: Cryosystem behavior during fault.

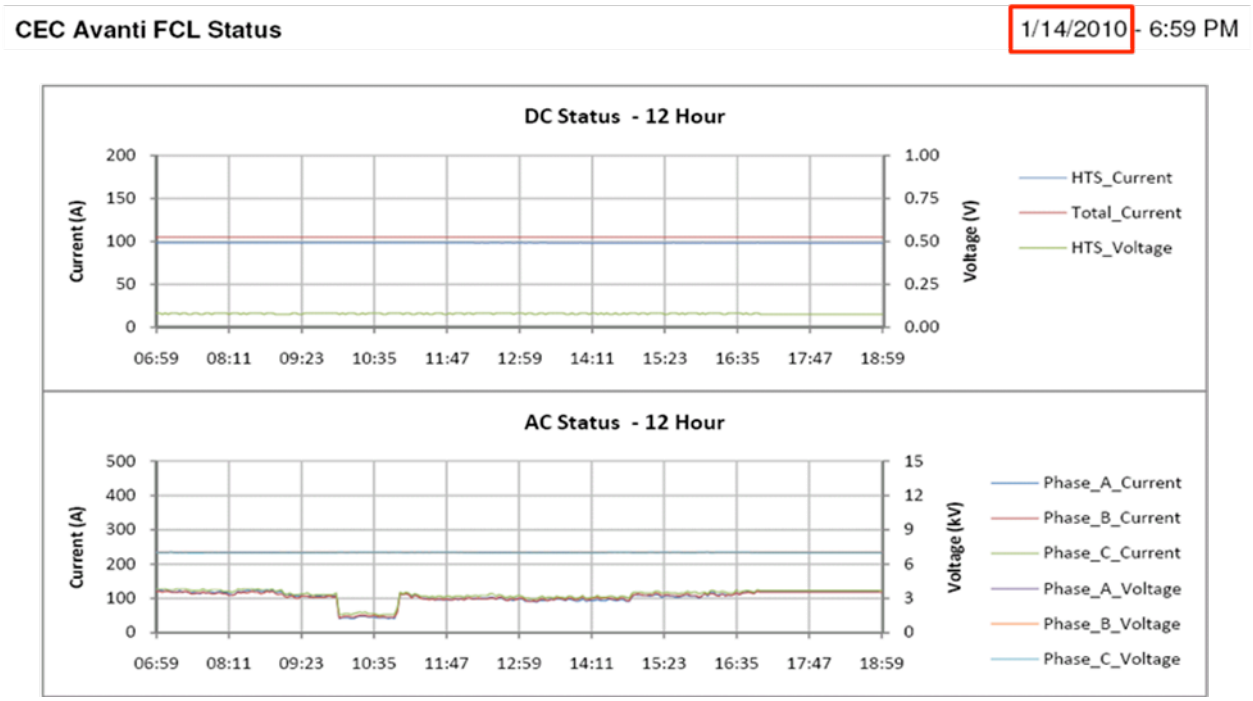

6.4 Summary

The prototype "Spider" saturable core HTS FCL was installed by Southern California Edison on the Avanti 'Circuit of the Future' in San Bernardino, California, for the field test. The FCL was energized on March 9, 2009 and decommissioned in October 2010, and removed in Decenber 2010. The Avanti Circuit is a dedicated 12.47kV feeder serving actual residential, commercial and light-industrial customers of SCE. The objective of the demonstration was to obtain service experience with state-of-the-art equipment and operating procedures that could result in increased system reliability and lower costs. The FCL was integrated into the utility's SCADA system. The FCL operated in real time to provide fault current protection to this distribution circuit of the California power grid.

The field demonstration provided a living laboratory to study the HTS FCL design, engineering, and operation. The experience gained from this demonstration has been invaluable to the evaluation and improvement of the FCL, contributing to a second-generation "compact" design, commercial sales, and migration to the development of a transmission-level HTS FCL.

CHAPTER 7:

Development of Zenergy Power Second Generation "Compact" FCL

Despite the success of the "Spider" FCL design, the large size and weight of the air-dielectric, closed-core FCL architecture relative to its electrical power rating challenged the economic value proposition at distribution voltages. At the same time, the air-dielectric design complicated scaling-up the device to higher voltages. In light of these issues, Zenery Power conceived an open-core FCL design that uses oil dielectric and conventional transformer design and manufacturing techniques to create a much smaller FCL with greater fault limiting performance and much higher voltage and power ratings. This new design is referred to as the "Compact" FCL.

7.1 "Compact" FCL Concept

The architecture of a single-phase Compact FCL is shown in Fig. 71. The FCL is built around two I-shaped iron cores. The AC coils are wound in opposite polarity, see Figure 71, and are connected in series with the load . Two DC coils are wound on top of the AC coils around both iron cores. The DC coils are wound with the first-generation HTS wires. The HTS coils form a strong magnet field by a low voltage high current DC power supply. Utilization of the HTS magnet allows reduction of the DC bias circuit resistance which helps to realize a high bias current and a high magnetic field intensity, as well as to reduce the losses in the DC bias circuit.

The principle of operation of the device is as follows. The two HTS bias coils are axially aligned and constitute a Helmholtz coil, which generates an almost uniformly distributed magnetic field in the cores with a higher magnetic field intensity than it would be possible using only a single DC magnet with same amount of ampere-turns. By regulating the DC coil current, the mmf-flux operating point of both cores is established in the vicinity of point B, see Figure 15, which is

Figure 71: The architecture of a single phase dual core saturated core FCL.

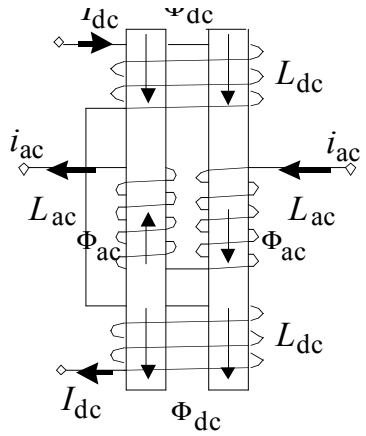

located in the saturation region of the core's B-H curve. As the AC line current flows through the AC coils, the core operating point is shifted. Due to the counter sense winding of the AC coils, the AC induced MMF in one core reinforces the DC mmf, whereas in the other core

weakens the bias mmf. Therefore, the operating point of one core shifts into a deeper saturation, point A, whereas, the operating point of the other core moves towards a shallower saturation, at point C, closer to the hysteresis knee point. In the normal state of the line, the shift is designed small enough such that both cores remain in saturation, as a result their combined impedance is low, with less than 1% voltage drop across the AC coils.

When a fault occurs, the abnormal amplitude of the fault current is capable of driving the core with the counteracting MMF out of saturation and into the steep region C-D of the hysteresis curve. Here, the permeance of the desaturated core sharply increases, resulting in a considerable increase in coil inductance and, consequently, higher impedance which helps to limit the fault current. Depending on the AC line current polarity the coils alternate in and out of saturation to reduce the current in each half cycle.

The advantage of the proposed concept is that it has a rather wide range of potential operating envelope. There are several variables that can be adjusted, such as the iron core length, core cross-section area, number of AC coil turns, DC coil turns and DC bias current. These parameters can be tuned to obtain the desired steady-state impedance, Z_{min}, the percent of fault current reduction in the worst case, the faulted state impedance, Z_{max}, and the knee point current, I_{knee}, at which the limiting effect commences.

A unique feature of the compact FCL is that there is no physical interface between the "AC side" of the device (the line current and voltage in the circuit being protected) and the "DC side" of the device (the HTS DC bias coil and its associated power supply). The AC coils and bus-work are located inside a dielectric tank, and the HTS DC bias magnets are placed in cryostats that surround the tank.

Another important design innovation is the use of "dry-type" cryogenics to conductively cool the HTS coil without the use of liquid nitrogen. Conduction cooling allows the HTS coil to be cooled below the nitrogen freezing point, thereby improving the performance of the HTS wire and reducing the amount used in the magnets. The "Dry-type" conduction cooling method also alleviates the complication about large volumes of liquid cryogens in confined spaces creating potential pressure problems. Hence, maintenance is significantly simplified.

Figure 76 shows a recently completed 15kV class FCL with two "dry-type" conduction cooled coils surrounding an oil-filled dielectric tank with the AC coils. This device is 75% smaller and only slightly heavier than the spider FCL with a similar voltage and current ratings, but offers considerably more electrical performance.

7.2 Brief Comparison with Other Saturable Core FCL Designs

In the first generation spider-core FCL, each phase is constructed using dual CC iron cores as shown in Figure 72 (a). A pair of ordinary AC coils is wound on the outer legs of the cores. The HTS DC bias coil is wound around the combined center limb. This has the advantage of having a single HTS DC coil to be shared by the two cores. Another advantage is the closed magnetic path for both AC and DC coils, which facilitates relatively easy saturation of the core. A major disadvantage of this approach is the large volume and weight of the core. Another disadvantage is the large diameter of the HTS DC coil and, accordingly, the required length and cost of the HTS wire.

Figure 72: Architecture of a saturated core FCL with a spider-core design [34] (a) and of a saturated open core FCL [26] (b).

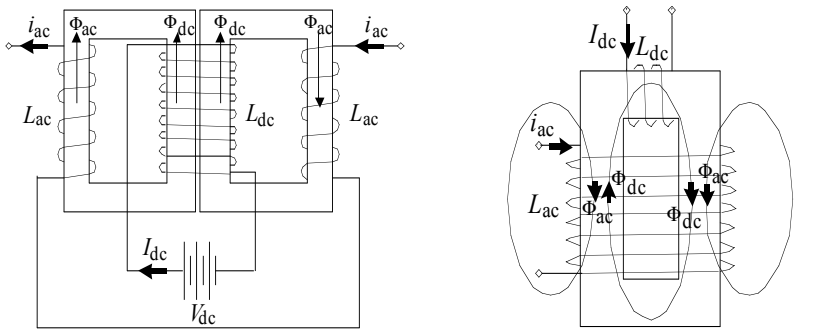

(a) **(b)**

The structure of the Saturated Open Core FCL [56] is shown in Figure 72 (b). This FCL uses a closed, strongly elongated "C" type magnetic core. This magnetic design provides a closed magnetic path for the DC bias flux, however, appearing as an open core to the AC flux.

A clear advantage of this type of FCL is that the iron core has low volume and weight, owing to its narrow and compact shape. Moreover, a narrow diameter of the HTS DC coil is needed which results in shorter HTS wire length and, accordingly, lower cost. Furthermore, lower HTS magnet volume requires lower cooling power. Another important advantage of this FCL is the orthogonal arrangement of the DC and AC coils which minimizes the AC to DC coupling.

The most significant advantage of the Compact FCL, see Figure 71, is that the I-cores have the lowest volume, weight and cost. Another major advantage is that the I cores are well suited for oil-filled dielectric design. Thus, the Compact FCL can be adopted for high voltage applications without over sizing the device. The main disadvantage of the Compact FCL is the low permeability magnetic path that requires stronger DC bias MMF to saturate the core. Therefore, two HTS magnets of an appropriate diameter and two sizable cryostat units are needed. Comparison of these three devices is summarized in Table 4.

Table 4: Comparison of main features of the spider core, open core and compact FCLs.

	Spider Core FCL	Open Core FCL	Compact FCL
Core Volume	Large	Medium-Small	Small
HTS coil diameter	Large	Small	Large
Copper coil diameter	Small	Large	Small
Cryostat	Medium	Small	Large
Dielectric type	Air	Air	Oil

7.3 Distribution Level "Compact" FCL Prototyping

A view of a three-phase Compact Saturable Core Reactor prototype FCL assembly is shown in Figure 73. A rectangular supporting frame design was used. The FCL is composed of six I cores combined in a single bundle. An AC coil is wound on each core. A pair of AC coils is needed per each phase. In order to attain an electro static isolation sufficient for high voltage applications, the cores are housed in an oil-filled tank. SF6 may also be used as an insulating media. The tank is placed inside the supporting frame to which the DC bias coils are also attached.

The prototype Compact FCL's main specifications are as follows: line-to-line voltage 12.47kV; line current 1.25kArms; prospective fault current 20kArms; line frequency 60Hz; normal state voltage drop 1%; and fault current reduction 25%. The FCL uses an oil-filled dielectric design and cryogen-free, conduction-cooled HTS magnets, resulting in a reduced coil size.

A comparison of weight, size and cost between the first-generation Spider FCL and the second-generation Compact FCL designs with similar electrical characteristics is given in Table 5.

Figure 73: Physical structure of a rectangular frame design three-phase Compact FCL prototype.

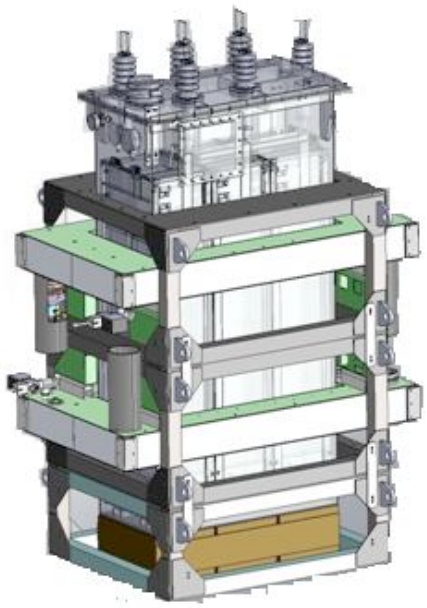

Table 5: Comparison of main features of the Spider Core and Compact FCLs designs.

	Spider Core FCL	Compact FCL
Iron Core Weight (lbs)	52K	67K
Cost of Iron @ $3.00/lb	$ 156K	$ 201K

FCL Size	19' x 19'	10' x 7'

As a learning experience, several additional three-phase and single-phase full-scale prototypes for medium-voltage applications were built. The prototypes were constructed as modular units. The supporting frame was designed to hold the Helmholtz HTS coils aligned at their position. Together with the cryostat, the power supply and the control electronics, the structure formed a standard test bed. One of the advantages of the proposed FCL structure is that there are no physical interconnections between the AC coils and DC magnets. This allowed the tank with the AC coils to be lifted and removed from the frame and replaced with a differently designed AC coils module. By such an approach, the experimental FCL could be reconfigured as a single-phase or three-phase device with a different set of parameters. Four full-scale Compact FCL prototypes were designed, built and tested. The specifications of these FCLs are summarized in Table 6.

Table 6: Specifications of prototype Compact FCLs.

Parameter	Units	FCL # 1	FCL # 2	FCL # 3	FCL # 4
Line-to-Line Voltage	kV	12.47	12.47	12.47	13.8
Number of Phases	#	3	3	1	1
Line Frequency	Hz	60	60	60	60
Prospective Fault Current	kA	35	46	80	25
Limited Peak Fault	kA	27	30	40	18
Prospective Fault Current RMS Symmetrical	kA	20	20	40	11
Limited Symmetric Fault Current	kA	15	11.5	18	6.5
Load Current Steady-State RMS	kA	1.25	1.25	1.25	2.5 – 4.0
Voltage Drop Steady-State Maximum	%	1	1	1	2
Line-to-Ground Voltage	kV	6.9	6.9	6.9	8.0
Asymmetry Factor	#	1.2	1.6	1.4	1.6
Source Fault Impedance	Ohms	0.346	0.346	0.173	0.724
Fault Reduction	%	25	43	55	41

Table 6 shows all four of the compact HTS FCL prototypes that were built and tested. These prototypes have the same nominal 15 kV design voltage and 110 BIL rating, but differ in their steady-state AC current ratings, the targeted AC steady-state current insertion impedance, and AC fault current limiting capability. The designed AC steady-state current levels ranged from 1,250 amperes RMS to 2,500 amperes RMS, and the targeted AC fault current reduction levels ranged from about 30% up to more than 50% of a 25 kA RMS potential steady-state fault current with an asymmetry factor yielding a first-peak fault current approaching 50 kA.

The compact FCL prototypes underwent full-power load and fault testing at Powertech Laboratories in July 2009 using essentially the same comprehensive test plan that was employed for the spider FCL. All 118 separate tests were performed on the four compact FCL prototypes, including 55 calibration tests, 12 load current only tests, and 51 fault tests. In many cases, the measured performance exceeded expectations, and the test program fully validated both the performance potential of the compact FCL design and the efficacy of Zenergy Power's design protocol.

A particularly important result from the compact FCL testing program was the fact that the AC coils and the DC HTS Coil exhibited very little electromagnetic coupling. The DC current in the HTS bias coil varied only by 5% as the compact FCL was subjected to up to a 30 kA peak fault current. These results were typical for all of the compact FCL devices during fault current testing.

Also, the steady-state voltage drop of the compact FCL typically remained low with increasing AC currents and also exhibited very "clean" AC power characteristics with Total Harmonic Distortion levels well within the requirements of IEEE 519-1992.

The rectangular design of the experimental FCLs was adopted for the reason that rectangular shaped HTS magnets of an appropriate size as well as their cryostats were readily available and allowed rapid prototyping. The rectangular shape, however, is not the best choice for a practical device, because it requires more structural components. Considering the electromagnetic forces, a better structural form for a coil is a round shape. Hence, circular HTS coils, a circular supporting frame as well as a circular oil tank, are more natural and easier to build. Therefore, a prospective compact FCL having a circular design was conceived.

The FCL evolution path to commercial product is shown in Figure 74. On the left is the first generation spider FCL that was tested, installed and operated in a commercially operating grid to verify performance and reliability. In the middle is the rectangular prototype Compact FCL, which was built and tested to validate a smaller and more efficient FCL. And on the right is the round compact FCL for distribution-class applications that takes advantage of all lessons learned throughout the prototyping.

Figure 74: FCL prototypes on the path to commercial product.

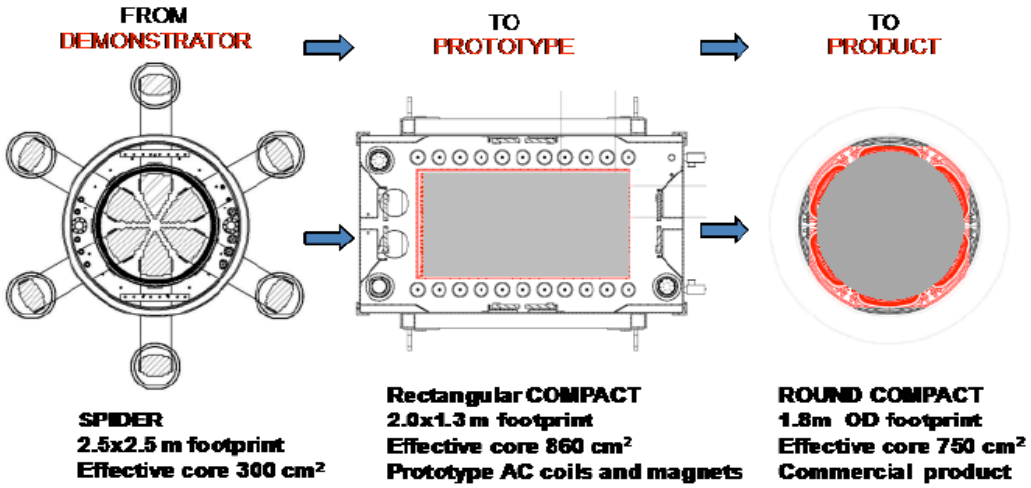

A perspective view of a circular frame design three-phase compact FCL is shown in Figure 75. Such FCL can be installed in a vault shielding it from the elements as well as from possible acts of vandalism. The auxiliary equipment such as the cryocoolers, chillers, power supplies and control electronics are installed in an adjacent control compartment having a safe access for maintenance personnel. Figure 76 shows the assembled three-phase distribution-level compact FCL.

Figure 75: Design and layout of commercial 15 kV-class medium-voltage circular-frame Compact FCL assembly.

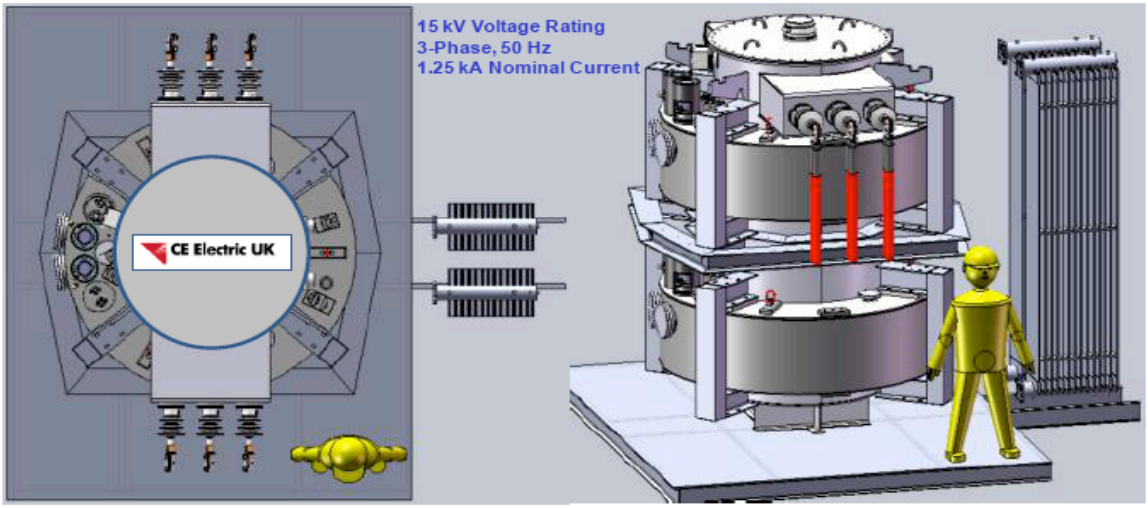

Figure 76: Three-phase distribution-level, 15kV class, Compact FCL prototype with "dry-cooled" HTS magnets surrounding an oil-filled dielectric tank with AC coils.

7.4 Transmission Level "Compact" FCL Development

A perspective view of a transmission-level single-phase compact FCL is shown in Fig. 77. A high-voltage three-phase compact FCL can be built using a bank of three single-phase compact FCLs and installed in a substation as shown in Fig. 78. Possible specifications of a prospective transmission-level compact FCL are summarized in Table 7. Such a device is feasible. Per a preliminary design, a single-phase FCL could require four HTS magnets. The estimated device dimensions are approximately 8.3m in length and 2.3m in diameter.

Zenergy Power has entered into an agreement with American Electric Power (AEP), Columbus, Ohio, to partner for the demonstration of a 138 kV three-phase FCL as a part of Zenergy Power's ongoing DOE-sponsored FCL development program. A single-phase 138 kV FCL prototype will be built and tested in 2011, and a three-phase FCL demonstration unit will be built, tested and installed in AEP's Tidd substation located near Steubenville, Ohio in 2012. This device will operate at 1.3 kA in the normal state and reduce an approximate 20 kA prospective fault by 43%, and recover instantaneously under load. The installation will be on the low side of the 345 kV to 138 kV transformer to protect the 138 kV feeder.

Figure 77: Perspective view of a transmission level single-phase compact FCL.

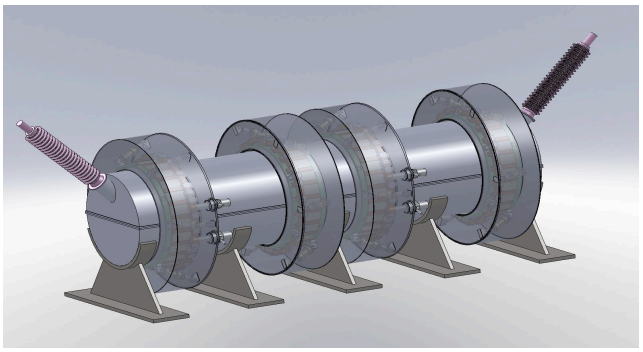

Figure 78: A perspective view of a compact FCL installation in a substation.

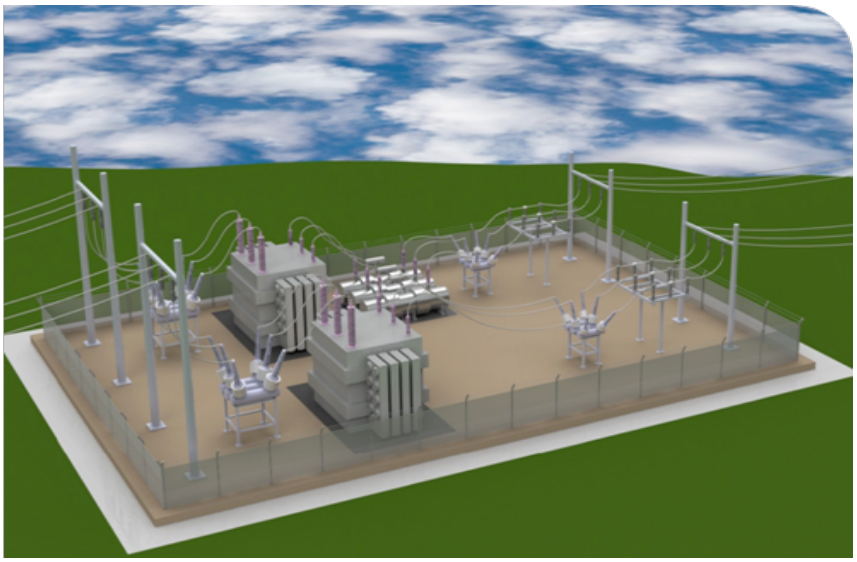

Table 7: Possible characteristics of a future transmission level Compact FCL.

Parameter	Units	Value
Line – to –Line Voltage	kV	230
Line Frequency	Hz	60
Rated Current	kA rms	2
Prospective Fault Current as Maximum Symmetric Fault Current	kA rms	63
Asymmetry Factor	#	2.75
Desired Limited Current	kA rms	52
Maximum Voltage Drop at Rated Current as a Line Voltage	kV	0.5

Prospective Peak Fault Current	kA	173
Maximum Voltage Drop at Rated Current as a Percentage of Line Voltage	%	0.37
Percent Fault Limiting Capability	%	17.5
Line – to – Ground Voltage	kV	132.8
Cryostat ID	m	1.34
Magnetic Core Volume	m^3	2.5
Magnetic Core Weight	kg	19,964

7.5 Summary

This chapter reported on recent development of a second-generation compact saturable core FCL for medium-voltage distribution systems. This device is an evolution of the first generation spider FCL sponsored by the CEC/CIEE program.

The compact FCL has several advantages: such as reasonably small core size, completely passive design, the ability to limit first-peak fault current, sufficient fault current reduction, automatic recovery and fail safe operation. The decoupled high-voltage and cryogenic systems allow simplified oiled-filled high-voltage design. This approach presents a relatively small heat load on HTS magnet and, therefore, cryogen-free, low maintenance, and commercial off-the-shelf cryogenic equipment can be used.

The compact FCL prototype is the second superconductive FCL to be successfully tested for US utilities. The compact FCL prototype is an advanced full-scale experimental model, which builds confidence in the new technology. While the development and prototyping of distribution level FCLs proved successful, the ultimate objective is to develop commercially feasible, full size transmission-level FCL.

Research and development of FCLs has been conducted for many years. The compact FCL system described here seems a promising, practical, efficient and economically feasible device that meets utility needs. The emerging compact FCL is a viable candidate to make a break-through into commercialization.

CHAPTER 8:

Lessons Learned

While the first generation FCL demonstration program was a technical success, the objectives of the program, specifically with respect to the electrical performance of the FCL devices, were modest. The devices had a relatively low electrical rating, with maximum potential ratings on the order of 25 MVA, while the high duty-cycle ratings are significantly lower, and a high cost. The development and demonstration results clearly point out that the FCL technologies must be expanded to higher voltage, higher power applications in order to be cost effective.

The cost effectiveness can be addressed in two directions, firstly, the FCL technology is being improved to reduce basic device manufacturing cost, and secondly, the FCL technology is being improved to work reliably at higher voltages and currents. The latter is more important in terms of FCL technology cost effectiveness and value proposition, especially in the short term.

Higher voltage substations can often be more crowded and have fewer options for expansion, due to electrostatic clearance issues, and higher voltage components (switchgear, insulators, transformers, buss-work) are exponentially more expensive than their low-voltage counterparts. Furtermore, high-voltage substations have become increasingly more common where large renewable power generators desire to connect to the electric grid, and high-voltage tie-lines have increased as more power is wheeled from long distances and as grid interconnections become more necessary to improve the reliability and better control power flows. Economic studies and performance models show that at the current performance levels and price points, FCL technologies can be very cost-effective compared to major upgrade projects at high voltages.

The FCL demonstration project also clearly highlighted the shortcomings of the current spider FCL with respect to reliability. While the FCL device performed satisfactorily while "in the grid," a large number of interventions were needed to keep the FCL completely operational. The demonstration suggested that cryogenics are a key shortcoming, and it is clear that cooling the HTS coil must be more reliable, less costly, and less intrusive. At a minimum, the FCL cryogenics need to target "5-nines" reliability with only a single, scheduled, short-duration annual maintenance outage. Even better would be extending the maintenance interval to two-years or longer.

If the FCL is to be relied upon for protection (which is essential to the economic value proposition), it must be installed such that it can be bypassed and removed from service temporarily for maintenance, while fault currents will remain acceptable. This may be accomplished by splitting buses or otherwise configuring the electric grid in manners that are acceptable for short durations, but which may not be optimal for long-term operation.

If such a alternate grid configuration is not acceptable or available, then the FCL must be designed, to the maximum extent possible, to allow essential routine maintenance, such as cryogenic maintenance, to be performed while the unit is energized, through measures such as locating the cryogenic coolers remote from the FCL itself. Also, the FCL must be designed to remain in the protected circuit indefinitely in the failed state, if the resulting higher voltage drop is tolerable, until replacement or repair can be arranged.

Ultimately, the FCL must be as reliable as a transformer of similar voltage class, and exhibit a similar maintenance profile. Then, even though major outages will occur, they will be infrequent and tolerable, as corresponding transformer failures are accommodated today. FCL

developers and manufacturers are taking these reliability issues to heart and are aggressively modifying their FCL technologies for reduced maintenance requirements, higher MTBF, and lower MTTR. They are also working with key industry partners and suppliers, such as cryogenic cooler manufacturers to reduce the cost and improve the performance of enabling technologies.

One important weakness identified during the field test was that the nitrogen cooling system could be problematical for maintenance since it requires periodic maintenance of the cryostat, including drying the volume and replacing liquid nitrogen. This may not be practical considering the fact that the unit is typically installed in a high-voltage area. However, this weakness was resolved in subsequent FCL designs by replacing the nitrogen cooling system with a liquid cryogen-free, "dry-type" conductive cryogenic cooling system, commercially available off-the-shelf, resulting in a more reliable and robust system.

Overall, the Zenergy FCL is considered as an important success and it has already led to a scaled up design for transmission level (138kV) application. Further fast-paced and more advanced development of FCL technology is strongly recommended. This project has demonstrated the benefits of FCL technology, but has also shown that realizing those benefits will require accumulating significant operational experience with beta hardware essentially the same as eventual series production items and extrapolating the FCL technology to considerably higher power levels.

While the private sector will eventually "get there" and achieve these objectives, this trajectory will take too many years. In the meantime, tremendous investment in general grid upgrades will have to be made on a fast-track in order to maintain required levels of reliability. Significant amounts of this investment are potentially avoidable and represent tremendous value to ratepayers, if suitable FCL technologies are available to California utilities, and if California utilities are given reasonable incentives to deploy new technologies. The CEC and PUC can perform a valuable service for California ratepayers and workers, and the economy in general, if an accelerated program of high-voltage, high-power FCL technology is implemented under a consortium involving the PUC, the CEC, the State's electric utilities, and private industry.

CHAPTER 9:

Application Matrix of FCL

This chapter suggests several possible applications of the FCL in the power transmission and distribution systems (see references [15] and [72]).

A. Fault Current Limiter in the Coupling

Instead of designing the two systems for the total short-circuit current, the FCL is installed in the bus coupling position as shown in Figure 79. In case of a fault, the FCL reduces the peak short-circuit current at the first current rise. The advantages of this application are given below:

The parallel connection of the transformers (two systems) will result in an even distribution of the currents supplied; reduction of the required short circuit capability of the system; reduction of the network impedance; no disconnection of the feeding transformers after tripping of the FCL.

Figure 79: FCL installed in the coupling.

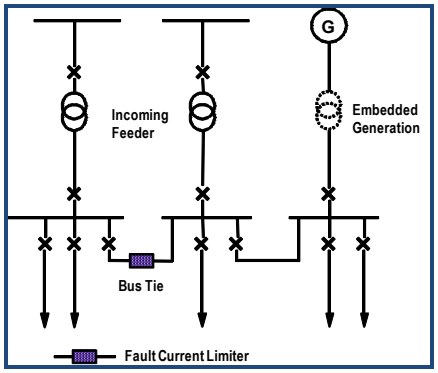

B. Fault Current Limiters in the Incoming Feeders

Instead of designing the two systems for the total short-circuit current, the FCL is installed in the incoming feeders as shown in Figure 80. In case of a fault, the FCL reduces the peak short-circuit current at the first current rise. The advantages of this application are:

The parallel connection of the transformers (two systems) will result in an even distribution of the currents supplied; reduction of the required short circuit capability of the system; reduction of the network impedance.

Figure 80: FCLs installed in the incoming feeders.

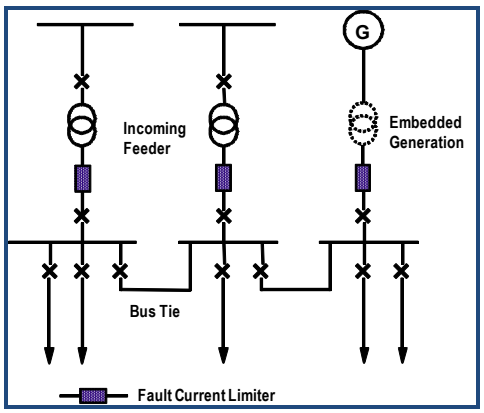

C. Fault Current Limiters in the Outgoing Feeders

Instead of designing the two systems for the total short-circuit current, the FCL is installed in the bus coupling position as shown in Figure 81. In case of a fault, the FCL reduces the peak short-circuit current at the first current rise. The main bus must be capable of carrying the full fault current. The advantages of this application are:

Reduction of the required short circuit capability of the feeders on which the FCL's are installed; reduction of the network impedance; no disconnection of the transformers after tripping of the FCL.

Figure 81: Fault Current Limiters installed in the Outgoing Feeders.

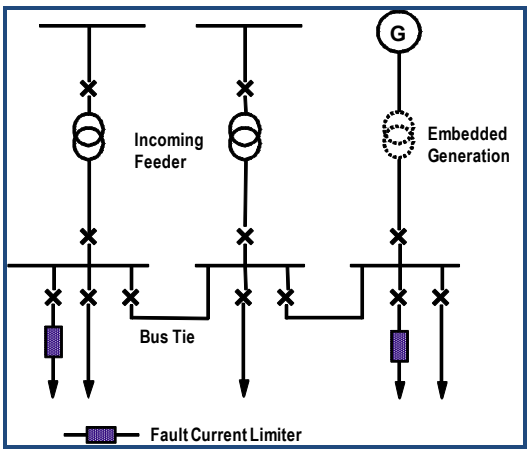

D. Grid coupling

The subgrids are fed via transformers from the 220 kV and 380 kV voltage level. The transformer capacity feeding into a 110 kV subgrid is approximately 1000 MVA taking into account the n −1 reliability criterion commonly used in utility applications. Advantages of this application are:

FCLs in the grid coupling, as shown in Figure 82, can reduce the surplus in transformer capacity without exceeding the admissible fault current level. This leads to the same technical benefits as in distribution levels with a considerable additional economical benefit by saving a 110/380 kV transformer and the associated switchgear components. In the specific case shown in figure 82 two transformers can be saved: the first one because of the introduction of the FCLs and the second one because a small increase in the loading capacity of the other transformers is permissible.

Figure 82: Two sub-grids coupled by FCL.

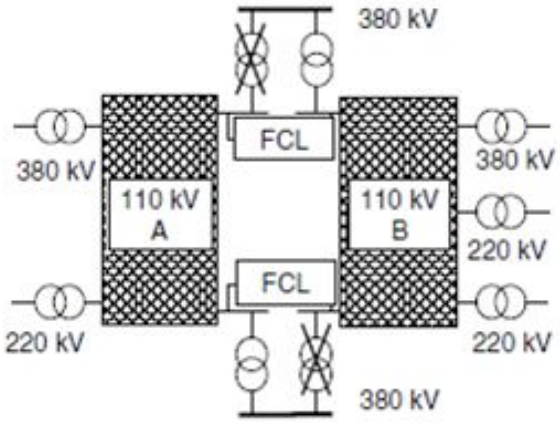

E. Power plant auxiliary power feeder

The power plant auxiliaries are usually connected to the power plant generator via a transformer. This is in general a location with high short-circuit capacity because of the vicinity

to the power plant generator. Hence, an FCL should be inserted at these points as shown in Figure 83.

The advantages, the FCL can bring in this application, is that the energy of arc faults is reduced significantly, which means that additional measures to protect against these arcs are no longer needed. Savings can also be obtained from reduced stresses on switchgear components mainly at the medium-voltage level, and the possibility to use cables with reduced cross section. Because of the fault current limitation it is no longer required to use separate cables for each phase, which results in much faster and cost-effective cable installations.

Figure 83: Location of FCLs in power plant auxiliaries: (a) medium voltage; (b) medium voltage; (c) low voltage.

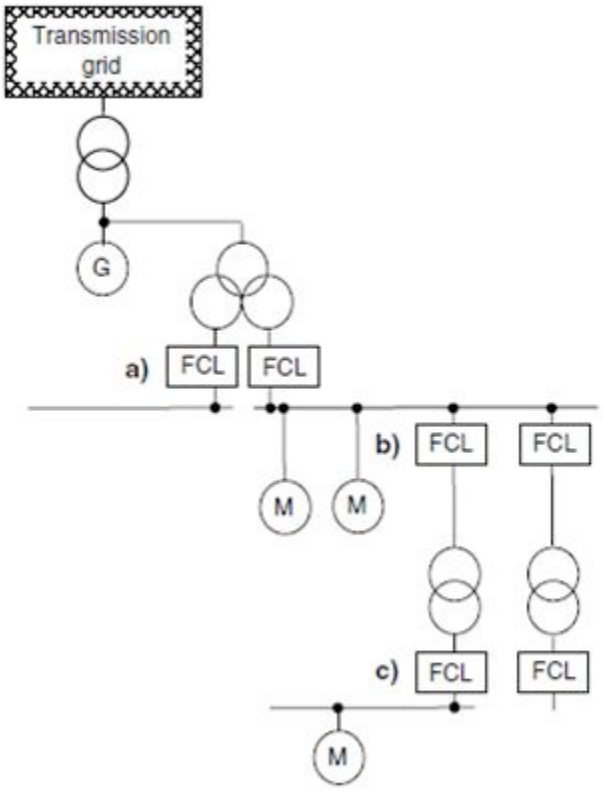

CHAPTER 10:

Installation of Zenergy Power FCL

10.1 Site Preparation to Accommodate the FCL

As there are no industry-accepted standards for FCL testing, the National Electric Energy Testing Research and Applications Center (NEETRAC) in close collaboration with several of its member utilities, including SCE, developed a detailed FCL test program based on Institute of Electrical and Electronics Engineers (IEEE) and Conseil International des Grands Réseaux Électriques (CIGRE) standards for transformers and reactors.

The following measures were taken in order to test the FCL for acceptance by SCE and to prepare for the FCL's installation at the site.

10.1.1 Pre-installation High Power and High Voltage Testing

The FCL was first subjected to heat runs at a full prospective normal load current and full DC bias current to verify the maximum temperature rise of the AC coils and the HV terminations. All measurements were within the limits specified in IEEE Std C57.16-1996.

A total of 65 separate tests were performed at PowerTech Labs, Vancouver BC, including 32 full-power fault tests with first peak fault current levels up to 59 kA all at rated voltage. Fault tests included individual fault events of 20-30 cycles duration, as well as multiple fault events in rapid sequence (to simulate automatic re-closer operation) and extended fault events of up to 82 cycles duration, simulating primary protection failure scenarios.

The FCL was tested under full lightning impulse for:

- One reduced (1.2 x 50 μs) full wave– 50 percent or 55 kV peak wave
- One full (1.2 x 50 μs) wave – 100 percent or 110 kV peak wave
- One reduced chopped wave – 50 percent or 60 kV peak wave (chopped at 2 microsec.)
- Two full chopped waves - 100 percent or 120 kV peak waves
- Two full (1.2 x 50 μs) waves (within 10 minutes after the last chopped wave)

10.1.2 On-site Commissioning Test

Continuity and insulation resistance measurements were performed to verify the device's internal components were not disrupted during shipping. Source-side and load-side bushing terminations were measured separately.

Commissioning tests at the site consisted of coil resistance, power factor, and megger measurements of all phases. These measurements were performed as a safety and reliability check every time work was conducted in the HV compartment to verify that the HV insulation had not been disrupted. The change of the FCL's insertion inductance as a function of the DC bias current was also measured as the cryogenic system was first energized and de-energized.

10.1.3 Special Bypass Switch

To help assure service reliability an innovative FCL bypass/isolation switch conceptualized by SCE and custom built by a leading circuit breaker supplier was installed. The design includes a three-phase pad mount device with fixed input and output elbow connections for line and load side of the circuit. The device has two sets of elbow connections for insertion of any three-phase device (device input & device output) also elbow connectors are used for this connection. On the device there are 3 independent switches used manually/remotely to open and close the vacuum bottles on the device-input and device-output connection as well as one to control the bypass (or parallel the device-input and device-output) connections as depicted in Figure 84.

The purpose of the bypass switch is to easily and quickly reconfigure the electrical arrangement consisting of the source transformer, the Avanti Circuit, and the FCL without the need to take a circuit outage.

The bypass switch has redundant controls and can be programmed to operate either totally automated, remote control, or manual under local control (overriding the remote control for safety reasons). Physically the bypass switch is similar to a pad mounted gas switch.

Figure 84. By-Pass Switch for Zenergy Power FCL.

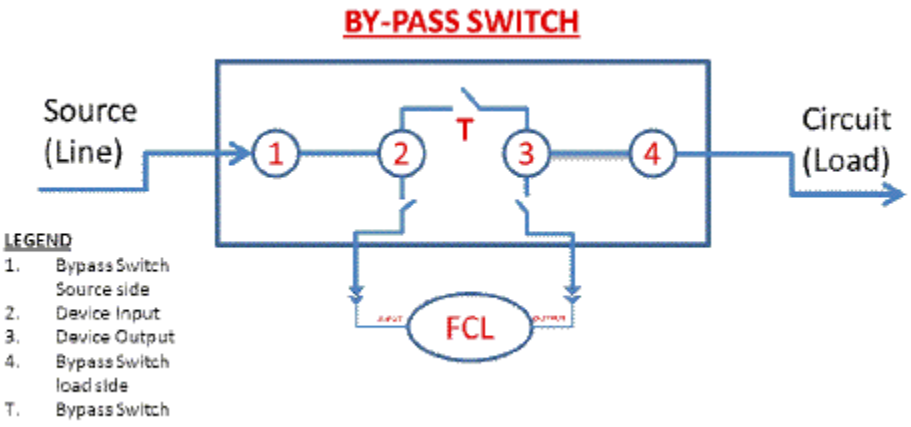

By means of the bypass/isolation switch the FCL can be connected in series with the source only, thus applying 12 kV to the FCL's AC coils, but without any load current flowing through the unit. A second arrangement connects the FCL in series with both the source and the load, which is the normal mode. The third arrangement completely isolates the FCL from the SCE system.

10.1.4 Civil Engineering

Seismic modal analysis of the FCL unit was performed by the manufacturer to determine any structural requirements to withstand a 0.5 G zero period acceleration. Finite element modeling and spectrum analysis up to 40 Hz with 2 percent damping were performed to verify that stresses and deflections were limited to within the allowable values per IEEE Standard 693.

SCE's civil engineering group was consulted to determine the best option for the physical installation of the FCL and to design the anchorage and stress release for the electrical connection according to the reaction forces.

One alternative considered for the foundation was to use railroad ties over the existing crushed gravel in the substation's yard. Another option was to build a traditional concrete foundation to ensure that the FCL would remain level in seismically active area. The civil engineering team's recommendation was to set the FCL on compacted and leveled crushed gravel without any additional support because the FCL's enclosure is welded to steel I-beam skids.

10.1.5 High Voltage Connections and Grounding

The next element in the site preparation was to interface the high voltage (HV) power terminations allowing the FCL to be easily connected to the circuit via the bypass switch. Elbow terminations were selected. The advantage here is that elbow connection at 12KV would reduce cost and provide dead front installation as oppose to live front and costly civil work to enable overhead installation.

Deadbreak premolded cable connectors penetrating the FCL's enclosure three feet above ground level were installed for the 12 kV cable connections from the FCL to the bypass switch. This facilitated the physical connection and disconnection of the FCL and also eliminated cable splicing. The connectors are 25 kV Voltage Class, 125 kV basic insulation level (BIL), current rated at 900 A continuous, and 25 kA momentary. Stainless steel flanges were specified for these connectors to reduce induced eddy currents. The flanges and cable shields were grounded to the FCL's common grounding circuit, which in turn was connected to the substations ground mat.

10.1.6 Auxiliary Power

The SCE and Zenergy team worked closely to define the auxiliary power need to supply the FCL's electrical load. First, the most practical voltage to use was determined. Then the total power requirement for the FCL's peak load scenario was calculated. This reduced the cost and additional time requirements should have the device control voltage be at a non standard voltage value that is not typically supported at SCE substations.

The available voltage at the site was 120/240 volts, three-phase delta. Consequently, FCL's low voltage components were designed accordingly. To meet the FCL's 100 kVA requirement, the site's station light and power were upgraded, allowing the FCL to operate without affecting the substation's normal load. A 100 Amp three-phase circuit breaker was installed as a dedicated source for the FCL power. Six-hundred feet of 2/0 copper conductor were pulled from the AC panel to a connection box next to the FCL.

10.1.7 Noise Ordinance Compliance

A local city ordinance allows no more than 55 db total sound energy be emitted during the daytime and 45 db at night as measured at the perimeter of the substation. Sound measurements with the unit on and off were performed. To comply with the stated limits, the FCL was sound insulated to better contain the sound emission of the compressors and cold heads. The FCL enclosure was also oriented so as to reduce the noise projected to the closest neighbors.

10.1.8 Connection to HV side (Input & Output)

The connection, depending on the voltage class should be carefully discussed before the test unit is built for field demonstration. Initially ZenergyPower had planned to have overhead potheads installed for the high voltage interconnection, but SCE provided timely input to change to a better concept. SCE suggested that the input and output be equipped with 15 kV volt elbow connections as shown in the picture above. The resulting advantage was that elbow connection at 12KV reduced the cost of installation and provided quicker and safer dead front connection and disconnection, which was done more frequently because of the development nature of this project. In contrast pothead/live-front installation would have necessitated additional costly civil work to enable a safe overhead installation and more time to make the actual connections.

For future demonstration units the interconnections means should be carefully discussed with the host site to determine the optimal connection method.

10.1.9 Metering PT's and CT's and Interconnection Cabinet

This interconnection cabinet was not part of the original installation, but was added later for monitoring purposes. The location where terminal blocks were added to provide 3-phase output voltage was limited to the side bypass alarm cabinet/opening.

It is highly desirable to have relay class PT's and CT's installed both on the input and the output of the FCL device as illustrated in Figure 85. This makes possible the installation of Digital Fault Recorders and Power Quality (PQ) instrumentation on the input and the output of the device to operate at the required bandwidths to monitor the expected transient events and operate stand-alone high speed PQ monitoring. This arrangement would allow the utility to capture fault profiles before and after the device, producing a more accurate data retrieval for analysis and validation of the unit's operation.

The secondary of the monitoring voltage and current transformers will need to be in a weather resistant enclosure mounted on the outside of the FCL unit, giving unrestricted safe access to utility personnel An Auxiliary 120VAC receptacle should also be made available in this cabinet.

Figure 85. Installation of Zenergy Power HTSFCL Voltage and Current Monitors.

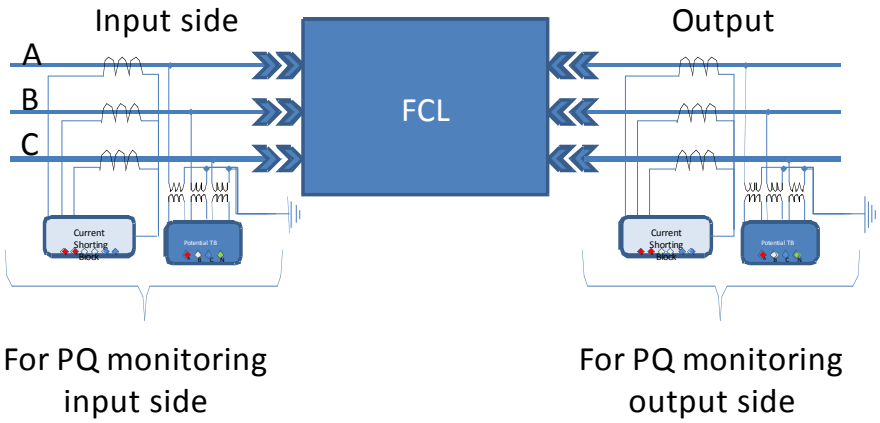

10.1.10 Communication Interconnection Point

For alarms and possible remote control (in this case there was no remote control by host utility), there should be some communication means to provide a secure and accessible point and physical area where utility can receive alarms and if needed Data Acquisition System signals for monitoring and alarming use by the operations personnel. During the FCL field test, one single alarm point to the control screen at the control center was necessary. It was set up to provide an alarm to the operator in case of an FCL abnormal condition.

10.1.11 Bypass Relay and Alarm Cabinet

As part of operations requirement, the host utility at minimum should receive a single bypass condition alarm to safely isolate the FCL device from service and generate alarms accordingly. This alarm should be in the form of a latching relay to maintain the condition until the event is acknowledged physically by an operator. The bypass switch can also be automated to expedite isolation of the device during abnormal conditions.

CHAPTER 11:

Summary and Recommendations

After three-year and 9 months of team works, the project is towards its completion. Two different types of FCLs, one solid-state type and one saturable core type, were selected for the development and field demonstration.

From the earliest stage of FCL's development work, an important step taken was "design for the test"! Significant efforts were dedicated to the development of the test plans that are acceptable to SCE and workable for the teams. Zenergy worked closely with NEETRAC and several of its member utilities, including SCE, developed a detailed FCL test program based on IEEE and CIGRE standards for transformers and reactors. EPRI/Silicon Power created their plan based on ANSI C39.09-1999 and ANSI C37.06-2000 covering the entire spectrum of possible tests that need to be carried out on their equipment, including component level factory tests, system level factory tests, acceptance tests, and system field tests. Many technical issues related to laboratory test and field test interface were resolved during a series of meetings with knowledgeable SCE engineers who provided valuable design and test guidelines. Both teams completed their test plan, which provided a valuable design and test guideline.

11.1 Development of a Solid-State Fault Current Limiter

The Solid-State Fault Current Limiter (SSFCL) was developed by EPRI/SiliconPower Corp. This SSFCL employs a modular and scalable design, applicable to a range of voltage classes. The advantages of the emerging SSFCL approach are immediate recovery after fault, no voltage or current distortion, no cryogenics, low losses and reduced size and weight.

The major technical issues with the SSFCL have been resolved and the detailed design of the system has been completed. One of the lessons learned from the first generation SSFCL was that the auxiliary circuit that is the cause of many timing problems and control complications and also requires multi-channel high voltage isolated charging power supply. This increases system's cost as well as reduces the reliability. Therefore, in designing the second generation SSFCL the auxiliary thyristors and resonant current shaping inductor were removed. Instead, a simple capacitive snubber was fitted to soften the main SGTO hard turn off.

The second generation single-phase SSFCL was constructed under the scope of a different research funding. Till date, the results of the hardware design and elemental testing are promising and, so far, encouraging. The single-phase second generation SSFCL underwent testing at KEMA-Powertest Laboratories, Chalfont, PA in May 2011. The SSFCL had successfully passed the normal state testing at 15kV and 1200A full load current and successfully reduced a 23 kA prospective fault current to 9kA. In the near future, construction of the full size three-phase 15kV, 1.2kA SSFCL for a 23kA symmetric rms fault current rating will be initiated. This will include an extension of existing design by duplication of the already tested power stack. Some additional tasks to be performed are to extend the control from a single-phase to a three-phase system, include additional diagnostics, design a full size three-phase thermal management system, and build a full size enclosure. Then, the complete SSFCL will be sent out for field testing.

The EPRI/Silicon Power FCL represents a potential cost-effective solution to the rapidly rising available fault currents seen in utility systems. One advantage of this type of FCL is the flexibility to be interruptive or non-interruptive. Furthermore, the solid state FCL may be used

to limit the current of superconducting cable to enable the use of smaller cable sizes. The solid state FCL also has a unique capability to limit inrush current, even for capacitive loads.

EPRI/Silicon Power identified some thermal management issue in their initial design. An improved system design was complete, and the major technical design challenges, such as the thermal management system and control architecture, have been resolved. However, the resulted cost increase was constrained by the project budget, thus this FCL did not advance to whole system laboratory test and field demonstration stage under this program.

According to the design prediction the system size and weight would be 6.5'X12'X12' and weight would be 62,000lbs with oil cooling. This size and weight is acceptable.

The SSFCL employs a modular and scalable design. The SSFCL designed for the 12kV line in this project period is composed of 10 SBBs in series. Voltage sharing to maintain all the SBBs under the blocking voltage under dynamic condition may be a technical challenge for transmission level applications where the voltage level is above 100kV.

11.2 Development of a Saturable Core Type High Temperature Superconductive Fault Current Limiter

The first in its class 15kV saturable Core type High Temperature Superconductive Fault Current Limiter (HTS FCL) prototype has been built by Zenergy Power Inc. It underwent a successful laboratory testing, and was connected in the Southern California Edison (SCE) 'Avanti' Circuit of the Future for field demonstration. The HTS FCL was energized on March 9, 2009 and decommissioned October 2010 after successfully completing its field testing period. This superconducting FCL was the first to be in commercial service in the United State.

This report presents the design, testing, and application issues as well as a systematic approach to modeling the electrical behavior of this type of fault current limiter. The derived computer model provided an excellent tool for predicting the overall fault current reduction of a saturated core HTS fault current limiter. The model was useful in designing and operating an innovative distribution class 15kV saturated core FCLs.

The important results of this project were the development of the simulation model, design tools, operations and maintenance experience gained, and valuable protocols for the design, installation, control, monitoring, and employment of FCLs in an electric power system.

Also under CIEE support, Zenergy Power has gained experience in:

- Designing, building, installing and operating a fault current limiter in the electrical grid including integration with the SCADA system.
- Both Zenergy Power and SCE have gained invaluable experience by operating an HTS FCL in real-world conditions through all four seasons.
- Zenergy Power learned to address unplanned events such as loss of station power and loss of FCL bias current.
- The host utility learned about preventive maintenance and how the FCL responded to real fault events.

The FCL performed well throughout the field demonstration, but several significant modifications were made in collaboration with SCE. Significant observations from the demonstration project include:

- The FCL's enclosure environmental conditions must be maintained within a narrow band to maintain the reliability of the control and monitoring instrumentation, cryogenic refrigeration, and DC power supply equipment. Additional air conditioning was installed in the FCL enclosure to meet hot-day cooling requirements.
- Air-cooled cryogenic refrigerators were satisfactorily employed (with sufficient enclosure air conditioning), but water-cooled cryogenic refrigerators may be more robust in the field.
- A sub-cooled liquid nitrogen re-condensing cryogenic system was successfully employed. Zenergy Power's current FCLs will use a "dry-type" conduction-cooling cryogenic system free of liquid cryogens, which is more reliable and easier to maintain..
- The FCL control system was able to shut itself down in an orderly and safe sequence under loss of station power events. Several substation blackouts were experienced. The FCL is capable of automatically restarting when station power is restored, including the restoration and stabilization of cryogenic refrigeration, but this feature was disabled for safety purposes.
- A UPS was installed to provide control, instrumentation and DC bias current for up to two hours during station outages.
- While multiple channels for the FCL's system "health" data were provided, SCE desired a "watch-dog" monitoring system that provided a "Go" (all systems normal) or a "No-Go" (some system off-specification) with an automatic bypass switch to remove the FCL from service in the event of a "No-Go" condition.
- The FCL control system was successfully integrated through a secure Ethernet connection into the SCE SCADA system; a secure physically separated and independent MODBUS control scheme enabled secure, real-time monitoring and operation from the SCE Control Room.
- If the FCL is being relied upon for system protection, the system must be configurable (through temporary buss-splitting, for example) to control fault duty levels in the event the FCL must be removed for maintenance or repair.
- Saturated-core FCL's, seen as almost transparent inductors during steady-state conditions and large inductors during fault conditions, must be evaluated for compatibility with existing circuit resistance and capacitance values to ensure voltage stability on the protected circuit – a separate paper on resonance discusses this requirement.
- The effects of saturated core FCL's on circuit breaker transient recovery voltage must be considered to assure adequate rating of circuit breakers and determination of maximum allowable interruption currents. A separate journal paper on this topic was also published by Zenergy.

The research in this period has led to the successful field demonstration of the Zenergy Power HTS FCL, marking a milestone event in the history of FCL development in the United States. The experience gained from the research led to a more reliable controller, a dramatic reduction

of the FCL's size and weight, and the replacement of liquid nitrogen cryogenic refrigeration by a low maintenance dry cooling system.

The Zenergy Power HTS FCL was first laboratory tested successfully against an FCL specification and test criteria developed by US utilities, including the host utility Southern California Edison. The HTS FCL was then successfully demonstrated in actual field operation. The HTS FCL unit is rated at 15kV, 1200A, 110kV (BIL), steady state insertion impedance <1%, and a fault current reduction capability of 20% at 23kA.

The first generation Spider core HTS FCL had a dry-type transformer (air dielectric) structure, a total overall dimensions of about 19'X19'X7', and weighed approximately 50,000 lbs. The second generation Compact HTS FCL that followed from this research employed innovative core architecture and oil dielectric transformer construction techniques that led to a much more compact size of approximately 8'x10'x11' (including electric bushings for AC circuit connection, which protrude from the side in a customer-required air-filled cable box) and a weight of approximately 67,000 lbs. The compact FCL had a similar power rating and much higher fault current limiting performance. The new Compact FCL design is an attractive option where real estate requirements are tight.

Regarding the cost-effeteness is concerned, since the first generation device has a relatively low electrical rating, with maximum potential ratings on the order of 25 MVA and high duty-cycle ratings significantly lower, the present manufacturing cost may not represent a high value proposition. This issue has been addressed, in two directions – FCL technology is being improved to reduce basic device manufacturing cost, and FCL technology is being scaled up for higher voltages and current. The latter may be more important in terms of cost effectiveness and value proposition, considering the fact that higher voltage substations can often be more crowded and have fewer options for expansion, due to electrostatic clearance issues, and higher voltage components (switchgear, insulators, transformers, buss-work) are exponentially more expensive than their low-voltage counterparts. Further, large renewable power generators desire to connect to the electric grid, and high-voltage tie-lines have become increasingly more common as more power is wheeled from long distances and as grid interconnections occur to improve reliability and better control power flows. All of these factors are projected to continue to increase energy levels within the grid, leading to potentially unsafe fault current levels. In some cases, higher-rated components cannot be retrofitted in the available space, leading to lengthy and costly major upgrades of grid infrastructure. Economic studies and performance models show that at current performance levels and price points, FCL technologies can be very cost-effective compared to major upgrade projects at high voltages.

The FCL demonstration project also brought to light an issue with respect to the device's reliability and maintenance requirements.. While the FCL device was kept operable and performed satisfactorily while "in the grid," a number of interventions were needed to keep the FCL completely operational. As a prototype, it was acceptable, but as a commercial product, it is being improved. A desirable FCL needs to target "5-nines" reliability with only a single, scheduled, short-duration annual maintenance outage. Even better would be extending the maintenance interval to two-years or longer, but an annual outage of a day or less would be acceptable if the FCL were reliable and required no other maintenance.

If the FCL is to be relied upon for protection, then bypassing it from service temporarily for maintenance can be a risk for the circuit. Perhaps, a scheduled bypass can be accomplished by splitting buses or otherwise configuring the electric grid in manners acceptable for short durations; but it may not be optimal for long-term operation, or not acceptable at all. Thus the FCL shall be designed, to the maximum extent possible, to allow essential routine maintenance, such as cryogenic maintenance, to be performed while the unit is energized. Zenergy Power is aggressively modifying their FCL technologies for reduced maintenance requirements, higher MTBF, and lower MTTR.

One important weakness identified during the field test was that the nitrogen cooling system could be problematical for maintenance since it requires periodic maintenance of the cryostat, including drying the volume and replacing liquid nitrogen. This may not be practical considering the fact that the unit is typically installed in a high-voltage zone. However, this weakness was addressed in second generation HTS FCL design by replacing the liquid nitrogen cooling system with a cryogen-free, "dry-type" conductive cryogenic cooling system, available as a commercial off-the-shelf unit, resulting in a more reliable and robust system.

Overall, the Zenergy Power HTS FCL project is considered as an important success, which has already led to a scaled up design for a transmission level (138kV) commercial application.

11.3 Recommendations

Electricity is a vital force of our economy. It is an important goal of the California Institute for Energy and Environment and the California Energy Commission to support the technologies required satisfying a reliable, safe and environmentally responsible electrical energy supply. As such, FCC technology is a potentially cost-effective alternative to the capital-intensive upgrades of the power system that would ordinarily be required to meet growth in electrical demand. The demonstration projects in this phase have already resulted in two test plans, two full designs, and contributed to one commercial sale and one migration to a transmission-level application.

The consortium has accumulated extensive experience in the development of FCL technology, the operation, and support of field demonstration at Southern California Edison's Avanti Circuit. Further fast-paced and more advanced development of FCL technology is strongly recommended. As the demand for electrical energy rapidly increases, particularly in response to renewable power and "green technology" initiatives, tremendous investment investments on system upgrades will have to made on a fast-track in order to maintain the required levels of system availability and reliability. Significant amounts of these investment are potentially avoidable, if suitable FCL technologies are available to California utilities, and if California utilities are given reasonable incentives to deploy the new technologies. An accelerated program of FCL technology focused on reducing the cost, improving the reliability, and increasing the voltage and current ratings of FCC technology is needed in order for California utilities and ratepayers to reap the benefits. New and promising technologies are also important for the recovery of the economy and the creation of new jobs.

APPENDIXES

APPENDIX I:
SILICON POWER SSFCL TEST PLAN

APPENDIX II:
ZENERGY POWER HTS FCL TEST PLAN

APPENDIX III:

ZENERGY POWER HTS FCL DIELECTRIC AND HV TEST

APPENDIX IV:

ZENERGY POWER HTS FCL NORMAL STATE TEMPERATURE RISE TEST

APPENDIX V:
ZENERGY POWER HTS FCL SHORT CIRCUIT TEST

APPENDIX VI:
ZENERGY POWER HTS FCL HV TESTING

APPENDIX VII:
ZENERGY POWER HTS FCL OPERATION MANUAL

APPENDIX VIII:

HTS FCL CREOSTAT EVACUATION AND MOISTURE REMOVAL

APPENDIX IIX:
HTS FCL LIQUID NITROGEN FILL.

REFERENCES

[1] Anatomy of a Short Circuit, Siemens TechTopic no. 44, rev1. Dec. 12, 2003.

[2] L. A. Kojovic, S. P. Hassler, K. L. Leix, C. W. Williams and E. E. Baker. "Comparative analysis of expulsion and current-limiting fuse operation in distribution systems for improved power quality and protection" *IEEE Transactions on Power Delivery*, Vol. 13, No. 3, pp. 863-869, July 1998.

[3] "Using Current-limiting Fuses to Increase Short Circuit Current Ratings of Industrial Control Panels," Littelfuse App. Note, 2007.

[4] F. Pinnekamp, "The Circuit Breaker," ABB Review, Jan. 2007. Available at: http://library.abb.com/global/scot/scot271.nsf/veritydisplay/737de0b7f522f9b2c125728b00474780/$File/75-78%201M720_ENG72dpi.pdf

[5] T. Taylor, A. Hanson, D. Lubkeman, M. Mousavi, Fault Current Review Study, ABB Report No.: 2005-11222-1-R.04, pp. 41-45, December 22, 2005.

[6] P. G. Slade, R. E. Voshall, J. L. Wu, J. J. Bonk, E. J. Stacey, W. F. Stubler, J. Porter, L. Hong, "The Utility Requirements for a Distribution Fault Current Limiter," IEEE Trans. on Power Delivery, Vol. 7, No. 2, April 1992.

[7] M. Noe, B. R. Oswald, "Technical and Economical Benefits of Superconducting Fault Current Limiters in Power Systems," IEEE Trans. on App. Supercond., vol. 9, no. 2, June 1999, pp. 1347-50.

[8] A. Neumann, "Application of Fault Current Limiters," BERR report, pp. 3-14, 2007. Available at: http://www.ensg.gov.uk/assets/dgcg00099rep.pdf

[9] S. Eckroad, "Utility Needs Survey for Fault Current Limiters, EPRI," *International Workshop on Coated Conductors for Applications (CCA08)*, p. 7, December 4-6, 2008.

[10] D. Haught, "Fault Current Limiters," DOE newsletter, Available at: *www.oe.energy.gov/DocumentsandMedia/hts_fcl_110609.pdf, Nov. 6 2009.*

[11] J.C. Krause, "Short-Circuit Current Limiters- Literature Survey 1973 – 1979," TH-Report 80-E-109, ISBN 90-6J44-109-9, Eindhoven Univ. of Tech., July 1980.

[12] A.J. Power, IEE Colloquium on Fault Current Limiters - A Look at Tomorrow, pp. 1 – 5, Jun. 8 1995.

[13] E. M. Leung, "Superconducting fault current limiters," Power Engineering Review, IEEE, vol. 20, pp. 15-18, 30, 2000.

[14] C. Meyer, S. Schröder, R. W. De Doncker, "Solid-State Circuit Breakers and Current Limiters for Medium-Voltage Systems Having Distributed Power Systems," IEEE Trans. on Pow. Elect., vol. 19, no. 5, pp. 1333-40, Sep. 2004.

[15] M. Noe, M. Steurer, "High-temperature superconductor fault current limiters: concepts, applications, and development status," Supercond. Sci. Technol., vol. 20, pp. R15-29, 15 January 2007.

[16] D. Larbalestier, et al,"Power Applications of Superconductivity in Japan and Germany," World Technology Evaluation Commission Report, pp. 45-48, 1997. Available at: http://www.wtec.org/loyola/scpa/toc.htm.

[17] M. M. Lanes, H. A. C. Braga, P. G. Barbosa, "Limitador de Corrente de Curto-Circuito Baseado em Circuito Ressonante Controlado por Dispositivos Semicondutores de Potência," IEEE Latin America Trans., vol. 5, no. 5, Sep. 2007, pp. 311-320.

[18] C. Meyer, P. Köllensperger, R. W. De Doncker, "Design of a Novel Low Loss Fault Current Limiter for Medium-Voltage Systems" pp. 1825-1831.

[19] B. Chen, A. Q. Huang, M. Baran, C. Han, W. Song, "Operation Characteristics of Emitter Turn-Off Thyristor (ETO) for Solid-State Circuit Breaker and Fault Current Limiter".
[20] T. Genji, O. Nakamura, M. Isozaki, M. Yamada, T. Morita, M Kaneda, "400 V class highspeed current limiting circuit breaker for electric power system", *IEEE Transactions on Power Delivery*, vol. 9, issue 3, pp. 1428 – 1435, July 1994.
[21] M. M. R. Ahmed, G. Putrus, Li Ran, R. Penlington, "Development of a Prototype Solid-State Fault-Current Limiting and Interrupting Device for Low-Voltage Distribution Networks," IEEE Trans. on Pow. Deliv. vol. 21, no. 4, Oct. 2006, pp. 1997-2005.
[22] M. M. R. Ahmed, G. A. Putrus, L. Ran, L. Xiao, "Harmonic Analysis and Improvement of a New Solid-State Fault Current Limiter," IEEE Trans. on Ind. App., vol. 40, no. 4, pp. July/August 2004.
[23] H. J. Boenig and D. A. Paice, "Fault current limiter using a superconducting coil," *IEEE Transactions on* Magnetics, Vol. 19, No.3, pp. 1051-1053, May 1983.
[24] M. T. Hagh, M. Abapour, "DC reactor type transformer inrush current limiter," IET Electric Power Applications, vol. 1, Iss. 5, 2007 , pp. 808 – 814.
[25] Takahiro Nomura , Mitsugi Yamaguchi , Satoshi Fukui , Kazuya Yokoyama , Takao Satoh and Koji Usui, "Single DC Reactor Type Fault Current Limiter for 6.6 kV Power System," IEEE Trans. on App. Superconductivity, vol. 11 , no. 1 , Mar. 2001.
[26] Zhengyu Lu, Daozhuo Jiang and Zhaolin Wu, "A New Topology of Fault-Current Limiter and Its Parameters Optimization," IEEE Power Electronics Specialists Conference, PESC03, 2003, pp. 462-465.
[27] W. Fei and Y. Zhang, "A novel IGCT-based Half-controlled Bridge Type Fault Current Limiter," IPEMC 2006.
[28] W. Fei, Y. Zhang and Z. Meng. "A Novel Solid-State Bridge Type FCL for Three-Phase Three-Wire Power Systems," IEEE Applied Electronics Conference and Exposition, Anaheim, California, U.S.A., vol.2, pp. 1084-1088, 2007.
[29] W. Fei, Y. Zhang and Q. Wang, "A Novel Bridge Type FCL Based on Single Controllable Switch," PEDS 2007, pp. 113-116, 2007.
[30] W. Fei; Y. Zhang; Z. Lu, "Novel Bridge-Type FCL Based on Self-Turnoff Devices for Three-Phase Power Systems," IEEE Transactions on Power Delivery , Vol. 23, Issue 4, Oct. 2008 Page(s): 2068 – 2078.
[31] V. K. Sood, S. Alam, "3-Phase Fault Current Limiter for distribution Systems," International Conference on Power Electronics, Drives and Energy Systems, PEDS '06, pp. 1-6, 2006.
[32] T. Hoshino, K. M. Salim, A. Kawasaki, I. Muta, T. Nakamura, M. Yamada, "Design of 6.6 kV, 100 A saturated DC reactor type superconducting fault current limiter," IEEE Trans. Appl. Superconduct., 2003, vol. 13, no. 2, pp. 2012–2015.
[33] E. Yokoyama, T. Sato, T. Nomura, S. Fukui and M. Yamaguchi, "Application of Single DC Reactor Type Fault Current Limiter as a Power Source," IEEE Trans. on App. Superconductivity, vol. 11 , no. 1 , Mar. 2001.
[34] Z. Caihong, W. Zikai, Z. Dong, Z. Jingye, D. Xiaoji, G. Wengyong, X. Liye, L. Liangzhen, "Development and Test of a Superconducting Fault Current Limiter-Magnetic Energy Storage (SFCL-MES) System," IEEE Transactions on Applied Superconductivity, vol. 17, issue 2, pp. 2014-2017.
[35] T. Hoshino, K. M. Salim, M. Nishikawa, I. Nuta, and T. Nakamura, "DC Reactor Effect on Bridge Type Superconducting Fault Current Limiter During Load

Increasing," IEEE Trans. on Appl. Supercond., vol. 11, no.1, pp. 1944–1947, March 2001.
[36] T. Nomura, M. Yamaguchi, S. Fukui, K. Yokoyama, "Study of a Single DC device type FCL for three phase power system," Cryogenics, vol. 41, 2001, pp. 125-130.
[37] M. T. Hagh, M. Abapour, "Nonsuperconducting Fault Current Limiter With Controlling the Magnitudes of Fault Currents," IEEE Trans. On Power Electr., vol. 24, no. 3, March 2009, pp. 613-619.
[38] M. M. Lanes, H. A. C. Braga, P. G. Barbosa, "Limitador de Corrente de Curto-Circuito Baseado em Circuito Ressonante Controlado por Dispositivos Semicondutores de Potência," IEEE Latin America Trans., vol. 5, no. 5, Sep. 2007, pp. 311-320.
[39] G. G. Karady, "Principles of fault current limitation by a resonant LC circuit," *Generation, Transmission and Distribution [see also IEE Proceedings-Generation, Transmission and Distribution], IEE Proceedings C*, vol. 139, pp. 1-6, 1992.
[40] S. Sugimoto, J. Kida, H. Arita, C. Fukui and T. Yamagiwa, "Principle and characteristics of a fault current limiter with series compensation", *IEEE Transactions on Power delivery*, vol.11, no.2, pp. 842-847, 1996.
[41] C. S. Change, P. C. Loh, "Designs synthesis of resonant fault current limiter for voltage sag mitigation and current limitation", in *Proceeding of IEEE Power Engineering Society Winter Meeting*, vol. 4, pp. 2482 – 2487, Jan 2000.
[42] M. Hojo, Y. Fujimura, T. Ohnishi, T. Funabashi, "Experimental Studies on Fault Current Limiter by Voltage Source Inverter with Line Voltage Harmonics Compensation," European Conference on Power Electronics and Applications 2007, pp. 1-8.
[43] S. S. Choi, T. X. Wang, D. M. Vilathgamuwa, "A series compensator with fault current limiting function," IEEE Trans. on Power Delivery, vol. 20, pp. 2248-2256, 2005.
[44] M. Hojo, N. Kuroe, T. Ohnishi, "Fault current limiter by series connected voltage source inverter," IEEJ Trans. on Industry Applications, Special issue on IPEC-Niigata, Vol.126, No.4, pp.438-443, 2006.
[45] B. P. Raju, K. C. Parton, and T. C. Bartram, "A Current Limiting Device Using Superconducting DC Bias, Applications and Prospects," *IEEE Trans. Power Appar. & Syst.*, vol. 101, pp. 3173–3177, 1982.
[46] G. A. Oberbeck, W. E. Stanton, A. W. Stewart: *Saturable reactor limiter for current*, US Patent 4152637, May, 1979.
[47] Yanxia Pan, Jianguo Jiang, "Experimental Study on the Magnetic-controlled Switcher Type Fault Current Limiter," Third Int. Conf. on Electric Utility Deregulation Restructuring and Power Technologies 2008, DRPT 2008, pp. 1987 – 1991.
[48] D. Cvoric, S. W.H. de Haan, J.A. Ferreira, "Improved Configuration of the Inductive Core-Saturation Fault Current Limiter with the Magnetic Decoupling," IEEE Industry Applications Society Annual Meeting IAS'08, pp. 1-7, 2008.
[49] D. Cvoric, S. W.H. de Haan, J.A. Ferreira, "New Saturable-Core Fault Current Limiter Topology with Reduced Core Size," IEEE 6th Int. Power Electronics and Motion Control Conference IPEMC'09, pp. 920 – 926, 2009.
[50] M. Iwdiara, S. C. Mukl, S. Yaniada, et al. "Development of Passive Fault Current Limiter in Parallel Biasing Mode," IEEE Transactions on Magnetics, 1999, vol. 35, nom. 3, pp. 3523-3525.
[51] Hongshun Liu, Qingmin Li, Liang Zou, Yuan Ma, Wah Hoon Siew, "An Equivalent Magnetic Circuit Coupled Model of PMFCL for Transient Simulation," Proc. of 4th Int. Universities Po. Eng. Conf. UPEC, 2009, pp. 1-5.

[52] S. Young, F. P. Dawson, A.Konrad, "An extended magnet in a passive dI/dt limiter," *Journal of Applied Physics*, vol. 76, num. 10, pp. 6874-6876, Nov. 1994.
[53] J-L, Rasolonjanahary, J. P. Sturgess, E. F. H. Chong, A. E. Baker, C. L. Sasse, "Design and Construction of a Magnetic Fault Current Limiter," The 3rd Int. Conf. on Power Electronics, Machines and Drives, 2006, pp. 681-685.
[54] S. Young, F. P. Dawson, A.Konrad, "A three-material passive dI/dt limiter," *Journal of Applied Physics*, vol. 76, num. 10, pp. 6871-6873, Nov. 1994.
[55] S. Young, F. P. Dawson, M. Iwahara, S. Yamada, "A comparison between a two-material and three-material magnetic current limiter," *Journal of Applied Physics*, vol. 83, num. 11, pp. 7103-7105, June 1998.
[56] V. Rozenshtein, A. Friedman, Y. Wolfus, F. Kopansky, E. Perel, Y. Yeshurun, Z. Bar-Haim, Z. Ron, E. Harel, and N. Pundak, "Saturated Cores FCL—A New Approach," IEEE Trans. On Appl. Superconductivity, vol. 17, no. 2, pp. 1756-1759, June 2007.
[57] H. Hong, Z. Cao, J. Zhang, X. Hu, J. Wang, X. Niu, Bo Tian, Y. Wang, W. Gong, and Y. Xin, "DC Magnetization System for a 35 kV/90 MVA Superconducting Saturated Iron-Core Fault Current Limiter," IEEE Trans. On Appl. Superconductivity, vol. 19, no. 3, pp. 1851-1854, June 2009.
[58] Y.F. He, J.H. Li, X.H. Zong, J. Sun, Y.N. Wang, C.L. Wu, J.X. Wang, "The high voltage problem in the saturated core HTS fault current limiter," Physica C, vol. 386, pp. 527–530, 2003.
[59] Y. Xin, J. Zhang, W. Gong, "Voltage Surge Protection Circuit for Superconducting Bias Coil," IEEE Trans. Appl. Supercon., vol. 20, no. 3, pp. 1118 - 1121, 2010.
[60] V. Temple, "Super GTO's Push the Limits of Thyristor Physics," IEEE PESC Aachen, Germany, June 2004, vol. 1, pp. 604-610.
[61] V. Temple, "GTO's Fight Back", Power Electronic Europe, Feature Article, Issue 6, 2004, pp 32-34.
[62] V. Keilin, I. Kovalev, S.Kruglov, V.Stepanov, I.Shugaev and V.Shcherbakov, "Model of HTS Three-Phase Saturated Core Fault Current Limiter", IEEE Trans. Appl. Supercon, vol. 10, No. 1, 2000, pp. 836-839.
[63] Y. Xin, "Development of saturated iron core HTS fault current limiters," IEEE Trans. Appl. Supercon., vol. 17, no. 2, pp. 1760–1763, 2007.
[64] F. Moriconi, N. Koshnick, F. De La Rosa, A. Singh, "Modeling and Test Validation of a 15kV 24MVA Superconducting Fault Current Limiter," Trans. and Dist. Conf. and Expo. 2010 IEEE PES, April 19-22, 2010, pp. 1-6.
[65] S. B. Abbott, D. A. Robinson, S. Perera, F. A. Darmann, C. J. Hawley, and T. P. Beales, "Simulation of HTS Saturable Core-Type FCLs for MV Distribution Systems," IEEE Tran. on Power Delivery, Vol. 21, no. 2, April 2006.
[66] A. Nelson, L. Masur, F. Moriconi, F. De La Rosa, D. Kirsten, "Saturated-Core Fault Current Limiter Experience at a Distribution Substation," 21st International Conference on Electricity Distribution, Frankfurt, 6-9 June 2011.
[67] F. Moriconi, F. De La Rosa, F. Darmann, A. Nelson, L. Masur, "Development and Deployment of Saturated-Core Fault Current Limiters in Distribution and Transmission Substations," IEEE/CSC & ESAS European Superconductivity News Forum (ESNF), No. 14, October 2010.
[68] C. R. Clarke, F. Moriconi, A. Singh, A. Kamiab, R. Neal, A. Rodriguez, F. De La Rosa, N. Koshnick, "Resonance of a distribution feeder with a saturable core fault current limiter," IEEE PES Transmission and Distribution Conf. and Expo., 2010.
[69] A. Abramovitz, K. Smedley, "Review of the Saturable Core Fault Current Limiter Technology", submitted to IEEE Trans. on Power Delivery, Nov. 2010.

[70] A. Abramovitz, K. Smedley, et al, "Prototyping and Testing of a 15kV/1.2kA Saturable Core Reactor High Temperature Superconductive Fault Current Limiter," submitted to Trans. on Power Delivery, April, 2011.
[71] A. Abramovitz, K. Smedley, "A Survey of Solid State Fault Current Limiters".
[72] Fault Current Limiters: Report on the Activities of CIGRE WG A3.10, ELECTRA No. 194, February 2001, pp. 23-29.
[73] Available at: http://www.siliconpower.com/documents/comp_data/spt315.pdf
[74] Available at: http://www.siliconpower.com/_documents/sscl-datasheet.pdf